# Microfacies Analysis and Diagenetic Overprints of Pirkoh Formation in Zindapir Anticline, Sulaiman Province, Dera Ghazi Khan, Pakistan: Reservoir and Source Rock Implications

By

**ZUBAIR AHMED**



**DEPARTMENT OF EARTH SCIENCES**

**QUAID-I-AZAM UNIVERSITY,**

**ISLAMABAD.**

**SESSION: 2021-2023**

# Microfacies Analysis and Diagenetic Overprints of Pirkoh Formation in Zindapir Anticline, Sulaiman Province, Dera Ghazi Khan, Pakistan: Reservoir and Source Rock Implications




A thesis submitted to Quaid-I-Azam University Islamabad in partial fulfillment of the requirement for the degree of Master of Philosophy in Geology.

**By**

**ZUBAIR AHMED**

**Supervised by**

**Dr. Abbas Ali Naseem**

**DEPARTMENT OF EARTH SCIENCES**

**QUAID-I-AZAM UNIVERSITY, ISLAMABAD.**

**SESSION: 2021-2023**

**DEDICATION**

This research work is to dedicated my father, mother, and siblings.

## ABSTRACT

The present study is revealing the depositional facies, diagenetic overprints, reservoir properties and source rock potential of middle to late Eocene Pirkoh Formation in Zindapir Anticline of eastern Sulaiman Province, Dera Ghazi Khan, Pakistan. The microfacies analyses of Pirkoh Formation is representing total fifteen microfacies (MF1-MF15) categorized in three major facies assemblages i.e., inner, middle, and outer shelf based on their depositional setting on carbonate platform. The facies assemblages are typical representative of Tethyan carbonate shelf. The inner shelf facies are deposited on tidal setting (MF1), open lagoons (MF2), backreef shelf (MF3), reef patch (MF4), forereef shelf (MF5-MF7). The middle shelf facies are represented by (MF8-9) characterized by lime mudstone texture and low P/B ratio less than 5%, while the outer shelf facies are (MF10-15) consist of wackestone and packstone texture display high P/B ratio greater than 90% with co-occurrence of extensive echinoid fragments and large flat and well-preserved nummulites and orthophragminids in pelagic matrix. The diagenesis overprints of the Pirkoh Formation are studied in chronological sequence from early to late diagenetic stage. The early diagenetic stage is characterized by micritization, and dolomitization in shallow marine setting, which is followed by the first generation isopachous rim cementation during eogenesis. The mesogenetic phase of diagenesis display fabric selected dissolution in vadose zone of meteoric regime, which is subsequently followed by precipitation of blocky calcite cementation. The physical and mechanical compaction is found to be significant in burial stage of diagenesis resulting to suture seems and selective dolomitization along the fluid pattern. In the latest stage of diagenesis fracturing and telogenetic calcitization take place during tectonic uplift of late Eocene. The depositional facies of the Pirkoh Formation display reservoir potentiality index (RPI) as tight reservoir displaying air porosity (2.67 to 5.64 %) and air permeability (0.06 to 0.29 mD). The source rock results are indicating fear to good quality, but immature source rock with good TOC (1.28 to 1.58 wt.%), indigenous hydrocarbons, mix type II & III kerogen of more anoxic environment in pre-oil window. The Pirkoh formation is secondary reservoir based on the high-density fractures at the outcrop scale and can be a good source rock at certain depth of favorable thermal maturation.

## ACKNOWLEDGEMENTS

All praise to Almighty ALLAH, the most gracious, compassionate and ever merciful, who blessed me the power to do, the sight to observe and mind to think, judge and analyze. In completion of this work and I am core heartedly thankful to ALLAH Almighty. I firmly have faith in, without His gracious help this completion would not have been possible. I am grateful to many people as without their help, guidance and most sincere assistance I could not have achieved my aim of study.

First and foremost, I am deeply grateful to my thesis supervisor Dr. Abbas Ali Naseem for their invaluable guidance, expertise, and continuous support throughout the research process. Their insights and feedback have been instrumental in shaping this work.

I would like to extend my appreciation to the faculty members of Department of Earth Sciences. Quaid-I-Azam University, whose dedication to teaching and research has provided me with a strong academic foundation. Their courses and lectures have broadened my understanding and sparked my interest in the subject matter of this thesis.

I am indebted to the participants of this study, whose willingness to share their time and insights has made this research possible. Their contributions have added depth and significance to the findings presented in this thesis.

I would like to acknowledge the help of Mr. Ijaz, and Mr. Hassan at rock cutting lab. Their support has been crucial in conducting lab work and making quality thin sections.

I am grateful to my family and friends for their unwavering encouragement, patience, and understanding throughout this demanding academic journey. Their support has been a constant source of motivation and inspiration.

I want to express my heartfelt thanks to Qurat ul Ain, Faizan Sabir, Nowroz Khan, Jawad Arif, Khuda Baksh, Awais Haderani, Sheroon Shezad, Umer Khitab, Naveed Iqbal, Khalid Ali Khan, Arshad Jan, Adnan Khan, Adnan Sami Ullah, Abdul Bari Qanit, and Tousif Javed who supported me in ways big and small but may not be mentioned explicitly. Your encouragement, advice, and belief in my abilities have been invaluable.

The last but not the least, I am very thankful to HEC for research funding for access to scientific instrumentation via Access to Scientific Instrumentation Program (ASIP).

## TABLE OF CONTENTS

## LIST OF FIGURES

## LIST OF TABLES

# CHAPTER 1

## INTRODUCTION

Carbonate rocks broadly classified as limestone and dolomite differentiated based on their chemical composition i.e., $CaCO_3$ and $CaMg(CO_3)_2$ respectively. The limestone can be formed by the direct precipitation from concentrated fluids or may biologically evolve from living organism termed as chemical and biologically formed limestone. Limestone mostly formed in shallow depth warm water by the process of living organism to extract the calcium from the marine for the growth of their shelly skeletal parts. The carbonaceous skeleton of these organisms eventually precipitated along with the other constituents the allochemical components such as detrital grains, peloids, lumps, and coated grains including ooids, pisoliths and algal encrusted grains with cements and matrix formed the limestone with pore spaces, throat geometry and interconnected network of wide spectrum in different depositional and diagenetic facies. The texture of limestone highly variform in the term of sedimentary structures and fossils that give important information about the paleo marine environments, paleoecology of that time and/or the progression of lives, principally the marine dwelling organisms through geological time. The carbonate rocks precipitate more abundantly in various geological periods i.e., during Devonian till the late Paleozoic, further during the Jurassic and the Cretaceous of Mesozoic era and Tertiary period of the Cenozoic era. Also, these rocks are significantly recognizable since Precambrian and rest of the Phanerozoic eras (Greenlee et al., 1993; Kiessling et al., 1999; Kiessling, 2002). The successions of carbonate rocks exhibited by the Precambrian and Paleozoic bears mainly abundant of dolomite while that of Mesozoic and Cenozoic is chiefly limestone.

The existence of carbonate rocks has great importance in stratigraphic successions as half of the world's hydrocarbon reserves are host by carbonate rocks. More precisely, the statistics of proven hydrocarbon bearing deposits shows that almost half the hydrocarbons productions from carbonate rocks, in which oil is 60% and gas is 40%, although these rocks make only 20% of the sedimentary strata. In North America 80% of the hydrocarbon's reservoirs are in dolomite (Zenger et al., 1980); 50% of the carbonate reservoir in offshore China (Zhao et al., 2010) are also hosted carbonate reservoirs. Thus, it yields considerable volumes of fossil fuel resources. However, the hydrocarbons the carbonate reservoirs can be followed by the fracturing as it is air tight if nonfractured and/or non-altered limestone (Davies & Smith, 2006; Yoo et al., 2000; Coniglio et al., 1994; Middleton et al., 1993; Hurley &

Budros, 1990; Taylor & Sibley, 1986; Prouty, 1988). Besides, the carbonate rocks can also host the ore bodies such skarn deposits, which also make it more valuable in the stratigraphic succession.

The production of carbonate rocks is the interplay of various elements that includes the tectonic stresses, eustasy, accommodation space, ocean water chemistry, temperature, hydrodynamic regime, siliciclastic input, and the nature ecologies that produce the carbonate skeletal material. The combine effect of all later factors that influence the production of carbonate rocks has great impact on the different reservoir quality that vary from mudstone to grainstone. However, the carbonate rocks are highly suspectable to diagenetic fluids which make it suspicious irrespective of their recognizable depositional texture and display different reservoir behavior. The carbonate rocks facies in the hydrocarbon reservoir are always misleading in exploration and production due to multi face behavior that has been its part since ever these facies are deposited and till influenced by diagenesis. As soon as the carbonate rocks precipitated, it is eventually subject to shallow burial depth. Since the stage of initial burial and before these rocks are subject to regime of metamorphism the diagenesis actively influences carbonate rocks, and in the various realm of the diagenesis carbonate sediments go through various changes in their fabric, texture, composition, spore spaces, throat geometry and its physical strength. Further changes include, chemical and mechanical compaction, the precipitation of various cements cementation phases, dissolution, neomorphism, micritization, and mineral replacement by dolomite (Lapponi et al., 2013).

The influence of diagenesis is varying from process to process and vary differently by the same process. The depositional imprints of carbonate rocks upon various diagenetic events may destroy or enhance in the term of their reservoir quality while these processes operate in any of diagenetic realm i.e., near surface marine, meteoric or the deep burial diagenetic realm. The heterogeneities in carbonate rocks are very important to understand. Therefore, the paragenetic sequence is important to be determined in the chronological order of their respective environment. Which return correctly interpret various boundaries and the detail pattern of depositional facies and their diagenetic fluences at various stages to successfully play the evaluation of hydrocarbon prospects as a first and fundamental stage (Martin et al. 2013). Additionally, the heterogeneities distribution of carbonate rocks is essentially controlled by depositional lithofacies units, diagenetic imprints, and structural framework (Martin et al., 2013).

Reservoir quality is important parameter to understand as it the key factor in the effectiveness of a well (Taylor et al., 2010). Various authors (Mansurbeg et al., 2009;

Deschamps et al., 2012; Lan et al., 2016; Zahid et al., 2016) show their interest in the assessment of carbonate rocks' reservoir quality, to understand the controlled by major factors such as original depositional facies, diagenesis, and sequence stratigraphic. On other hand, prior to diagenetic influence, structural and stratigraphic position of these the carbonates rocks also influence the textural and reservoir characteristics of carbonate rocks as function of variation in facies (Machel, 2004; 2005). The most important factor is the variation is microfacies and the influence of various diagenetic processes that significantly affect the reservoir quality (Machel and Mountjoy, 1986; Machel and Anderson, 1989; Machel and Lucia, 2007; Buschkuehle, 2008 ; Ahr, 2008; Koehrer et al., 2010; Moore and Wade, 2013; Daraei et al., 2014; Shen et al., 2015; Amel et al., 2015; Enayati-Bidgoli and Rahimpour-Bonab, 2016; Beigi et al., 2017). The present study focuses on the detailed microfacies analysis, diagenesis, reservoir and source quality of the Pirkoh Formation in Zindapir Anticline, Dera Ghazi Khan, Central indus basin, Pakistan.

### 1.1 Location and Accessibility of the Study Area/Studied Section

The area of interest for research purposes make part Dera Ghazi Khan is located in the Punjab province of Pakistan. The Zindapir section is accessible through following Zindapir shrine route through streams, undeveloped road and local tracks covering distance up 60 km from Shādan Lund to Zindapir section, while the D.G cement factory section is at 40 km from Shādan Lund. The later section located at geographic coordinates of 30°19'59.04"N and 70°29'30.14"E, while the former section is at geographic location of 30°24'48.81"N and 70°30'50.32"E.

### 1.2 Climate

Dera Ghazi Khan has a hot desert climate with scorching summers and cool winters. The summer season starts in April and lasts until October, with temperatures often exceeding 40 degrees Celsius (104 degrees Fahrenheit). During this time, the weather is extremely hot and dry. The winter season, from November to March, brings relatively cooler temperatures ranging from 5 to 20 degrees Celsius (41 to 68 degrees Fahrenheit).

### 1.3 Precipitation

Dera Ghazi Khan receives most of its rainfall during the monsoon season, which typically occurs from July to September. The average annual precipitation in the region is around 200-300 millimeters (8-12 inches). The monsoon rains bring relief from the scorching heat and contribute to the agricultural productivity of the area.

### 1.4 Local Culture

Dera Ghazi Khan has a rich cultural heritage. The region is known for its distinct folk music and dance forms, including the famous "Jhoomar" and "Dhamal." The people of Dera Ghazi Khan, like other areas in Punjab, have a vibrant and colorful culture. Traditional Punjabi dresses, such as the "shalwar kameez" for men and the "ghagra choli" for women, are commonly worn. The local cuisine of Dera Ghazi Khan is renowned for its flavors and includes dishes like "sajji," "biryani," and "siri paye." The city also hosts various festivals and events that showcase the traditional music, arts, and crafts of the region.

### 1.5 Zindapir

Zindapir also known as Zinda Pir, is a historical and revered shrine located in Dera Ghazi Khan, Pakistan. The shrine is dedicated to a Sufi saint named Hazrat Syed Ahmed Saeed Kazmi, who is commonly referred to as Zindapir. The architecture of the shrine reflects a blend of Islamic and local architectural styles. Annually, a large Urs (death anniversary) celebration is held at the Zindapir shrine, attracting thousands of devotees who gather to commemorate the saint's life and teachings. During the Urs, there are special prayers, religious gatherings, recitations of Sufi poetry, and performances of Qawwali (devotional music). Zindapir holds a significant place in the spiritual and cultural landscape of Dera Ghazi Khan. It serves as a symbol of religious harmony, unity, and devotion, and continues to attract both locals and tourists interested in Sufi traditions and spirituality. The Zindapir Anticline is named after Zindapir shrine.



### 1.6 Aims and Objectives

The present focus on the following objectives;

1. To study the microfacies and interpret the depositional environment.
2. To study the diagenetic overprints and determine the paragenetic sequence.
3. To characterize the reservoir quality.
4. To study the source rock quality.

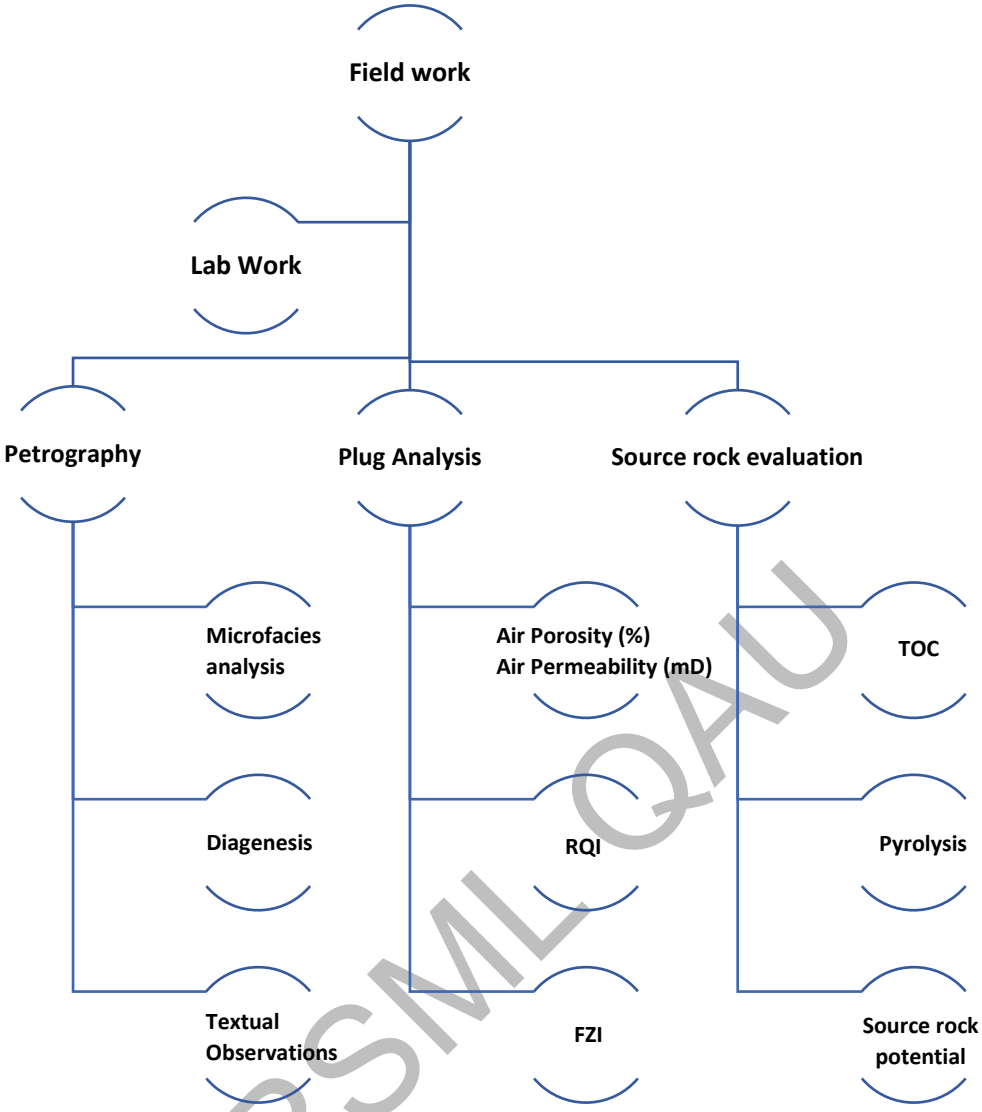


Fig. 1.1 shows flow chart of aims and objectives via methodology.

# CHAPTER 2

## PALEO-TECTONIC SETTING AND STRATIGRAPHY

### 2.1 Paleo-Tectonics

Pakistan and its surrounding regions are evolved from the Gondwanan and Tethyan domain. The southern-eastern Pakistan belongs to Indo-Pakistan crustal plate, while the northernmost and western Pakistan belong to the Tethyan domain. Overall Pakistan is located on Junction between Tethyan and Gondwanian domains (Kazmi & Jan, 1997). The brief evolutionary history of Pakistan and component tectonic domains.

In the late Paleozoic, there was a supercontinent known as Pangea surrounded by a universal ocean called Panthalassa. During the late Triassic, a wedge of Panthalassa i.e., the Tethys entered from east to west which breaks the Pangea into northern and southern sub-supercontinent by Tethys seaway (Kazmi & Jan, 1997). The Laurasia and Gondwana in the North and south respectively, forming the Paleo-pacific oceanic extension, forming the todays Central Atlantic Ocean (Khan & Tewari, 2016).

Continental drift is a continuous process that occurs over geologic time. Since the late Devonian- Triassic, it results in the further splitting of Laurasia and Gondwana into seven major tectonic plates, other microplates, oceans spaces, and sea landforms. The present South American, African, Antarctician, Indian and Australian plates are derived from Gondwana, while the North American and Eurasian plate derived from Laurasia.

The Eurasian plate comprises of initial Laurasian landmass, the Laurasian domain, "initial Laurasian landmass and former fragments of Gondwanaland" and the Gondwanan domain, "the accreted assemblage of the terminal former fragments i.e., Indian & Arabian shields of Gondwanaland at the south of Tethyan domain (Kazmi & Jan, 1997). Following (Sengor et al., 1988) Laurasian domain is term as the Tethyan domain.

The Gondwanan domain is characterized by the crystalline basement, the continental crust of Precambrian that developed to a platform type in Paleozoic. In Eurasia, it mainly comprises of Indian shields and Arabian crystalline basement rocks. The former is the present Indo-Pakistan subcontinent building the norther Himalayan orogeny extended from east to west (Kazmi & Jan, 1997). The Indian plate separated from its Gondwanaland about 130 Ma, drifted 5000 km northward, and collide with the Kohistan-Ladakh arc along with Main Mantle Thrust (MMT) in northern Pakistan in Paleocene-Eocene. Similarly, about 55 -60 Ma it collided with the afghan block in northwestern Pakistan along Main Waziristan Thrust (Kazmi & Jan, 1997). During the Late cretaceous Kohistan-Ladakh Intra oceanic arc had collided with Karakoram

palate along Main Karakoram Thrust (MKT) (Petterson & Windley, 1985). Both the MMT and MKT extended westward and terminates in eastern Afghanistan by Waziristan ophiolite (Treloar & Izatt, 1993).

The Tethyan domain from east to westward encompassing India and the northern borders of Africa and Arabia. It stretches from the Pacific Ocean to the Mediterranean Sea. Its shape is resembling ancient Tethys seaway i.e., wide in the east and narrow in the west. It is largely comprised of mosaic several orogenic continental blocks that stitch together in the form of a complex network of suture (Kazmi & Jan, 1997). During the middle to late Paleozoic rifting and successive fragmentation of continental blocks from Gondwanaland started drifting northward and later its collision with the Laurasian landmass result to the Tethyan domain. Its evolution is linked with the opening and closing of several ocean spaces by different geologic events i.e., rifting, subduction, and collision of crustal blocks. During Middle Carboniferous, the Pangea was intact and the earliest known ocean space between Gondwanaland and Laurasia was known as Paleo-Tethys. In the Late Triassic, most of these blocks collide with Laurasia and the Paleo-Tethys get closed in Early Jurassic. During Early Jurassic, Paleo-Tethys had closed and by late Jurassic, Neo-Tethys grow. The later upon the closing event mark the plate boundary upon the collision of Indian and Arabian shield with Eurasia resulting in Indus-Tsangpo suture and Zagros suture, respectively. The Alpine-Himalayas orogenic belt developed as part Indus-Tsangpo and Zagros sutures collage and colliding blocks refer to as Alpines.

The Himalayas orogeny development occurs due to the convergence of Eurasian and Indian Plate (Ding et al., 2016; Qasim et al., 2018). The MMT and MKT marks the Himalayan collision (Jin et al., 1996) which is divided into a northern suture called Main Karakoram, and a southern suture called as the Main Mantle Thrust (Tahirkheli, 1979). The MMT marks the collision zone of Kohistan Island Arc with Indian plate and the MKT marks the collision between the Karakoram block of Eurasian plate with Kohistan Island Arc at south and north respectively shown in (Fig. 2.1) (Searle, 1999; Ding et al., 2016).

The Chaman transform fault (left-lateral strike-slip) mark the active deformation zone along the east of Indian Eurasian collision zone while in the west it is mark by Bela-Zhob Ophiolites shown in (Fig. 2.1) (Lawrence et al., 1981, 1992; Siddiqui and Jadoon, 2012).

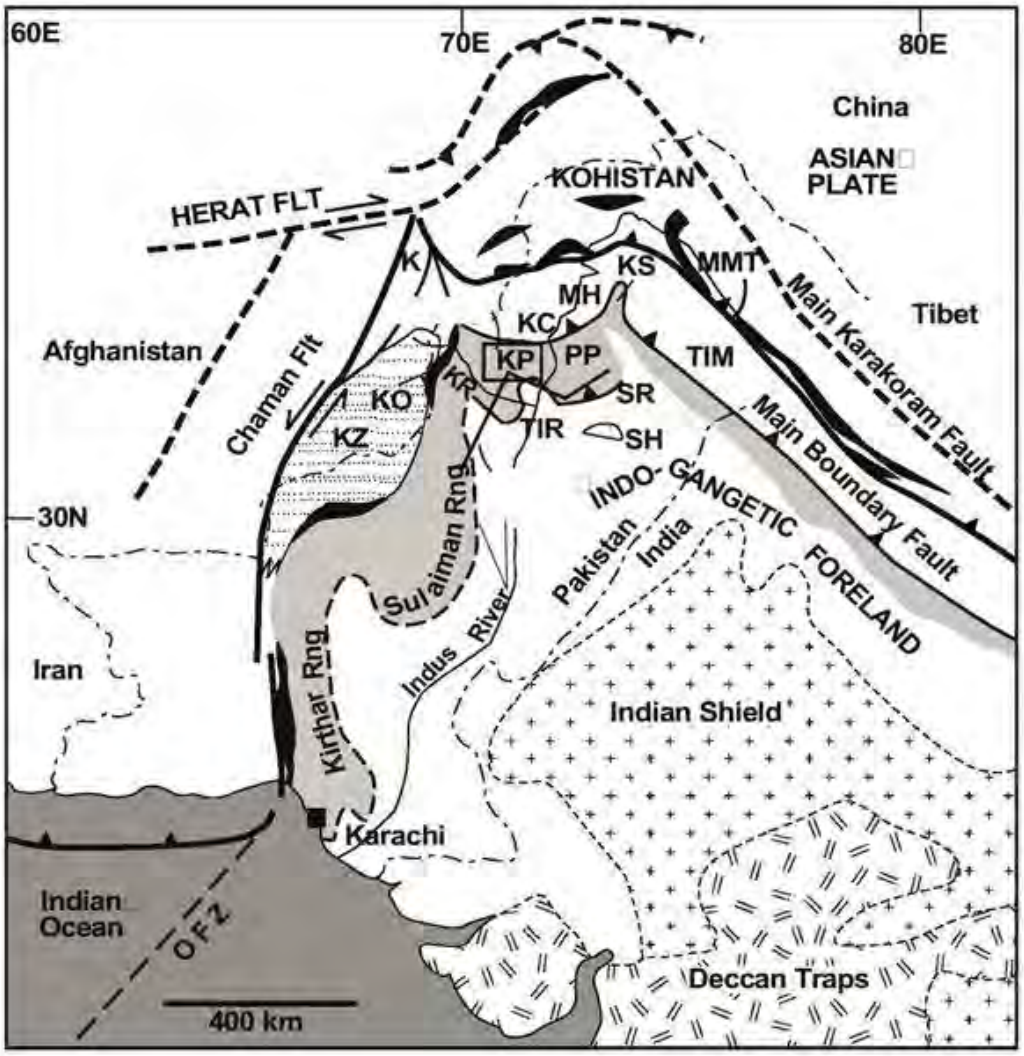


Fig 2.4: shows tectonic map of Pakistan (Ahmad et al., 2011)

### 2.1.1 The Sulaiman Fold belt (SFB)

The Sulaiman Fold belt (SFB) is lobate tectonic prominent feature extended ~ 400 km along the western extreme of north-west Himalaya. The SFB comprises of Eocene and Permian- Triassic succession of carbonate platform in the foreland and hinterland respectively. The strike length of ~1000 km in the mountain front represents Zindapir and Sui Monocline/folds in eastern and southern Sulieman fold and thrust belt. The SFB is investigated extensively over a broad spectrum of Seismic reflection, structural deformation, gravity modeling to interpret the genetic model, the sum of all signifies thin skinned deformation of SFB because of Convergence over a decollement (Quittmeyer et al., 1984; Banks and Warburton, 1986; Jadoon et al., 1993, 1994a; Davis and Lillie, 1994; Bernard et al., 2000; Reynolds et al., 2015). The study of (Banks and Warburton, 1986; Humayon et al., 1991; Jadoon et al., 1993, 1994a) signify the SFB as a passive-roof duplex style hindward oriented. The southern SFB comprises of East-West oriented detachment folds namely Loti and Sui folds

(Jadoon et al., 1992), while the Zindapir Anticlinorium is the north-south is typical fault bend fold (Humayon et al., 1991). However, the study of (Iqbal and Helmcke, 2004; Peresson and Daud, 2009; Iqbal and Khan, 2012) signify the Zindapir Anticlinorium as a flower structure of basement segmentation due to twist tectonics.

The Suleiman Fold and Belt is showing faults and folds in the hinter part and foreland respectively (Kazmi and Rana, 1982; Jadoon and Zaib, 2018). The Sulaiman Range is marked the topographic front of North-South alignment with 2000 m as compared to the internal part of the system which about 1000 m and lacking the thrust fault at the foreland. In the study area is Zindapir Anticlinorium is North-South oriented with strike length of about ~130 km.

### 2.1.2 Zindapir Anticline

The Zindapir Anticline is the segment of Zindapir Anticlinorium with length of about 60 km located in the southern extreme. The Zindapir Anticline is about 60 km wide and is North-South oriented, east-verging fold axis. The Paleocene strata is exposed in the core, which is drilled in Triassic strata of the Zindapir-01 to 4406 m total depth. The Triassic strata show the highest relief of about 4 km as compared to the regional stratigraphy. The cross section shows the Anticline stack of two duplex horses surrounded between floor thrust over the basement at a depth of about 10 km, and a roof thrust in the Cretaceous Sembar shale. The horse length is different from each other, the outer horse larger in length as compared to inner.

The strata Molasse present along the hanging wall of ramp flat geometry of the Zindapir duplex, it is generally flat along about~25 km long with the representation of extensive syncline between the Zindapir and Fort Munro Anticlines and whole ramp flat structure. The Anticlinal stack structure is showed in the westward located Fort Munro Anticline (Humayon et al., 1991; Jadoon et al., 2019). An oblique convergence beside the edge of the fold belt is represented by the eastward propagation of the foreland thrusting. The propagation of mountain front is recorded in the Tertiary sedimentary marine and the continental strata in east (Waheed and Wells, 1990).

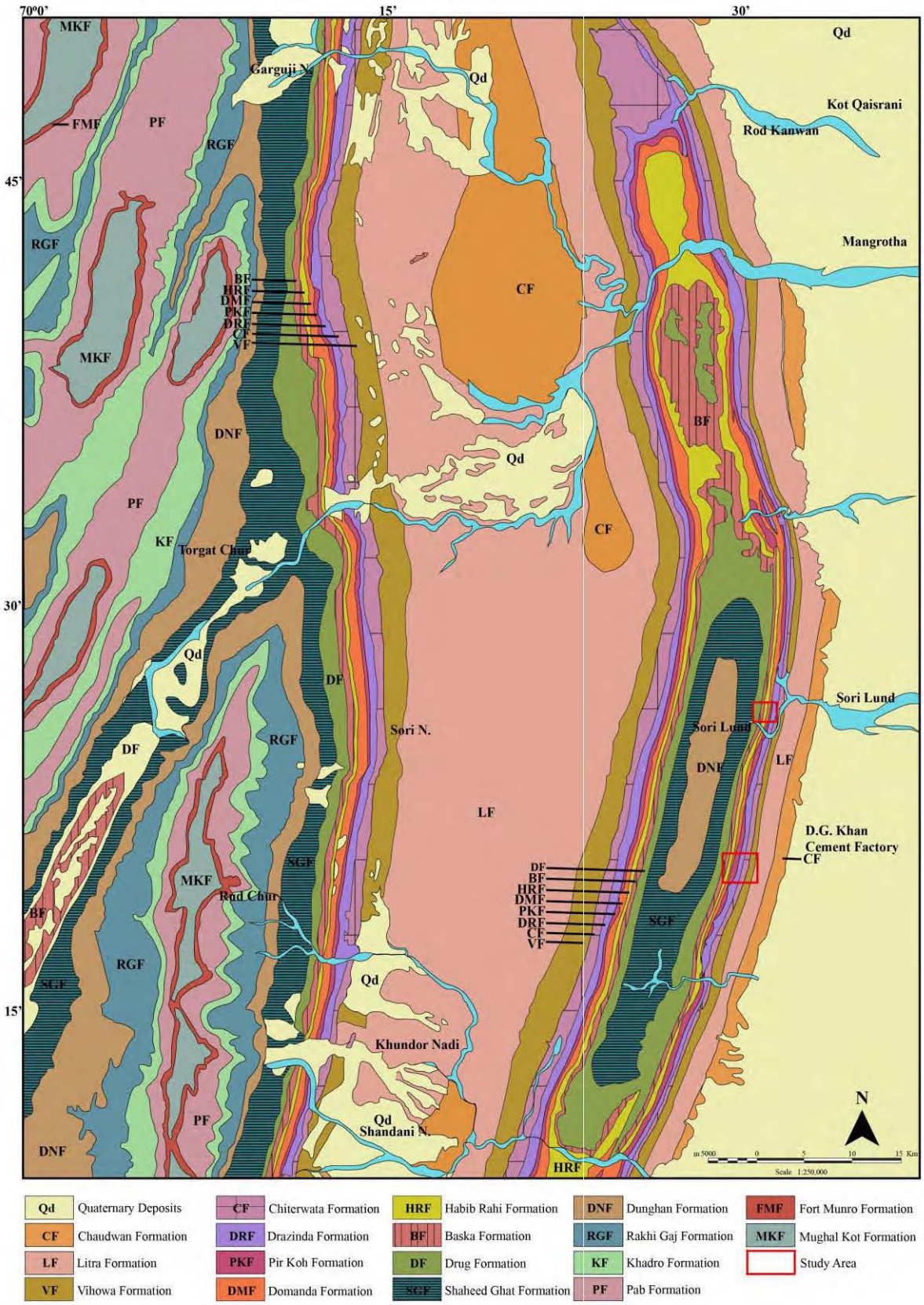


Fig 2.2: shows geological map of Zindapir Anticline (after Hassan et al., 2002) reference no. 39J, GSP, 2002.

## 2.2 Stratigraphy of Study Area

### 2.2.1 Recent deposits

The recent deposits consist of alluvium deposits comprising unconsolidated pebbles, gravel, sand, silt, and clay of Recent origin occupying stream beds. The meander belt deposits include sand, silt and clay of levees and bars of meandering channel deposits of Indus River. The active flood plain deposits are sand, silt, and clay derived from the Indus River flood plain liable to flooding seasonally, while the dune sand deposits in the Zindapir area are mainly aeolian sand and silt deposits lying over the Recent and sub recent surficial sediments.

### 2.2.2 Sub recent deposits

The sub recent deposits comprise of flood plain deposits, which are mainly clay, silt, and sand of older flood plain of Indus River. The sub piedmont deposits include finer detrital material comprising clay, silt, sand, and gravel derived from adjacent highlands and deposited between the flood plain deposits and the piedmont plain. The piedmont deposits are made of coarse grain detrital material comprising boulders pebbles. gravel, sand, and silt derived from adjacent highlands and deposited between the foothills and the sub piedmont plain. The alluvial Fan deposits in Zindapir area are mainly sandstone and limestone boulders, pebbles and gravel deposited as a continuous apron consisting of alluvial fans along the inclined base of the mountain range. The pediment deposits are pebbles, cobbles and boulders covering slopes and raised terraces. The terrace gravel deposits are the old stream deposits comprising boulders, cobbles and pebbles of sandstone and limestone, loosely cemented by gritty and sandy matrix. recently incised.



### 2.2.3 Dada Conglomerate

It has Light brownish grey color, massive conglomerate comprising boulders, cobbles, pebbles of sandstone and limestone in sandy matrix. The upper contact of Dada conglomerate is with surficial deposits unconformable. It has up to 9 m thickness in the Zindapir area. The Formation is considered of Pleistocene age.

### 2.2.4 Chaudhwan Formation

It has light brownish grey, massive conglomerate with brownish grey and grey sandstone and earthy claystone intercalations, capped by unconsolidated Quaternary sediments at places. It has upper contact unconformable with Dada Conglomerate and Quaternary surficial deposits. In Zindapir area it has thickness of + 1422m. The age of the Formation is late Pliocene.

### 2.2.5 Litra Formation

It has grey, greenish grey sandstone with minor brown clay. The sandstone unit of the Formation are thick bedded to massive, cross bedded, conglomerate, and contains vertebrate fossils. It has upper conformable contact with Chaudhwan Formation and attain thickness of 2002 m in Zindapir area. The age of the Formation is Middle Pliocene.

### 2.2.6 Vihowa Formation

The Vihowa Formation is showing bright red claystone/siltstone, intercalated with grey, greenish grey, thick bedded to massive sandstone contains remains of vertebrate fossils. It has upper transitional contact with Litra Formation and has thickness up to 975m. The age of the Formation is Early Pliocene.

### 2.2.7 Chitarwata Formation

The Nari Formation of Eames (1952) is given the Chitarwatta name by Hemphill and Kidwai (1973) in Sulaiman range, and the Stratigraphic Committee of Pakistan formalized it. It lies in the Sulaiman range to the east and south. It consists of grey, yellowish grey quarzitic sandstone with siltstone and vary colored claystone sandstone. It is oolitic and ferruginous in basal parts, silica sand developed in the middle and upper parts, it also contains vertebrate fauna. Claystone and siltstone are carbonaceous and contain thin coal beds, lea and root fragments. It has Upper disconformable contact with Vihowa Formation. It has thickness up to 320m in Zindapir area. Iqbal (1969b) assigned Oligocene age based on the Bivalves and gastropods of fresh water, and the fossil species are restricted to Oligocene.

### 2.2.8 Kirthar Group

The term ‘Kirthar’ is recognized by (Kadri, 1995). The sediments as defined were subdivided into four members as discrete Formations i.e., the Drazinda, Pirkoh, Sirki/Domanda, and Habib Rahi Formation (Raza et al., 2001) in the Sulaiman Range and the Central Indus Basin. According to (Raza et al., 2001), the Kirthar Formation is upper most Ypresian (Lower Eocene) to lower Lutetian (Middle Eocene).

#### 2.2.8.1 Drazinda Formation

The Drazinda Formation was designated the top Formation of the Kirthar Group by Iqbal and (Shah, 1980), although it was not recognized as such by (Raza et al., 2001). It consists of grey to brown non-calcareous shales with poorly developed interbeds of fossiliferous limestone, which are widely exposed throughout the eastern side of the SFB and Central Indus Basin. In Zindapir area it has upper unconformable contact with Chitarwata Formation and

lower transitional with the Pirkoh Formation. In other areas, a significant regional unconformity accounts for the absence of the Nari and Gaj Formations. The lithology in Zindapir area consist of brown and green shale/claystone with subordinate siltstone, marl, and limestone, gypsiferous, fossiliferous, fauna includes foraminifera, bivalves, gastropods, and remains of fish, sea cow and whales. The Chitarwata Formation attain thickness up to 583 m in Zindapir area.

The macrofossil content comprises gastropods, bivalves and echinoid remain (Oldham, 1890). Microfossil assemblages include ostracods and larger benthonic foraminifera mainly orthophragminids (Porth and Raza, 1990a). It Bartonian to Priabonian and display open marine setting.

#### 2.2.8.2 Pirkoh Formation

The term Pirkoh is introduced by (Hemphill and Kidwai, 1973). In Zindapir area it is light pale yellow to brownish limestone medium bedded in the middle unit and massive both in upper unit (argillaceous and marly fossiliferous) and lower unit comprising of abundant shallow benthic foraminifera. It is. Its faunal assemblage includes foraminifera, bivalves, gastropods and fish remains. The type locality for the Formation is the Pirkoh structure in the Dera-Bugti region. The Pirkoh Formation is present in the south of Sulaiman province, but it is often not represented in the north due to unconformity or non-deposition (arial photography view from satellite). The limestone consists of packstone and foraminiferal grainstone with subordinate marl beds and calcareous shales, with a discocyclinids bearing limestone bed at the base (present study). The Pirkoh Formation in the study area display well exposed contact with overlaying Drazinda Formation and underlain Domanda Formation, where the nature of contacts is transitional and conformable respectively (present study). The paleontological criteria of Pirkoh Formation suggest the Lutetian to Bartonian (Middle-Late Eocene) age and the facies interpretation signify to the depositional setting shallow to moderately deep marine on carbonate shelf (present study).

#### 2.2.8.3 Domanda Formation

The ‘Domanda’ is introduced by (Raza et al., 2001). It is widely exposed throughout the eastern Sulaiman basin. The sediments consist of grey, often chocolate-brown, non-calcareous shales and claystone. The fauna includes foraminifera, bivalves, gastropod, and remains of sea cow and whale. It has upper conformable contact with Pirkoh Formation and attain thickness up to 460 m in Zindapir area. It has both conformable contacts underlying Habib Rahi and overlying Pirkoh Formation. The Formation contains a rich macrofaunal

assemblage comprising gastropods, brachiopods, and fish remains. It is of Lutetian (Middle Eocene) age and depositional setting of shallow marine to brackish.

#### 2.2.8.4 Habib Rahi Formation

The 'Habib Rahi Limestone' formed the basal member of the Kirthar Formation as defined by Iqbal and Shah (1980) and was called the 'Platy Limestone' by (Eames, 1952). It was recognized as a separate Formation by (Raza et al. 2001). The 'Habib Rahi' Formation refer is equivalent to Kohat Formation (Kadri, 1995). The Formation consists of limestone of light grey color with shale intercalations in the lower part. The lower and upper boundaries are conformable with the underlying Ghazij and overlying Domanda Formation. It comprises of light grey brownish grey limestone, argillaceous, cherty, platy, massive at the base. It is highly fossiliferous, and the fauna includes foraminifera and fish. Up to 74m thick. It has age of Lutetian (Middle Eocene) and shallower, inner shelf depositional setting.

### 2.2.9 Ghazij Formation

#### 2.2.9.1 Baska Formation

Baska Formation of Ghazij group is introduced by (Hemphill and Kidwai, 1973). It has grey color, nodular in places, argillaceous limestone and intercalated green shale. The fauna includes foraminifera, bivalves, gastropods, and lamellibranches. It has upper transitional contact with Habib Rahi Formation and attain thickness up to 345 m thick. It is restricted to Lower Eocene (Iqbal, 1969).

#### 2.2.9.2 Drug Formation

The Drug Formation consist of greenish grey shale and brownish grey limestone. The shale intercalated with gypsum in the upper part. The fauna includes foraminifera and lamellibranches. In the Zindapir area it has conformable upper contact with Habib Rahi Formation and attain thickness of attain thickness of up to 356 m. The biostratigraphy age of Drug Formation is Early Eocene (Iqbal,1969), and display inner shelf depositional environment.

#### 2.2.9.3 Shaheed Ghat Formation

It has dark grey, olive grey, green fissile stale intercalated with siltstone and the gypsiferous, carbonaceous, fossiliferous limestone is present in the lower part. The fauna includes foraminifera, gastropods, and bivalves. In Zindapir area it has upper transitional contact with drug Formation and attain thickness about 1,870m. The biostratigraphy age of Drug Formation is Early Eocene (Iqbal, 1969).

### 2.2.10 Dungan Formation

It is dark grey to brown limestone, thick bedded to massive, nodular, intercalated with dark bluish grey shale dominating in the southern part. The limestone conglomerate bed developed at the top of the Formation, which grades into calcareous sandstone in places. The fauna includes foraminifera gastropods, bivalves, and algae. In Zindapir area it has upper conformable contact with the Shaheed Ghat Formation and attain thickness up to 211 m. The limestones, shales and marls of the Dungan Formation are widely distributed throughout the Central Indus Platform Basin and conformably succeed the Upper Ranikot Formation. The Formation contains a diverse and abundant macrofossil assemblage including bivalves and gastropods. The microfossils include melobesioidean calcareous algae and both shallow and planktonic benthonic foraminifera (Davies, 1941).

The Dungan Formation contains abundant fossils includes algae, bivalves, gastropods, and foraminifera. The foraminiferal assemblages of Dungan Formation include dictyoconoides, discocyclina, linderina, lockhartia, operculina, nummulites, miscellanea and other shallow benthic foraminifera. It Paleocene to Early Eocene (Latif, 1964), and display depositional environment of typical platform limestone.

### 2.2.11 Rakhi Gaj Formation

The Rakhi Gaj Formation consists olive-grey to dark greenish-grey shale intercalated with mostly brown to greyish red, purple and yellowish green thin to thick bedded sandstone, iron concretions developed in shale, and also bands of grey limestone developed at places. It is fossiliferous in places, while the faunal includes foraminifera, bivalves, and gastropods. In Zindapir area it has upper conformable contact with Dungan Formation, and lower conformable contact with Khadro Formation. It attains thickness of up to 357 m thick. The delta of the Rakhi Gaj Formation submerged and giving the overlying Formation to rise at its place. It has age of middle and late Paleocene based on superposition and equivalent chronostratigraphic unit in region.

### 2.2.12 Khadro Formation

The Khadro Formation consist of dark reddish brown to grey oolitic, shelly calcareous sandstone and limestone. The limestone units are intercalated with olive grey shale. The faunal assemblages of Khadro Formation include foraminifera, bivalves and gastropods and diagnostic fossil Cardita *Beaumonti*. In Zindapir area it has upper conformable contact with Rakhi Gaj Formation and attain thickness up to l54m thick.

### 2.2.13 Pab Formation

It has light grey, whitish to pinkish grey sandstone, thick bedded, and display mudstone intercalation. It is rarely fossiliferous reported, the fauna includes orbitoides mostly, but overall, poorly fossiliferous. In Zindapir area it has upper unconformable contact with contact with Khadro Formation and attain thickness up to 446 m, while in 469m thick in principle section. The sandy beds are devoid of any fossil content, but an assemblage of benthonic foraminifera has been recorded within the shales and is considered as of cretaceous age (Kadri, 1995).

In the Central Indus Basin, the Pab Formation is restricted to the southwestern and central areas; in the north and east, sediments of Upper Cretaceous age are probably absent. The sediments consist of thickly bedded, coarse-grained sandstones, with thin layers of calcareous shale in the lower unit. The Deposition of the Formation probably occurred in a marine shelf location, where the general lowering of sea level provided a significant source of sediment.

### 2.2.14 Fort Munro Formation

The limestone is fossiliferous and contains the remains of reef-building organisms such as hermatypic corals, ammonites, and echinoids, and abundant bioclastic debris, probably derived from bivalves. It has dark grey to black, medium to thick bedded limestone with alternating thinly bedded grey marly shale. The Fort Munro Formation is argillaceous in the lower part and sandy in the upper part. The faunal assemblage of the Formation includes foraminifera, especially orbitolites.

In Zindapir area, it has upper transitional contact with Pab Formation and attain thickness up to 139 m and it is about 100 m thick in the principal at Fort Munro Anticline, near the Dera Ghazi Khan Road. It is upper Campanian to upper Maastrichtian age based on the benthonic foraminiferal index species (Iqbal and Shah, 1980), and display shallow marine shelf environment.

### 2.2.15 Mughal Kot Formation

It is calcareous mudstone of grey color, with limestone and shale intercalations. The sandy upper unit display rare fossiliferous nature in places. The biota assemblage of the Mughal Kot Formation is including shallow benthic foraminifera orbitoides media, omphalocyclus macroporus and siderolites calcitrapoides, while the planktonic foraminiferal microfauna comprising Globotruncana *spp*., Globigerina *spp*., Guembelina *spp*., and associated forms has

also been recorded, but the assemblage is usually impoverished (Kadri, 1995). In Zindapir area the base of Mughal Kot Formation is buried, while it has upper conformable contact is with Fort Munro Formation. It is about 172 m in Zindapir area, while it is about 1170m thick in its principal section at Mughal Kot (Kadri, 1995).

The Mughal Kot Formation occurs over much of the Central Indus Basin, in the north and east, the Formation is absent either due to erosion or non-deposition. The Formation is heterogeneous, consisting of marls, shales, and siltstones with intercalations of sandstones and argillaceous limestones. The base of the Formation is characterized by huge slumping features. The age assigned to the Mughal Kot Formation, based on the above micro fauna confirming Campanian to lower Maastrichtian (Shah, 1977; Iqbal and Shah, 1980), and it has depositional environment of relatively shallow water, with the limestone indicating a shallow-water origin in shelf areas displaying thicker limestone sequences of outer shelf environment with access to the open ocean (Kadri, 1995).

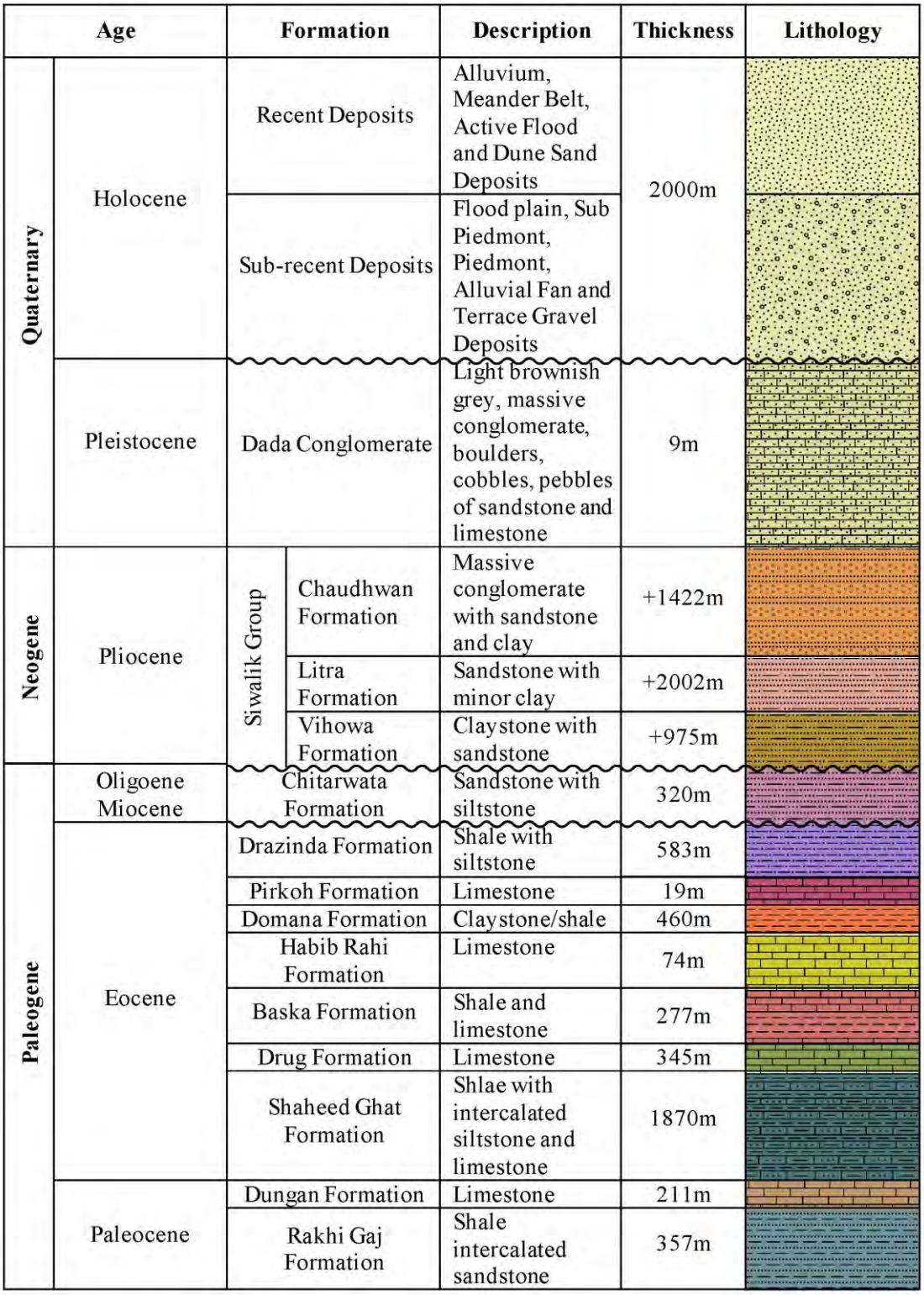


Fig 2.5: shows the Stratigraphic chart of Zindapir area of eastern Sulaiman province.

# CHAPTER 3

# RESEARCH METHODOLOGY

## 3.1 Field sample collection

In the field work the Zindapir section and DG cement factory section of the Pirkoh Formation is measured. Total 36 samples bed to bed were collected during field work. The collected samples were run in rock cutting laboratory for petrographic studies to determine the depositional facies of Pirkoh Formation. The porosity and permeability of selected samples were determined by conducting plug analysis. Furthermore, the source rock properties (TOC and rock eval pyrolysis) are studied in detail to investigate the source potential.

## 3.2 Petrography and microphotography

The systematic bed-to-bed samples are collected from outcrop and run in rock cutting laboratory at Quaid-I-Azam University, Islamabad.

### 3.2.1 Thin sections preparation

The transparent glass slides are polished with silicon carbide 1000 mesh to vanish the scratches and remove the dust and other impurities attached to the slide surface. After polishing, the glass slide is washed and clean with tap water and let it dry on hot plate. The outcrop samples are cut at different orientation to observe the maximum possible variation of biota assemblage and diagenesis in minimum area of rock slab. The desired rock chips are selected and polished with silicon carbide 1000 mesh to get evenly distributed surface for attachment to glass slide. After polishing, the selected rock chips are washed and clean with tap water and let it dry on hot plate to remove the moisture content.

Epoxy is carefully prepared by mixing the part “A” with part “B”, the hardener of the resin with fixed ratio (2:1) respectively. The prepared resin was used within 30 minutes after preparation to attached both polished surfaces of rock chip and glass slide. After the attachment, all the entrapped air is removed with nonstick metallic clips and placed the samples attached with clipped on hot plate for 5 minutes to cure the resin and dry the left-over moisture content in rock chip and placed the sample at room temperature for 48 hours to dry the resin completely.

The attached sample is grinded with silicon carbide 120 mesh on grinder, followed by grinding with silicon carbide 240, 320 and 400 mesh on large glass. Furthermore, the grinded samples are polished with silicon carbide 600, 800 and 1000 mesh for final touch to attain thickness of up to 30 microns. The flow chart is shown in (Fig. 3.1).

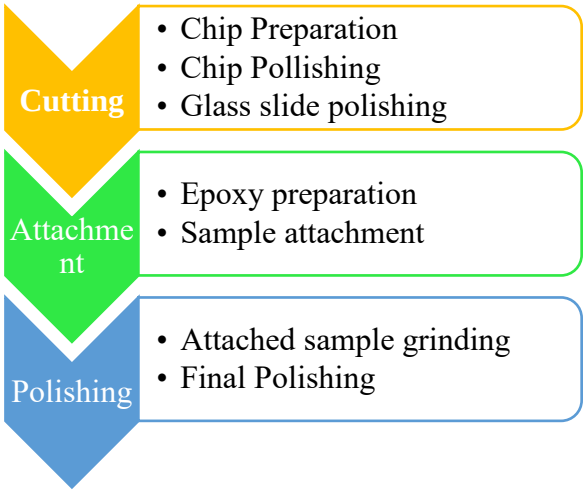


Fig 3. 2: shows flow chart of thin sections preparation.

### 3.2.2 Microphotography

The prepared samples are studied at petrography laboratory, Quaid-I-Azam University, Islamabad Leica with Leica DM750P with attached DFC290 camera and Leica application suite.



### 3.3 Plug Analysis:

The plug analyses of selected 15 samples were carried out in HDIP, Islamabad. The field samples after petrographic studies were further investigated for plug analysis to determine the air porosity and air permeability of depositional facies based on their texture.

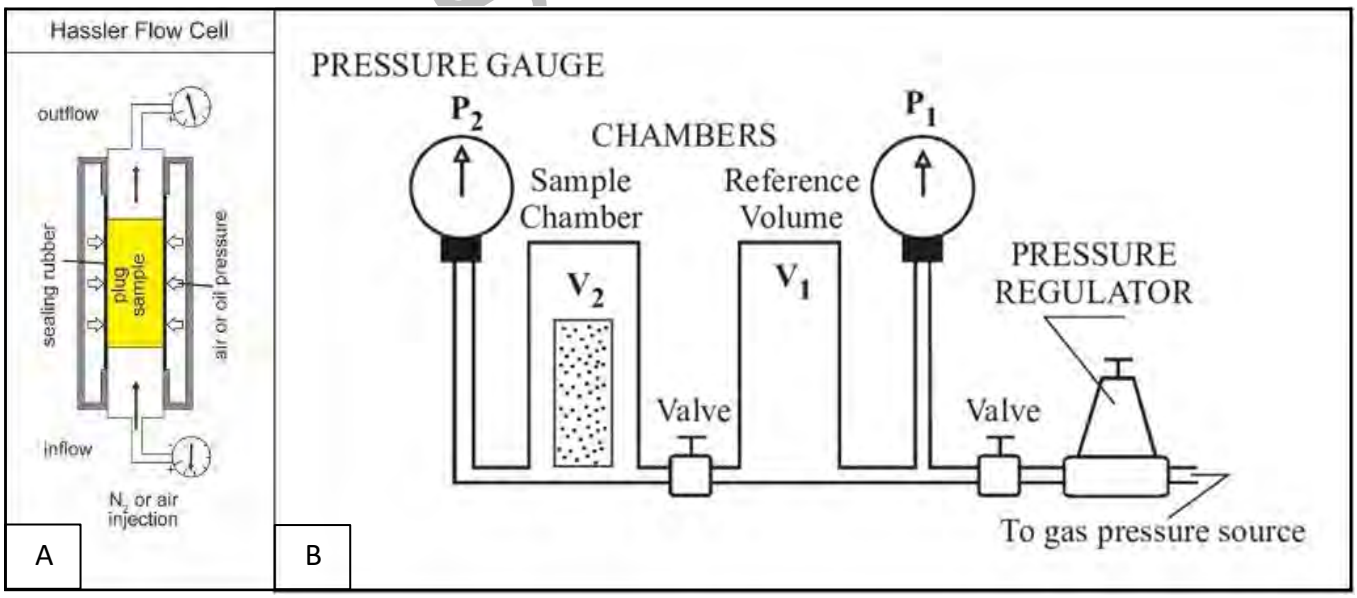


Fig 3.2: (A) showing Air Permeameter apparatus (Filomena et al., 2014), (B) Helium Porosimeter by (Torsæter & Abtahi, 2003).

### 3.4 Source rock evaluation

#### 3.4.1 Sample preparation

To find out the source rock potential the samples are prepared and run in the lab as follow:

1. To find TOC, initially the sample is grinded and meshed up to 2 mm.
2. The grinded powered samples are stored low temperature about $4^0$C.
3. In case of dry combustion techniques samples generally involves the removal of interferents or water while passing through the system with the help of sorbent. Excessive can be removed simply by air drying or oven drying usually at 130ºC.
4. If water is not removed, it tends to form carbon dioxide and can't differentiate between organic and inorganic derived carbon dioxide. Test done to find out if carbonates are present by the addition of acid (i.e., few drops of HCL) and observing if the sample shows effervescences. If inorganic particles are present, they are removed by the acid treatment.
5. The Manganese dioxide and sulfuric acid minimize the decarboxylation and oxidation by the addition of ferrous sulphate to the sample (Allison, 1960). The iron and chromium cause error in finding the TOC content and in the Manganese dioxide which is over and underestimation respectively (Schumacher et. al., 1995). These unwanted materials ($Fe^{2+}$) are removed with the help of oxidation and treatment of sample with $FeSO_4$ in case of excess of $MnO_2$.

#### 3.4.2 TOC measurements

The grinded and dried samples are neutralized with distilled water and dried again to remove the left-over water. Thee recorded weight samples are subjected in the crucible for analysis along with standard and blank for analysis. Prepared sediments were combusted at 1450ºC in the vicinity of oxygen containing atmosphere resulting to $CO_2$ which calculated to determine the organic richness.

It is calculated parameter rather than direct measurement by using the following equation.

$$TOC\ (wt.\%) = [0.082(S1 + S2) + S4] /10$$

#### 3.4.3 Rock Eval Pyrolysis

The Analytical method widely used in oil industries and many research institutes for the estimation of maturity and hydrocarbon generation potential (Peters, 1986). For the quantity, the nature of kerogen type and thermal maturity is given by this conventional

technique. This technique is primarily developed for detail investigations associated natural organic content present within the sediments.

Two peaks of hydrocarbons which is well defined as a function of temperature during pyrolysis $S_1$ first peak and S2 second peak. The earlier is signifying to free hydrocarbons and the later signify to thermal cracking of kerogen at 300-500ºC (Espitalié et al., 1977). According to Espitalié measuring of bitumen contents is the ($S_1$) and measuring of the insoluble kerogen content of the rock is ($S_2$), which is obtained by pyrolysis of kerogen. Production Index is represented by $S_1/[S_1 + S_2]$ which is the transformation of kerogen into oil. The temperature (Tmax) at which maximum hydrocarbon ($S_2$) is generated upon thermal heating. (HI) stands for Hydrogen Index is used for characterization of the type of kerogen and its origination. It is represented by the formula ($S_2$/organic carbon). Third peak ($S_{3)}$ represents the amount of $CO_2$ remained trapped in the sample. The detail of rock eval pyrolysis under controlled heating is shown in (Fig. 3.3).

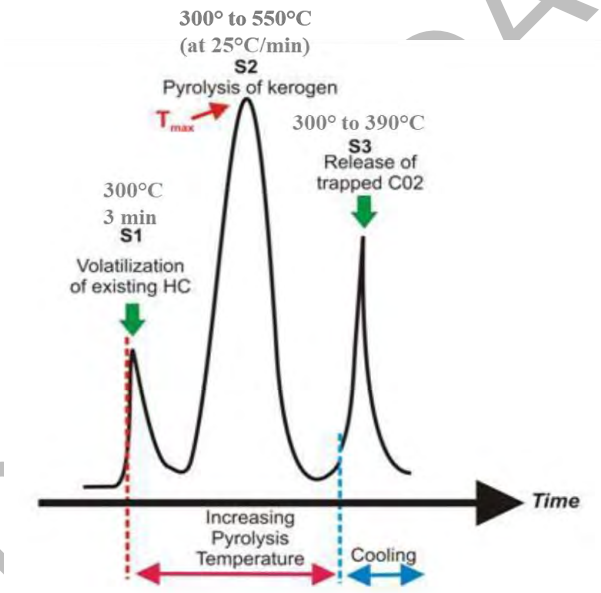


Fig 3.3: shows Rock-Eval pyrolysis parameters for source rock potential evaluation under controlled heating (Kamali and Rezaee, 2012).

## CHAPTER 4

# FIELD OBERSERVATION

The geological field is conducted at DG cement factory section and Zindapir section of Pirkoh Formation in Zindapir Anticline of eastern Sulaiman province, Dera Ghazi Khan. Total section 36 samples were from two detail measured sections to study faunal assemblage and diagenetic overprints.

### 4.1 DG Cement factory section

The Cement factory section of Pirkoh Formation at geographic coordinates (30°19'59.04"N and 70°29'30.14"E) is measure with total thickness of 18 meter. The contact of Pirkoh Formation with Drazinda Formation is buried under the overlain eroded materials (Fig. 3.1 A) and shows conformable contact with Domanda Formation (Fig. 4.1 B). In the DG cement factory section, the Pirkoh Formation in field work is divided into three units based on bedding size, and fauna assemblages at field scale. In DG cement factory section, the Pirkoh Formation show lower part as thick bedded limestone unit consisting of thick limestone bedding with shale intercalated (Fig. 3.2 A). In the middle unit it displays medium to thin bedded limestone unit consist with shale intercalations. While in the part of Pirkoh Formation medium bedded planktic foraminifera rich limestone bedding consist of thin shale intercalations. The Pirkoh Formation in DG cement factory section display fractures in the upper unit (Fig. 4.1 E), and the marine shale in distributed throughout the Formation (Fig. 4.1 A, C, D). It highly fossiliferous made of large benthic foraminifera nummulites, discocyclina, operculina, orthophragmina in the lower and middle units, while the lower units display planktonic foraminifera (Fig. 4.1 F-M).



### 4.2 Zindapir section

The Zindapir section of Pirkoh Formation at geographic coordinates (30°24'48.81"N and 70°30'50.32"E) is measured with total thickness of 9 meters. In Zindapir section, the Pirkoh Formation display transitional contact with Drazinda Formation and conformable contact with Domanda Formation (Fig. 4.2 B). In Zindapir section, the Pirkoh Formation is divided into three divisible units based on the appearance, bedding style, and fauna assemblage. The Lower unit is thick bedded Nummulitic limestone unit consist of massive bedding and highly fractured (Fig. 4.2 A, E). In the middle unit of the Pirkoh Formation display thin to medium bedding, highly fossiliferous and display shale intercalation, while the upper unit is medium bedded rich in planktonic foraminifera consisting of vertical oriented well exposed beds (Fig. 4.2 A, C).

The larger benthic foraminifera majorly consist of Bioclasts of reword biota and well preserved large flat discocyclinidea and nummulitids (Fig. 4.2 D-K)


Fig 4.3: (A) mosaic view of Pirkoh Formation in DG cement factory section, (B) contact Pirkoh and Domanda Formation, (c) lower thick bedded and middle thin to medium bedded units, (D) marine shale, (E) fracturing of lower unit, (F-M) bioclasts and shallow benthic foraminifera, (N) organic rich shale in the lower unit of Pirkoh Formation.

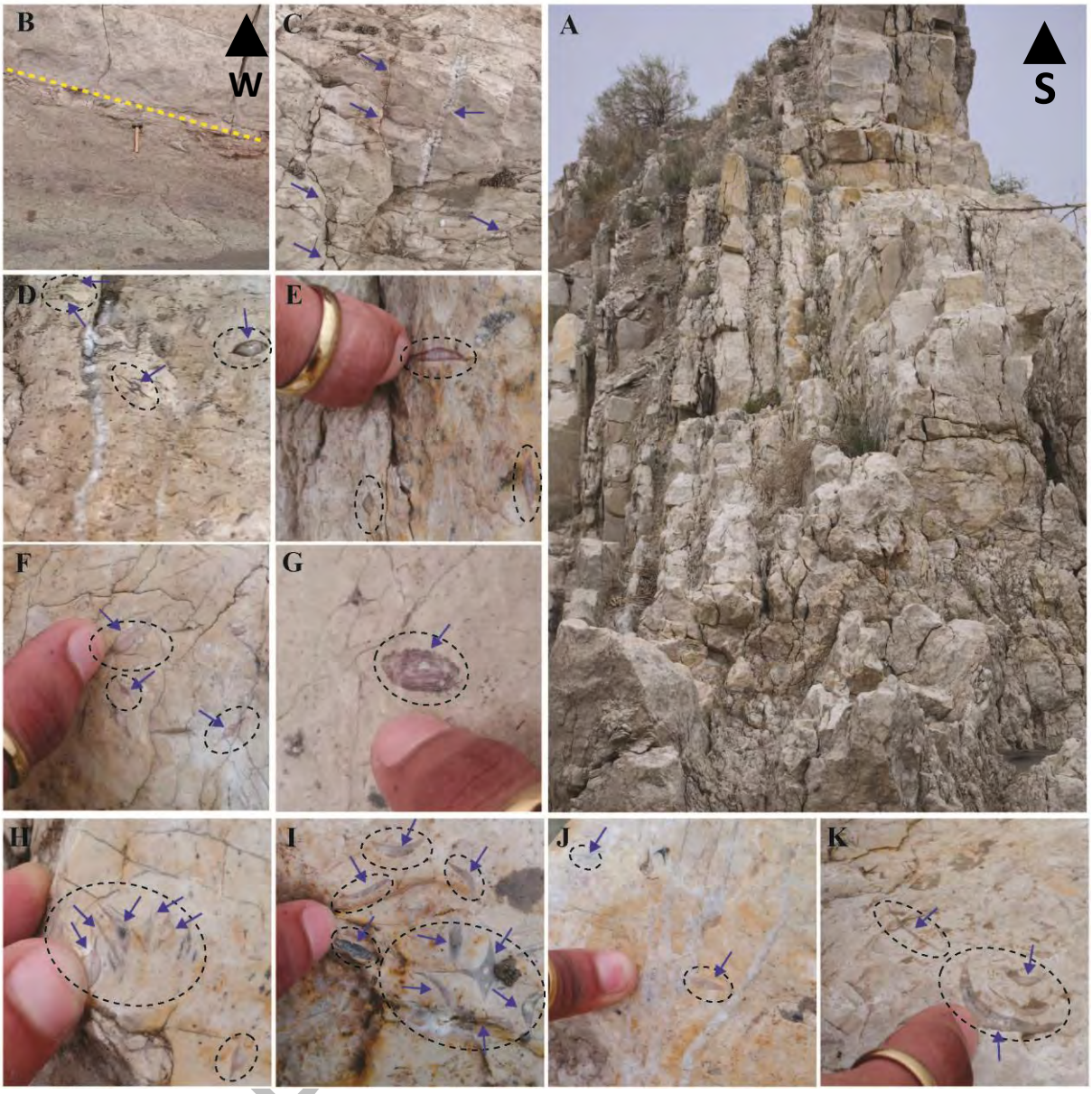


Fig 4.4: (A) showing mosaic view of Pirkoh Formation, (B) shows contact of Pirkoh and Drazinda Formation, (C, J, & O) shows factures and calcite fill veins (D-K) shows bioclasts and shallow benthic foraminifera.

**CHAPTER 5**

# MICROFACIES ANALYSES

## 5.1 Introduction

Brown (1943) and Cuvillier (1952) stated the word "microfacies" to microscopic identifications in thin sections. Though, nowadays microfacies is stated by Flügel, 2010 as, *"the total of all sedimentological and paleontological data which can be described and classified from thin sections, peels, polished slabs or rock samples".*

The microfacies analyses of carbonate rocks are very fundamental to determine the depositional environment to explore the carbonate platform. The petrographic studies with field lithofacies determine the depositional pattern of carbonate rocks. The carbonate rock classification introduced by Dunham (1962), is applied to categorize the textural attribute of rock units, and the paleontological parameters are further integrated with textural characteristics to develop the depositional environment.

## 5.2 Microfacies analyses of Pirkoh Formation

The microfacies analyses of Pirkoh Formation is studied in detail based on relative composition of carbonate rocks fundamental components. The percentage of allochemical components is determined based on point counting, in which total 200 grids were plotted on thin section slab and high resolution 4k images were studied on JMicroVision software. The relative percentage of each components classified the microfacies of Pirkoh Formation into total fifteen microfacies (MF1-MF15), which is further categorized into 3 facies assemblages based on their depositional setting i.e., 1) Inner (MF1-7), 2) middle (MF8-9) and 3) outer shelf (MF10-15).



### 5.2.1 Inner shelf environment

#### 5.2.1.1 Dolomitic lime mudstone (MF-1)

The dolomitic lime mudstone is present in the lower part of the Pirkoh Formation in DG cement factory section. This facie is overlain by bioclastic wackestone and underlain by orthophragminid nummulitid floatstone (Fig. 5.16). In the exposed outcrop, this facie attains thickness of 1.2 m at the lower part Formation and appear as pale-yellow medium bedded limestone. In the field at outcrop scale, it is slightly fractured (Fig. 4.1). The petrographic studies of this facie describe dolomicrite and very minor planktonic foraminifera. The dolomite rhombs show very fine anhedral crystal and a few fine grained well developed euhedral texture (Fig. 5.1 A-D).

***Interpretation:*** The dolomitic lime mudstone is interpreted to have been deposited in low energy restricted tidal flat environment of inner shelf setting. The low content of planktonic foraminifera indicates the depositional environment restricted lagoon to tidal environment and overall peritidal environment. Moreover, the presence of dolomite rhombs embedded in micritic matrix (dolomicrite) and indicates early diagenetic stage dolomitization in a peritidal environment (Tucker and Wright, 1990; Wanas, 2008). In addition, the lime texture further signifies in low energy restricted tidal flat environment of peritidal environment. It is equivalent to SMF23 and FZ8 (Wilson, 1975).

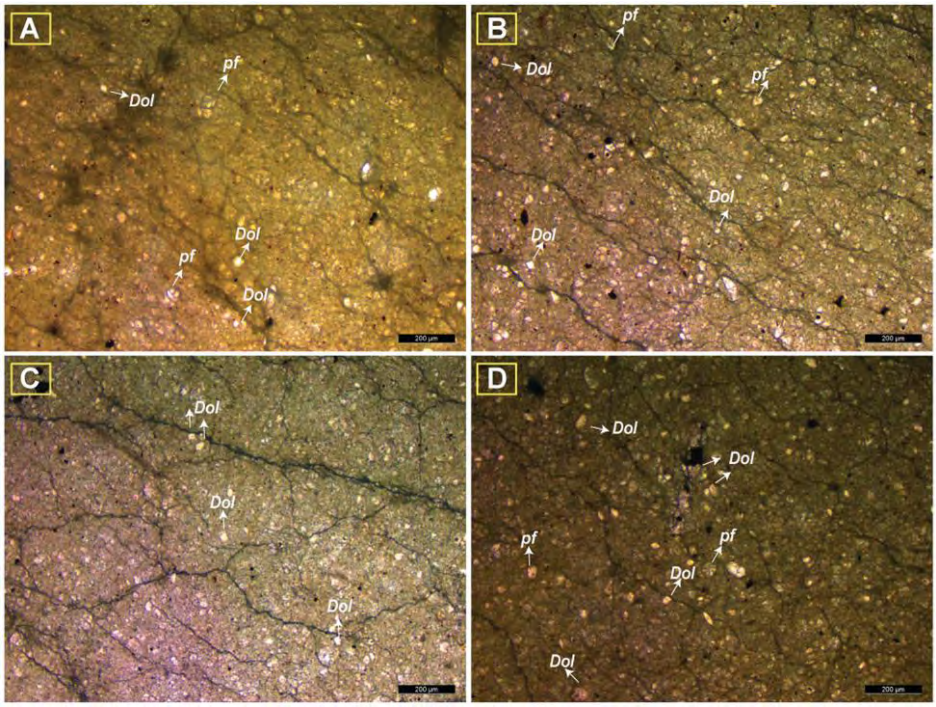


Fig 5.2: shows dolomitic lime mudstone (MF-1), (A-D) display the dolomite rhombs (*Dol*) are shown with arrows, (A, B, and D) planktonic foraminifera (*pf*).

### 5.2.1.2 Bioclastic wackestone (MF-2)

The bioclastic wackestone is represent in the lower part of the Pirkoh Formation in DG cement factory section. It is overlain by austrotrillina nummulitid bioclastic packstone and underlain by dolomitic lime mudstone (Fig. 5.16). In the exposed outcrop, this facie attains thickness of 1.3m at the lower part as medium bedded and display thin bedded shale intercalation in lower middle part of the Formation where the bed thickness is varying between 0.3-0.5 meters. It appears as light yellowish grey in color. In the field at outcrop scale, it is slightly fractured (Fig. 4.1). The petrographic studies of this facie describe the bioclasts (10-15%) as main skeletal component (includes broken fragments of shallow benthic foraminifera i.e., fragments of coralline algae, operculinoides, nummulites, transported hetrostegina,

cycloclypeus, lepidocyclinids discocyclinids, and asterocyclinids embedded in micritic matrix (Fig. 5.2 A-D).

**Interpretation:** The broken fragments of pelecypods as well as other shallow/larger benthic foraminifera indicate open lagoon with well circulation and well oxygenated regime (Wilson, 1975; Flügel, 2010). Contrary, the restricted lagoons are characterized by planktic foraminifera and smaller miliolids, which are not significant in this facie, thus the most probable depositional setting of open lagoonal environment.

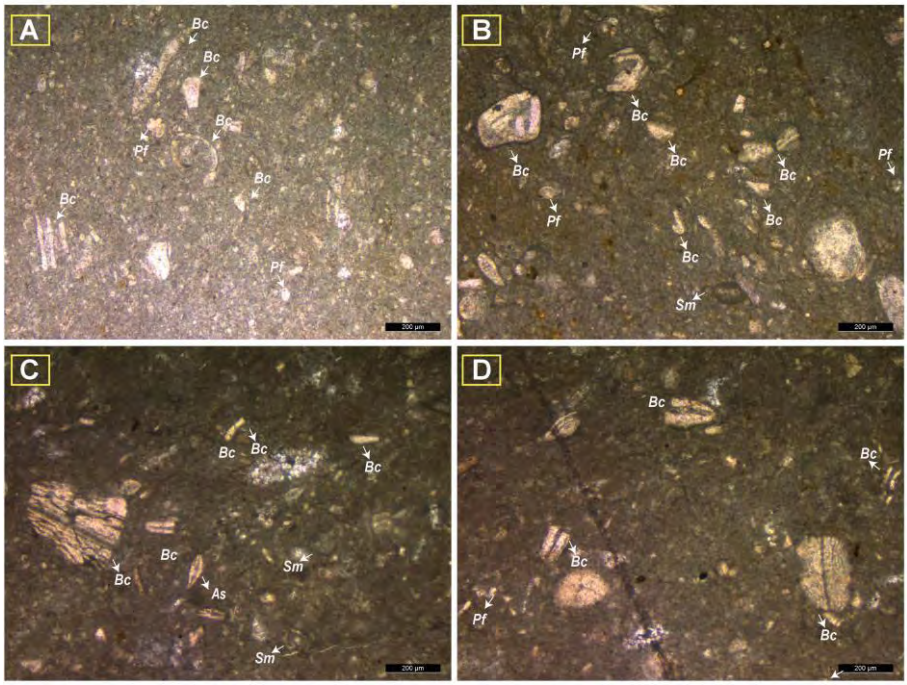


Fig 5.3: shows bioclastic wackestone (MF-2), (A-D) showing planktonic foraminifera (*pf*) reworked bioclast (*Bc*) of shallow benthic foraminifera majorly reworked nummulites, operculina, and orthophragminids, (C) showing assilina (*As*) and smaller miliolid (*Sm*).

### 5.2.1.3 Austrotrillina nummulitid bioclastic packstone (MF-3)

The austrotrillina nummulitid bioclastic packstone is present in the lower part of the Pirkoh Formation in DG cement factory section. It is overlain by contact with Domanda Formation and underlain by bioclastic wackestone microfacie (Fig. 5.16). In the exposed outcrop, this facie attains thickness of 3 m at the bottom of the Formation and 1 m and 2 m shale intercalated limestone. In the field at outcrop scale, it appears as thick bedded brecciated and highly fractured with light grey color appearance (Fig. 4.1). The petrographic studies of this facie describe the bioclasts (20-25%) as main skeletal component. The bioclasts are broken fragments of nummulites, operculina, assilina, bryozoan fragments. The only nummulites specie includes Nummulites *aturicus* (Fig. 5.3 A-B), while the other minor components include Operculina (Fig 5.3 A), Lockhartia *pustulosa*, Assilina *leymerie* (Fig 5.3 D) and miogypsinds

(10–15%) shown in (Fig. 5.3) This facie also displays green algae and well-preserved Caroline algae. The allochemical components are embedded in micrite matrix, in places minor fractures are observed and blocky calcite replaced the original aragonitic composition in the skeletal component.

***Interpretation:*** The relative abundance of austrotrillina is typical of back reef depositional environment with low hydrodynamic energy. Moreover, the genus austrotrillina most likely dependent on symbiotic relationship with algae. Thus, the presence of austrotrillina with well-preserved coralline algae signify to back- reefs (Fadel, 2018). Furthermore, the association of orbitolites and miogypsinds together with coralline algae and austrotrillina also support the back reef depositional (Fadel, 2018), while the other Nummulitid i.e., Operculina, nummulites and assilina indicates shallow and warm water condition (Wanas et al., 2020; Arni, 1965; Blondeau, 1972), and the presence of coralline algae along with shallow water biota further signify to proximal part of back reef shelf environment (Fadel, 2018).

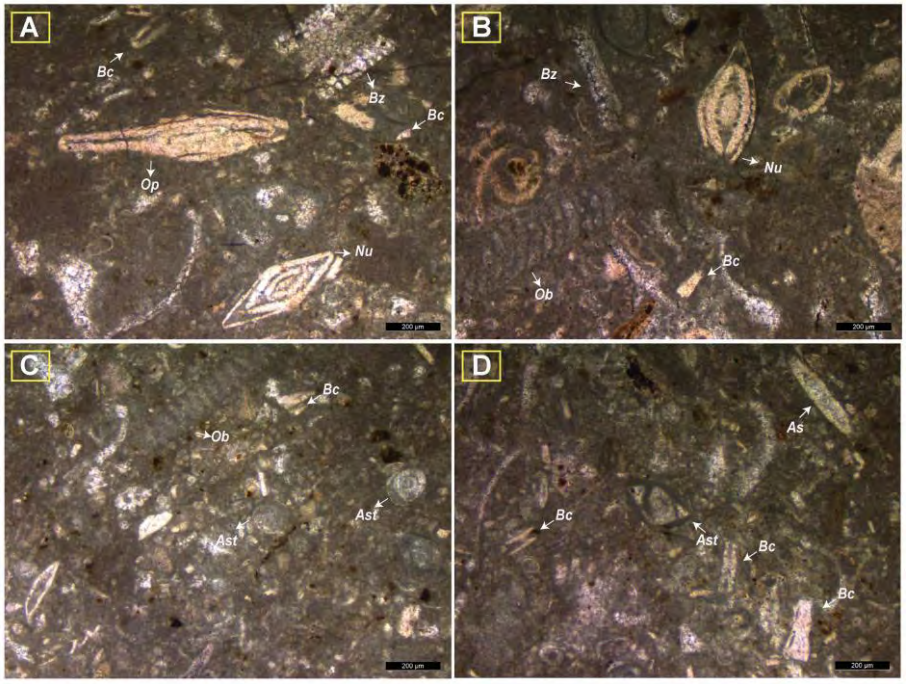


Fig 5.4: shows austrotrillina nummulitid bioclastic packstone (MF-3). operculina (*Op*) is shown in (A), Nummulites (*Nu*) are shown in (A, B) bioclasts. (*Bc*) are shown in (A-D), orbitolites (*Ob*) are shown in (B, C), austrotrillina (*Ast*) shown in (C, D) and assilina (*As*) is shown in (D).

### 5.2.1.4 Discocyclina nummulitic operculine bioclastic packstone (MF-4)

The discocyclina nummulitic operculine bioclastic packstone is present in the lower part of the Zindapir section of Pirkoh Formation (Fig. 4.2). This facie is overlain is by nummulitic operculine wackestone and underlain by bioclastic discocyclina floatstone (Fig.

5.17). In the exposed outcrop, this attains thickness of 1.7 m, and appear as medium bedded limestone, with light pale yellowish color. The petrographic studies of this facie describe the bioclasts as main skeletal component, which includes broken fragments of bryozoans, assilina, mollusks and other larger benthic foraminifera (15-25%). The species includes nummulites *bagelensis*, discocyclina *silla*, assilina species includes assilina *exponens*, assilina *leymerie*, the operculina species includes operculina *subsalsa* (show spins), and operculina *salsa* (no spines), and milioline genus austrotrillina, while the other contents include green algae linderina *schlumberger*, orbitolites, amphistigina, triloculina *trigonula,* and miogypsinds. The allochemical components are embedded in micritic matrix, also comprising patches of sparry calcite (Fig. 5.4).

***Interpretation:*** It is interpreted to be deposited on the reef patch based on the association of larger benthic foraminifera such as nummulites found together in association with operculina, discocyclina and assilina species (Aigner, 1983; Geel, 2000; Wanas et al., 2020). Moreover, it has diversity of larger benthic foraminifera of forereef shelf as well as backreef shelf along with abundant reworked bioclasts. The nummulites, operculina and cycloclypeus are typical of forereef shelf to reef patch indicators, while the orbitolites and austrotrillina indicates backreef shelf to reef patch. While the presence of discocyclina indicates a wide range of inner shelf. Overall, based on the biota assemblage this facie indicates reef patch depositional environment.

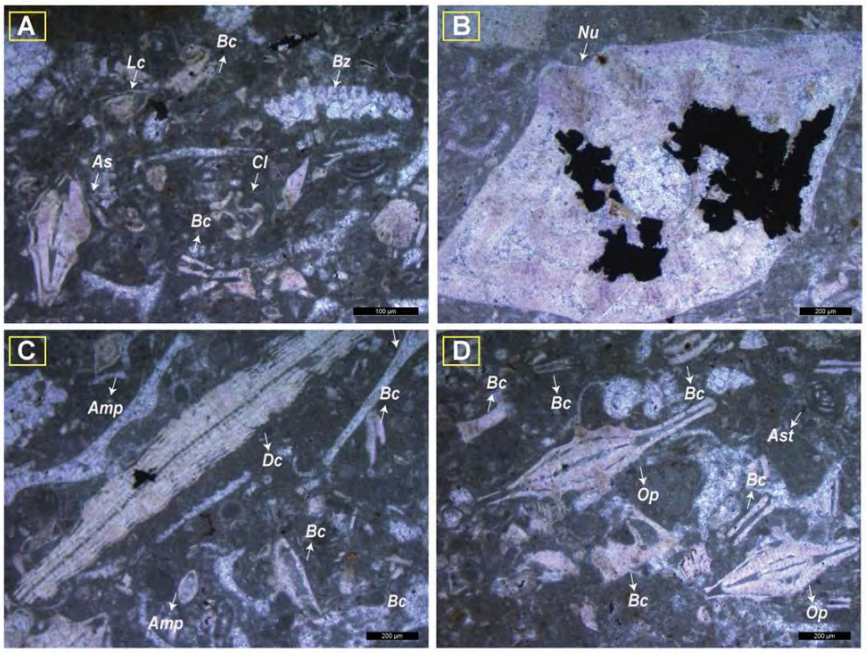


Fig 5.4: (A-D) shows discocyclina nummulitic operculine bioclastic packstone (MF-4). The figure display lockhartia (*Lc*), assilina (*As*), bioclasts (*Bc*), bryozoans (*Bz*), Coral (*Cl*), Nummulites (*Nu*), amphistigina (*Amp*). discocyclina (*Dc*), operculina (*Op*), austrotrillina (Ast).

#### 5.2.1.5 Bioclastic discocyclina floatstone (MF-5)

The bioclastic discocyclina floatstone microfacie is represent in the lower part of the Pirkoh Formation. This facie is overlain is by discocyclina nummulitic operculine bioclastic packstone and underlain by nummulitid orthophragminid rudstone (Fig. 5.17). In the exposed outcrop, this attains thickness of 0.4 m, and appear as light pale yellowish. The petrographic studies of this facie describe the presence of minor scattered bioclasts, amphistegina, and discocyclina *discus* (Fig. 5.5). The allochemical components are embedded in micritic matrix, also comprising patches of sparry calcite and calcite veins filled with blocky calcites and display scattered well-developed dolomite rhombs.

***Interpretation**:* The association amphistegina with discocyclina is typical of fore reef environment (Fadel, 2018; Asis and Jasin, 2015; Yazdi et al., 2021). The broken fragments signify high energy, while the well preserved autochthonous amphistegina, which is symbiotically dependent in shallow water about 70-80 m. Thus, it indicates the proximal fore shelf depositional setting on inner shelf (Branstätter, 1993, Yazdi et al., 2021).

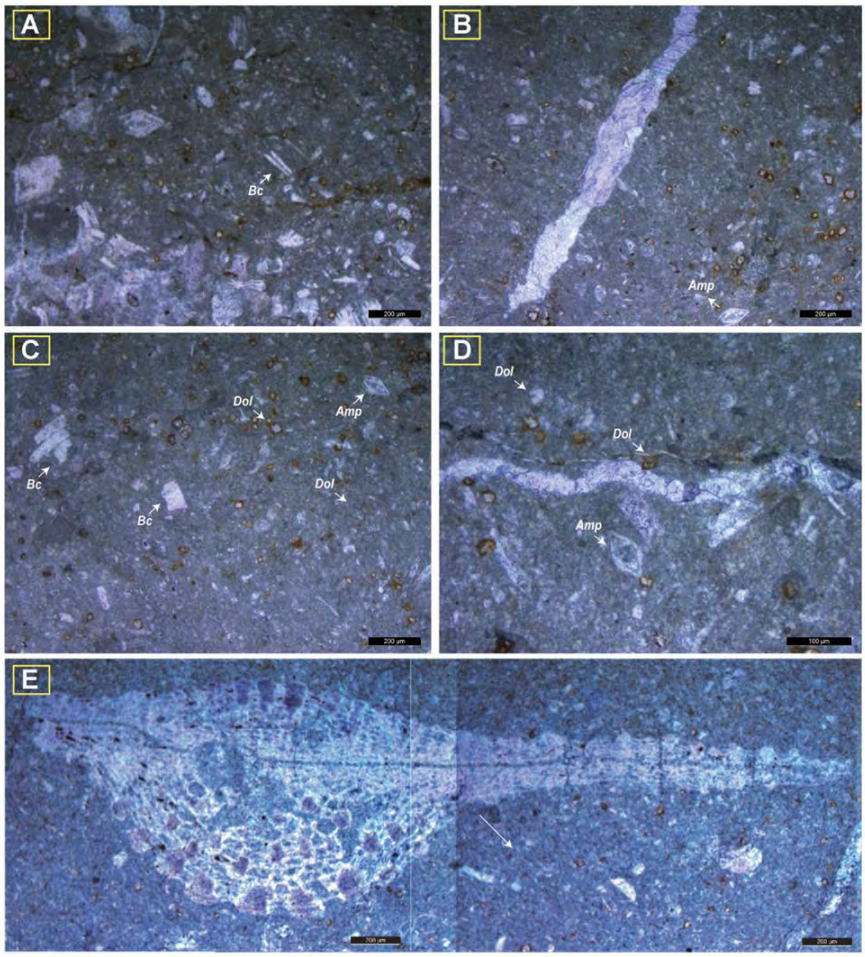


Fig 5.5: shows bioclastic discocyclina floatstone (MF-5). The figure display bioclasts (*Bc*), dolomite (*Dol*), amphistigina (*Amp*), and discocyclina discus.

### 5.2.1.6 Orthophragminid nummulitid floatstone (MF-6)

The orthophragminid nummulitid floatstone is represent terminal part of lower part of the Pirkoh Formation in DG cement factory section. This facie is overlain by dolomitic lime mudstone and underlain by the shale intercalated medium beds of bioclastic wackestone (Fig. 5.16). In the exposed outcrop, this facie attains thickness of 1.3 and appear as thick grey medium bedded limestone (Fig. 4.1). The petrographic studies of this facie describe the nummulitids (15-25%) as main skeletal components, which includes autochthonous nummulites, operculina, and assilina. The orthophragminid (Discocylina) species includes D. *Dispansa*, D. *Sulaimanensis*, broken fragments of D. *Kutchensis* about (5-10%) shown in (Fig.

5.6). This facie also displays amphistegina, cycloclypeus, and other minor components, that includes reef derived bivalve, coralline algae, minor bryozoans and allochthonous bioclasts. The skeletal components are embedded in micritic matrix in which the larger skeletal components are floating as coarse grained skeletal grains. In places, the minor fractures are observed along which dolomitization take place.

***Interpretation:*** The association operculina, cycloclypeus, and nummulites species along with Hetrostegina are typical of fore reef environment (Fadel, 2018), and the co-occurrence of amphistegina with discocylina further support forereef shelf depositional environment (Asis and Jasin, 2015; Yazdi et al., 2021). The broken fragments signify high energy, while the well preserved autochthonous amphistegina indiactes shallow water depth about (70-80 m) which symbiotically with other large/shallow benthic foraminifera and coralline algae, which specifically indicates the proximal fore shelf depositional setting (Rögl and Branstätter 1993, Miogysina paper). The shallow and proximal part of fore-reef shelf is also evident from the nummulites co-occurrence, which signifies neritic zone of shallow and warm water condition (Wanas et al., 2020; Arni, 1965; Blondeau, 1972). The assemblage of biota i.e., association of nummulite, operculina and discocylina species together indicates the deposition in banks setting of fore-reef shelf deposits (Wanas et al., 2020; Arni, 1965; Arni and Lanterno, 1972; Khalifa and Zaghloul, 1990).

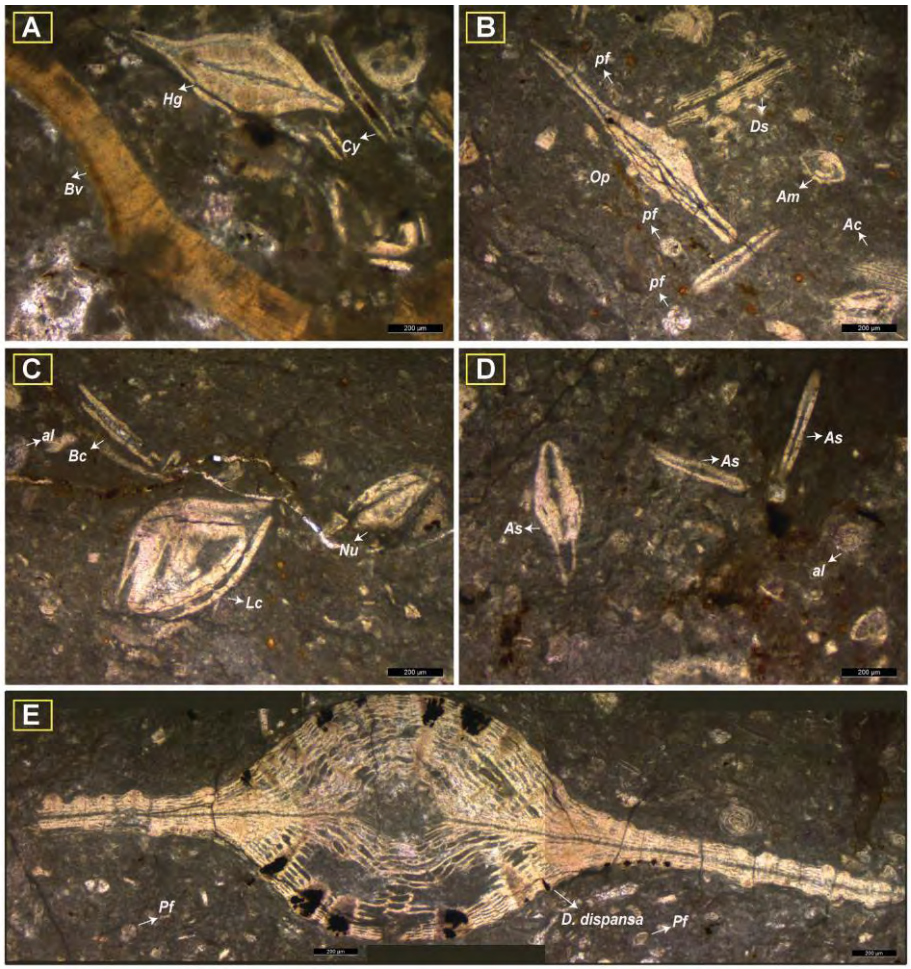


Fig 5.6: shows orthophragminid nummulitid floatstone (MF-6). The figure show heterostegina (*Hg*), bivalves (*Bi*) broken fragment of discocyclina (*Ds*), amphistigina (*Am*), algae (*al*). lockhartia (*Lc*), nummulites (*Nu*), assilina (*As*), planktonic foraminifera.

### 5.2.1.7 Nummulitic operculine wackestone (MF-7)

The nummulitic operculine wackestone is represent in the lower part of the Pirkoh Formation. This facie is overlain by contact with Domanda Formation and underlain by discocyclina nummulitic operculine bioclastic packstone (Fig. 5.17). In the exposed outcrop, this facie attains thickness of 1.5 m, and appear as light yellowish grey to pale white thick bedded limestone (Fig. 4.2). The petrographic studies of this facie describe the nummulites as main skeletal component species includes nummulite *sp.* (20 %) operculina *sp*. (10-15%) and minor assilina *sp*. (2-5%). Nummulite species includes nummulites *mamilla*, nummulites *aturicus*, operculina species includes only operculina *complanate*. It also exhabits lockhartia *pustulosa* rarely seen with assilina *leymerie*. The allochemical components are embedded in micritic matrix, also comprising patches of sparry calcite, and in places scattered well-developed dolomite rhombs shown in (Fig. 5.7).

***Interpretation:*** The presence of Nummulites signifies neritic zone of shallow and warm water condition (Wanas et al., 2020; Arni, 1965; Blondeau, 1972). The assemblage of biota i.e., association of nummulites, operculina and discocyclina species together indicates the deposition on banks setting of forereef shelf (Wanas et al., 2020; Arni, 1965; Arni and Lanterno, 1972; Khalifa and Zaghloul, 1990). The presence of textularia specie indicates shallow and warm water condition (Alabere et al., 2020), while the co-occurrence of Lokhartia signify to restricted conditions with low water turbulence conditions (Adabi et al., 2008; Beavington-penny, 2006), which is also supported by the wackestone texture. The sum of all imply the deposition on the distal part of fore reef shelf environment.

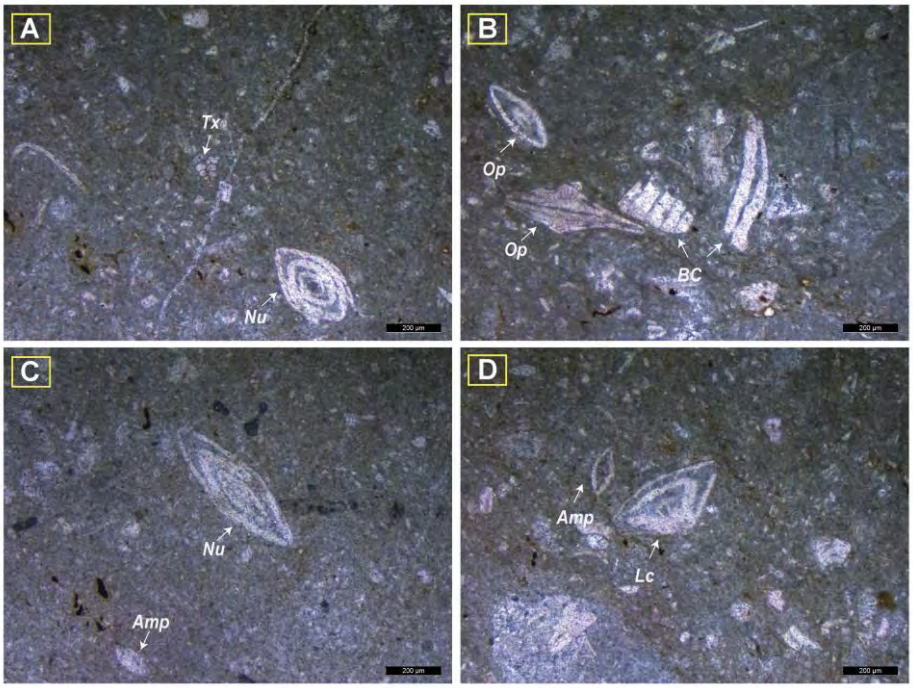


Fig 5.7: shows nummulitic operculine wackestone microfacie (MF-7). The figure shows Nummulites (*Nu*) operculina (*Op*), bioclasts (*Bc*), amphistegina (*Amp*) and lockhartia (*Lc*).

### 5.2.2 Middle shelf environment

#### 5.2.2.1 Bioclastic planktonic foraminiferal lime mudstone (MF-8)

The bioclastic planktonic foraminiferal lime mudstone is represent in the middle part of the Pirkoh Formation (Fig. 4.2). This facie is underlain is by nummulitid orthophragminid rudstone and overlain by Echinoid Operculine planktonic foraminiferal (Fig. 5.17). In the exposed outcrop, this attains thickness of 0.3 m, and appear as grey thin bedded limestone. The petrographic studies of this facie describe planktic foraminifera assemblage about 5 % embedded in dominate lime muddy matrix shown in (Fig. 5.8).

***Interpretation:*** The low Planktonic foraminiferal assemblage embedded in micritic sediments indicates the deposition on middle-shelf setting of proximal open marine environment with very low energy conditions (Wilson, 1975). The abundance of micritic sediments further signify to low energy environment and calm setting deposition (Wilson, 1975; Burchette and Wright, 1992).

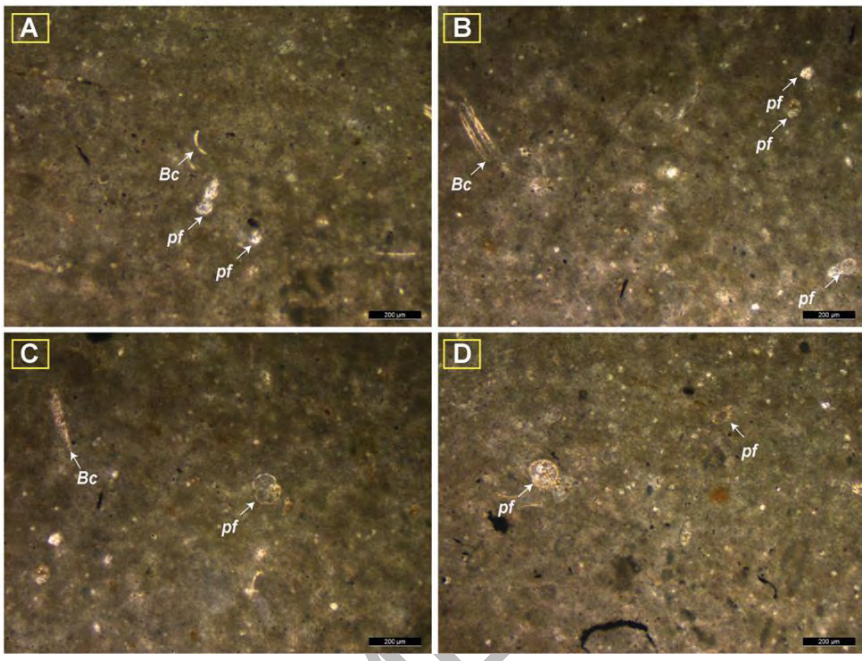


Fig 5.8: shows bioclastic planktonic foraminiferal lime mudstone (MF-9).



**5.2.2.2 Lepidocyclinid orthophragminid planktonic foraminiferal lime mudstone (MF-9)**

The lepidocyclinid orthophragminid planktonic foraminiferal lime mudstone is presenting upper part of the Pirkoh Formation in DG cement factory section. This facie is overlain bioclastic planktonic foraminiferal lime mudstone and underlain by echinoid discocylina planktic foraminiferal wackestone (Fig. 5.16). In the exposed outcrop, this facie attains thickness of 1.5m as shale intercalated medium bedded limestone bedding of grey to dark yellow color (Fig. 4.1). The petrographic studies of this microfacie describe the drthophragminids as main skeletal component, species: discocylina *Kutchensis* (Fig. 5.9 A), asterocyclina *sireli* (Fig. 5.9 B), while lepidocyclina specie includes eulepidina *elephantina* shown in (Fig. 5.9 B). This facie also comprises of large flat nummulites and open planktonic foraminifera, and other minor content includes reworked and transported fragments and nummulites and orthophragminids.

***Interpretation:*** The least abundance of planktonic foraminifera and its association with flat lepidocyclinids nummulitids symbolizes deeper oligophotic zone in the middle shelf open marine depositional environment of (Taheri et al., 2016). The dominancy of micrite, and large flag well preserved lepidocyclinids and orthophragminids signify to calm and low energy condition of open shelf condition (Sirotti, 1978; Fermont, 1982; Buxton and Pedley, 1989; Eichenseer and Luterbacher, 1992; Sinclair & Tucker, 1998; Racey et al., 2001; Penney and Racey, 2004; Cosovic et al., 2004; Beavington-Penney et al., 2006; Isvand et al., 2022).

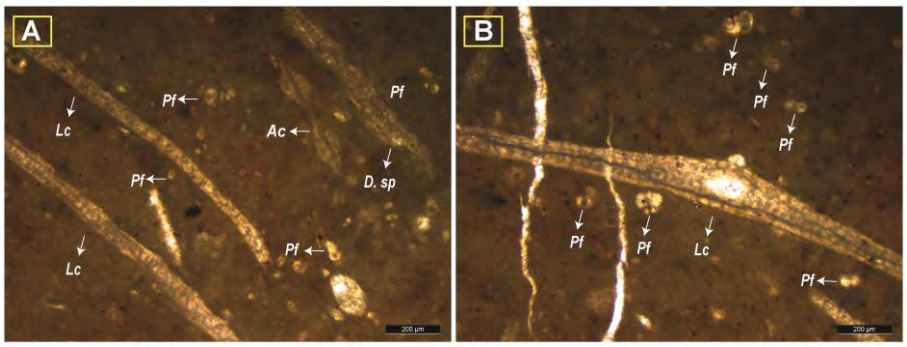


Fig 5.9: shows lepidocyclinid orthophragminid planktonic foraminiferal lime mudstone (MF-10). The figure shows planktonic foraminifera (*pf*), asterocyclina (*Ac*), discocyclina spp, lepidocyclina *eulepidina elephantina* (*Lc*).

### 5.2.3 Outer shelf environment

#### 5.2.3.1 Dolomitized Orthophragminid floatstone (MF-10)

The Dolomitized Orthophragminid floatstone microfacie is represent terminal part of middle part of the Pirkoh Formation in DG cement factory section. This facie is overlain bioclastic wackestone and underlain austrotrillina nummulitid bioclastic packstone (Fig. 5.16). In the exposed outcrop, this facie attains thickness of 0.4m and as appear as grey color medium to thick bedded limestone (Fig. 4.1). The petrographic studies of this microfacie describe the orthophragminids as main skeletal component includes species: discocylina *fortsi*, and D. *Kutcgensis*, and other minor components includes bioclasts, and very minor planktonic foraminifera shown in (Fig.5.10). This facie display dolomitization replaced the skeletal components and scatteredly dolomitized the groundmass. The facie display dolomite rhombs (euhedral to subhedral) and sparry calcites in the micritic matrix.

***Interpretation:*** The abundance of orthophragminids indicates the depositional environment of outer shelf depositional setting (Penney and Racey 2004; Cosovic et al. 2004). The dominancy of micrite, and association of large flat well preserved orthophragminid with planktic foraminifera signify to calm and low energy condition of open shelf condition below the fair-

weather wave base (Sayer & Tucker, 1998; Racey et al., 2001; Penney and Racey, 2004; Cosovic et al., 2004; Penney et al., 2006).

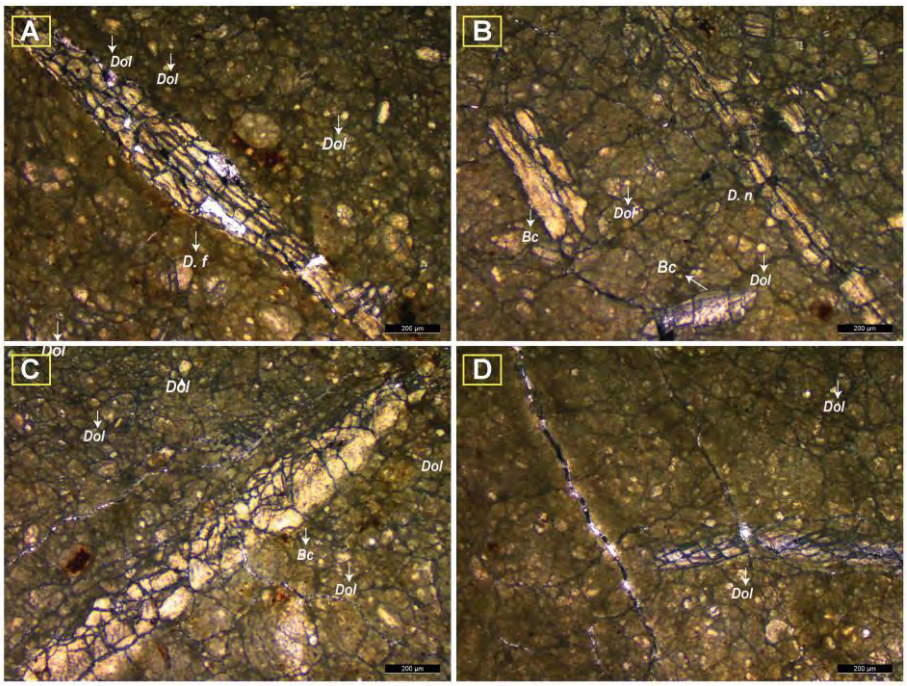


Fig 5.10: shows dolomitized orthophragminid floatstone (MF-10). The figure show dolomite (*Dol*), discocyclina fortisii, bioclasts (*Bc*), and discocyclina nandoroi (*D. n*).

### 5.2.3.2 Echinoid discocylina planktic foraminiferal wackestone (MF-11)

The Echinoid discocylina planktic foraminiferal wackestone is presenting upper part of the Pirkoh Formation in DG cement factory section. This facie is overlain lepidocyclinid orthophragminid planktonic foraminiferal lime mudstone and underlain by Planktic foraminiferal wackestone (Fig. 5.16). In the exposed outcrop, this microfacie attains thickness of 0.7 m and appear as grey color shale intercalated medium bedded of limestone (Fig. 4,1). The petrographic studies describe the Planktic *Foraminifera* as main skeletal component with echinoids fragments and discocylina (specie: D. Nandori) embedded in micritic matrix (Fig. 5.11).

***Interpretation:*** The extensive existence of echinoid fragments (10-15%) indicates the outer shelf of open marine deposition setting (Flügel, 2013). The packstone texture of planktonic foraminifera (15-20%) is typical indication of a low energy condition in outer shelf, open marine setting (Harris et al., 1997). The low energy condition is also evident from the occurrence of large flat discocylina in micritic matrix (Racey et al., 2001; Beavington-Penney and Racey, 2004; Cosovic et al., 2004; Beavington-Penney et al., 2006: Isvand et al., 2022).

Moreover, the dominance of planktonic foraminifera implies to deposition of sediments taken place below the fair-weather wave base (Wilson, 1975; Burchette and Wright, 1992).

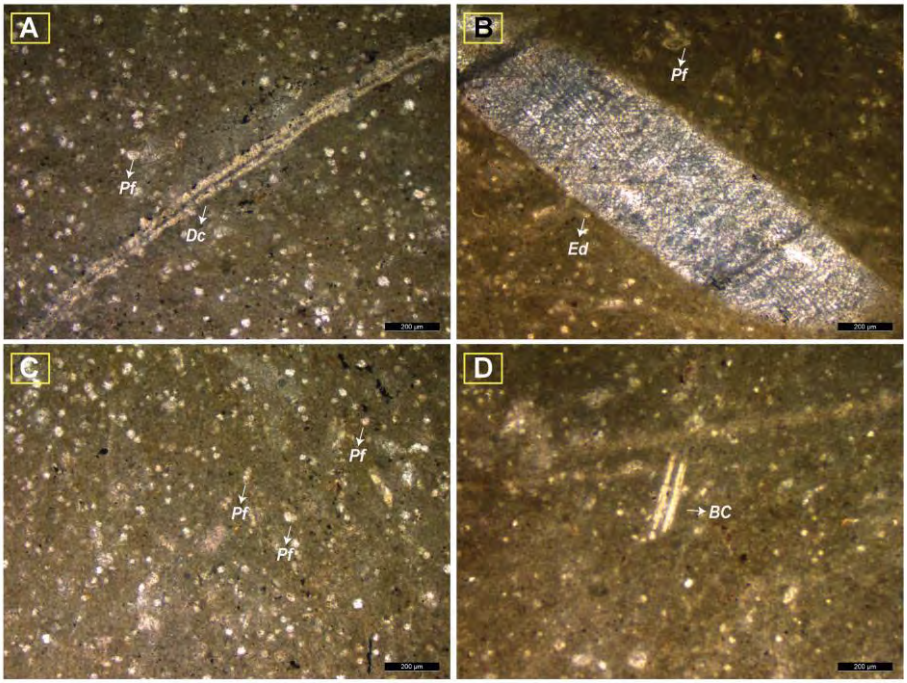


Fig 5.11: shows Echinoid discocylina planktic foraminiferal wackestone (MF-11). The figure shows planktonic foraminifera (*pf*), discocyclina *nandori*. (*Dc*) echinoderm fragment (*Ed*), and bioclasts (*Bc*).



### 5.2.3.3 Nummulitid orthophragminid rudstone (MF-12)

The nummulitid orthophragminid rudstone is present in the middle part of the Pirkoh Formation in Zindapir section (Fig. 4.2). This facie is overlain is by bioclastic discocyclina floatstone and underlain by bioclastic planktonic foraminiferal lime mudstone (Fig. 5.17). In the exposed outcrop section, it attains thickness of 0.75 m, and appear as medium bedded limestone with light grey color. The petrographic studies describe species discocyclina and asterocyclina as main skeletal component (70-80%) shown in (Fig. 5.12). The discocyclina species includes D. *Augustea*, D. *Zindapirensis*, D. *Rakhinalaensis*, D. *Discus*, D. *Silla* and D. *Nandori*, while the Asterocyclina species includes A. *alticostata* and A. *sireli* (Fig. 4.2 A-F). Nummulite about (5-10%), the Nummulites includes species present is N. *aturicus*. The Operculina about (5-10%), the Operculina species includes O. *aegyptiaca* and O. *complanate*, while the Assilina species includes A. *Azilensis*, and A. *laminose*. The planktic foraminifera is also present in this facie about (3-5%). The allochemical components are embedded in dominate micritic matrix.

***Interpretation:*** The abundance and association of orthophragminid (discocyclina and asterocyclina species) indicates the depositional environment of outer shelf depositional setting (Buxton and Pedley 1989; Eichenseer and Luterbacher 1992; Beavington-Penney and Racey 2004; Cosovic et al. 2004). The dominant assemblage of discocyclina as compared to Asterocyclina indicates shallow bathymetry (Less 1987, Nebelsick et al., 2005). The dominancy of micrite, and large flat well preserved orthophragminidae and abundance of planktonic foraminifera signify to calm and low energy condition of open shelf condition below the fair-weather wave base. (Wilson, 1975; Eichenseer and Luterbacher 1992; Sinclair et al., 1998; Racey et al., 2001; Beavington-Penney and Racey 2004; Cosovic et al. 2004; Beavington-Penney et al., 2006).

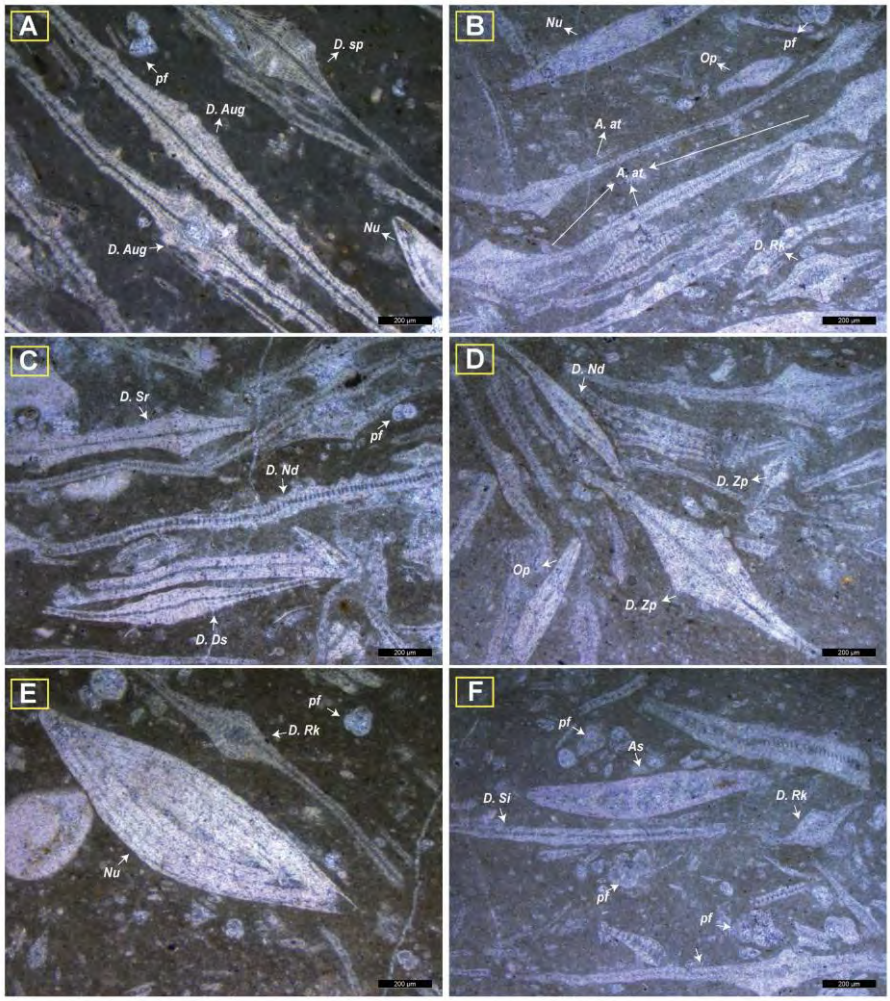


Fig 5.12: shows nummulitid orthophragminid rudstone (MF-12). The figure shows Discocyclina *augustea*, (D. *Aug*), D. *nandori* (D. *Nd*), D. *silla* (D. *Si*), D. *rakhinalaensis* (D. *Rk*), D. *zindapirensis* (D. *Zp*), D. *discus* (D. *Ds*), asterocyclina *alticostata* (A. *at)* and A. *sireli* (*A. sr*).

### 5.2.3.4 Echinoid operculine planktonic foraminiferal packstone (MF-13)

The echinoid operculine planktonic foraminiferal packstone is present in the middle part of the Pirkoh Formation (Fig. 4.2). It is overlain is by planktonic foraminiferal lime mudstone and underlain by planktonic foraminiferal wackestone (Fig. 5.17). In the exposed outcrop, this attains thickness of 0.45 m, and appear as grey thin bedded limestone. The petrographic studies describe abundant planktic foraminifera about 40-50 % embedded muddy matrix (Fig. 5.13). This facie also displays operculina (3-5%) and the echinoid fragments (10-15%) are present showing perforation arranged parallel to the spin long axis.

***Interpretation:*** The extensive existence of echinoid fragments indicates the outer shelf of open marine deposition setting (Flügel, 2013). The packstone texture of planktonic foraminifera is typical indication of a low energy condition in open marine setting (Harris et al. 1997). The association of operculina is allochthonous although it has a wide range of thriving, and less symbiotically dependent on coralline algae. Overall, the dominancy of open marine biota i.e., radiolarians, spicules and planktonic foraminifera indicates low energy environment of open marine environment depositional setting below the storm wave base (Wilson, 1975; Burchette and Wright, 1992).

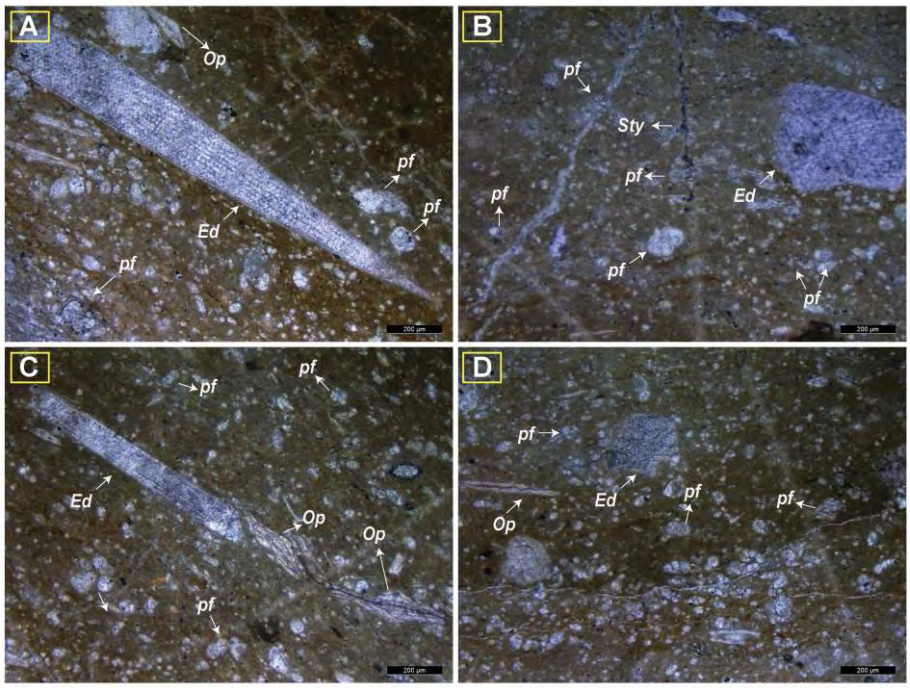


Fig 5.13: shows echinoid operculine planktonic foraminiferal packstone (MF-13). The figure shows echinoderm fragments (*Ed*), planktonic foraminifera (*pf*), and deformed operculina (*Op*).

### 5.2.3.5 Planktonic foraminiferal Wackestone (MF-14)

The planktonic foraminiferal wackestone is present in the upper part of the Pirkoh Formation (Fig. 4.2). It is overlain is by echinoid operculine planktic foraminiferal packstone and underlain by operculine Planktic foraminiferal wackestone (Fig. 5.17). In the exposed outcrop, this attains thickness of 1.2 m, and appear as medium bed of light grey color. The petrographic studies of this facie describe planktic foraminifera assemblage about 15-25 % embedded fine matrix shown in (Fig. 5.14).

***Interpretation:*** The dominancy of lime mud, complete absence of shallow marine neritic fauna and abundance of deep marine planktonic foraminifera support low energy hydrodynamic regime open marine environment of outer shelf environment depositional setting below the storm wave base (Wilson, 1975; Burchette and Wright, 1992; Harris et al., 1997; Flugel, 1982; Flugel,2010; Geel, 2000; Rikhtegarzadeh et al., 2016).

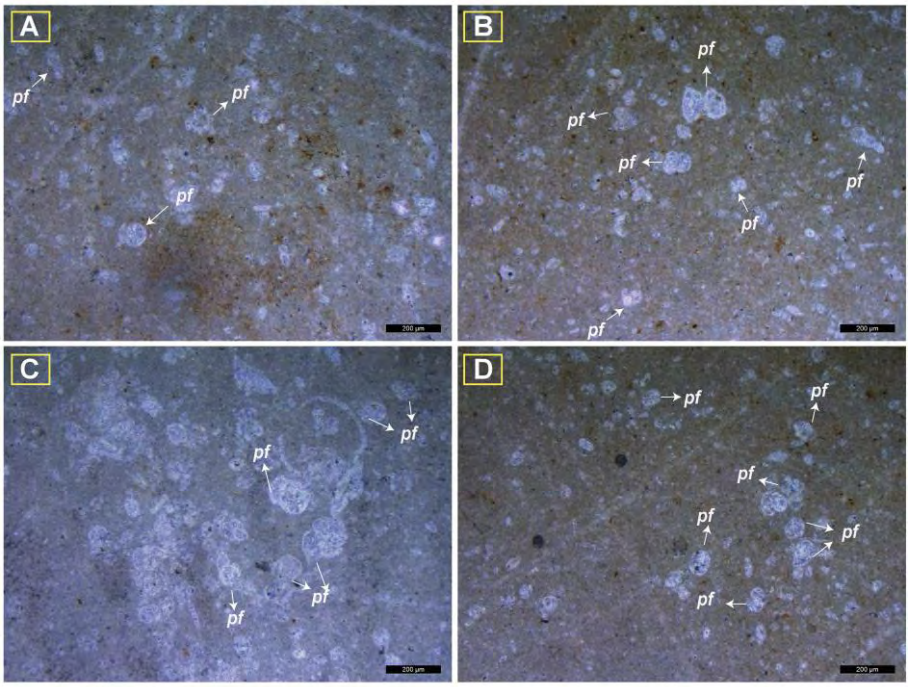


Fig 5.14: shows planktonic foraminiferal wackestone (MF-14). The figure shows planktonic foraminifera (*pf*).

### 5.2.3.6 Operculine planktonic foraminiferal wackestone (MF-15)

The operculine planktonic foraminiferal wackestone is present in the upper part of the Pirkoh Formation (Fig. 4.2). This facie is underlain is by contact of Dranzinda Formation and overlain by planktic foraminiferal Wackestone (Fig. 5.17). In the exposed outcrop, it attains thickness of 1.4 m, and appear as medium bedded limestone of light grey color. The petrographic studies of this facie describe planktic foraminifera assemblage about 20-30 %

embedded fine matrix accompanied by operculina and displaying teleogenetic white parallel calcite veins (Fig. 5.15).

***Interpretation:*** The operculina to less symbionts reliant on coralline algae thus signifying a wide range of depositional setting anywhere in carbonate platform as compared to other larger benthic foraminifera (Cole, 1957; Adams, 1965). However, the living species of operculina reported to thrive at depth 14 m in shallow water (Hottinger, 1983), on reef flats (McKee et al., 1959), assigned to reef shelf areas by (Maxwell et al.,1961; 1968), while the study of (Reiss and Hottinger, 1984; Banner and Hodgkinson, 1991) reported operculina to thrive in low-energy on soft-substrates at depth 30- 150m. On contrary, the Paleogene genus inhabits photic zone of inner shelf forereef high energy shallow setting (Chaproniere, 1975; Fadel, 2018) to quiet waters near the base of the photic zone. Thus, the association of operculina is allochthonous rather than in situ deposition. However, the abundant of planktic foraminifera embedded in mud dominated matrix irrespective of association with operculina is signify the deposition in outer shelf setting (Harris et al., 1997).

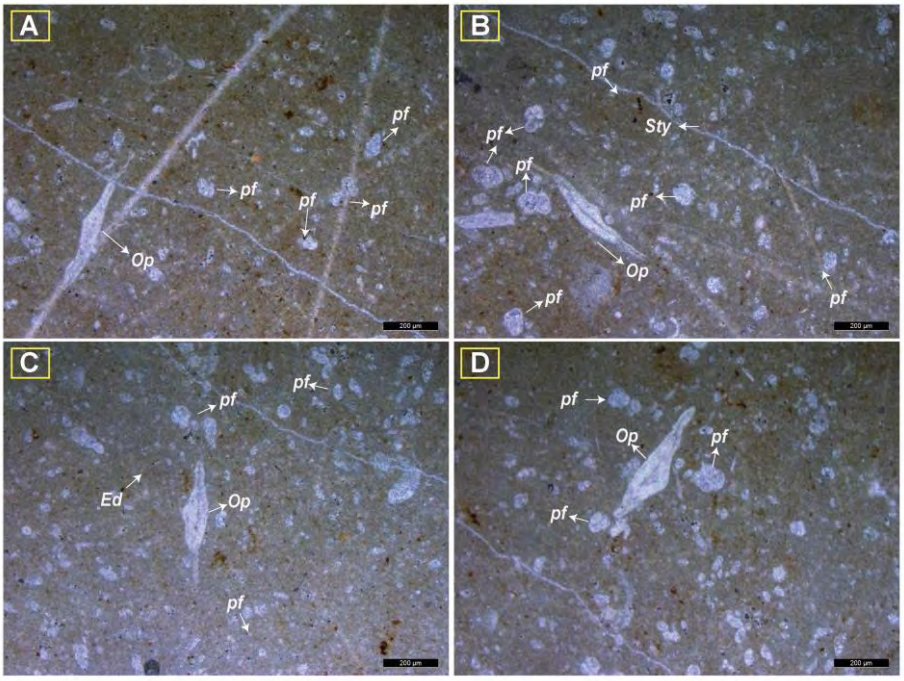


Fig 5.15: shows operculine planktonic foraminiferal wackestone (MF-15). The figure shows planktonic foraminifera (*pf*), and deformed operculina (*Op*).

### 5.3 Paleoecology of larger benthic and planktonic foraminifera

During the Eocene that the Nummulites fulfilled their unique rock- forming potential. They became abundant and formed the widespread nummulitic limestones of hydrocarbon reservoirs in offshore North Africa, India, and the Middle East. Their reservoir qualities are mostly due to the preservation of the intraskeletal porosity of the Nummulites test. Various depositional models have been proposed, and most of them described Nummulites accumulations as banks, bars or low- relief banks, sometimes related to palaeo- highs.

The behavior of Nummulites could explain the diversity of such depositional models. Depending on local hydrodynamic conditions, autochthonous Nummulites deposits can be preserved as in situ winnowed bioaccumulations or can be accumulated offshore, onshore or alongshore, away from the original biotope. But their most typical environment is forereef shelf of inner shelf setting (Fedal, 2018).

The nummulitids included genera with flattened to stoutly lenticular and even globular species, with a periphery varying from sharp to rounded or somewhat undulose (Beavington-Penney and Racey, 2004). The globose to ellipsoidal-flat Nummulites thrived in warm, tropical mesophotic zone, while the large flat forms are common in the oligophotic zone, either in shaded shallow water zones or deeper on the shelf (Mateu-Vicens et al., 2012, Pomar et al., 2017).

The operculina is the most "primitive" genus known and the least specialized (Cole, 1957; Chaproniere, 1975). For this reason, it is thought to be less dependent on coralline algae symbionts for food, and therefore it is inferred to have had a wider environmental range than the other nummulitids (Cole, 1957; Adams, 1965). Although the living nummulitids house symbiotic microalgae, they prefer calm water conditions and avoid highly illuminated areas near the water surface, since their flat tests could easily be damaged in a turbulent hydrodynamic regime (Hohenegger et al., 2000).

The living nummuliid Operculina appears to be restricted by oceanic salinities (Chaproniere, 1975). It has been found at depths as shallow as 14m (Hottinger, 1983). It has also been reported from the quieter parts of lagoons (McKee et al., 1959), channels on reef flats (Maxwell et al., 1961) and in off- reef shelf areas (Maxwell, 1968). Operculina lives on soft-bottomed substrates in the Gulf of Aqaba at depths of 30- 150m, with flatter forms most common between 60- 120m (Reiss and Hottinger, 1984). It dominates low- energy, muddy sea beds (Banner and Hodgkinson, 1991). In the Oligo- Miocene this genus is inferred to have inhabited environments ranging from high energy, shallow water forereef facies (BouDagher-Fadel et al., 2000) to quiet waters near the base of the photic zone (Chaproniere, 1975). The

alveolinids occur in a wide range of habitats, from deep lagoons and to forereef settings, existing down to depths of about 80m.

Heterostegina inhabited high energy forereef environments (Fadel et al., 2000), of 20 to 30 m depth (Banner and Hodgkinson, 1991), preferring to live on hard substrates (Reiss and Hottinger, 1984). Holocene Amphistegina has adapted to high energy conditions, however, it is also found in mud free sands in areas of sea grass or coralline algae and in reefal areas down to depths of 35m (McKee et al, 1959). Dead tests of Amphistegina have been found at greater depths (Chaproniere, 1975), but its main depth range is reported as 5 to 20m (Murray, 1973).

The orthophragminidea (Discocyclina and Asterocyclina) at the lower limit of the photic zone are very flat, and their lateral chamberlets are particularly low in shape (Fadel, 2018). The tendency towards flatter tests and thinner test walls with increasing water depth.

The Planktonic foraminifera inhabited various marine environments, but they were particularly abundant in warm, tropical to subtropical regions during the Eocene. Their fossil remains have been found in sedimentary rocks from shallow shelf areas to deep-sea environments. The remain are more commonly in lagoon setting of inner shelf setting with other larger benthic foraminifera such small rotaliids and small miliolids, and more abundant in outer shelf below the base of wave action (Fedal, 2018). In addition, the planktonic foraminifera in pelagic matrix support low energy hydrodynamic regime open marine environment of outer shelf environment depositional setting below the storm wave base (Wilson, 1975; Burchette and Wright, 1992; Harris et al., 1997; Flugel, 1982; Flugel,2010; Geel, 2000; Rikhtegarzadeh et al., 2016). The detail of paleoecology of larger benthic and planktonic foraminifera is illustrated in (Fig 5.18).

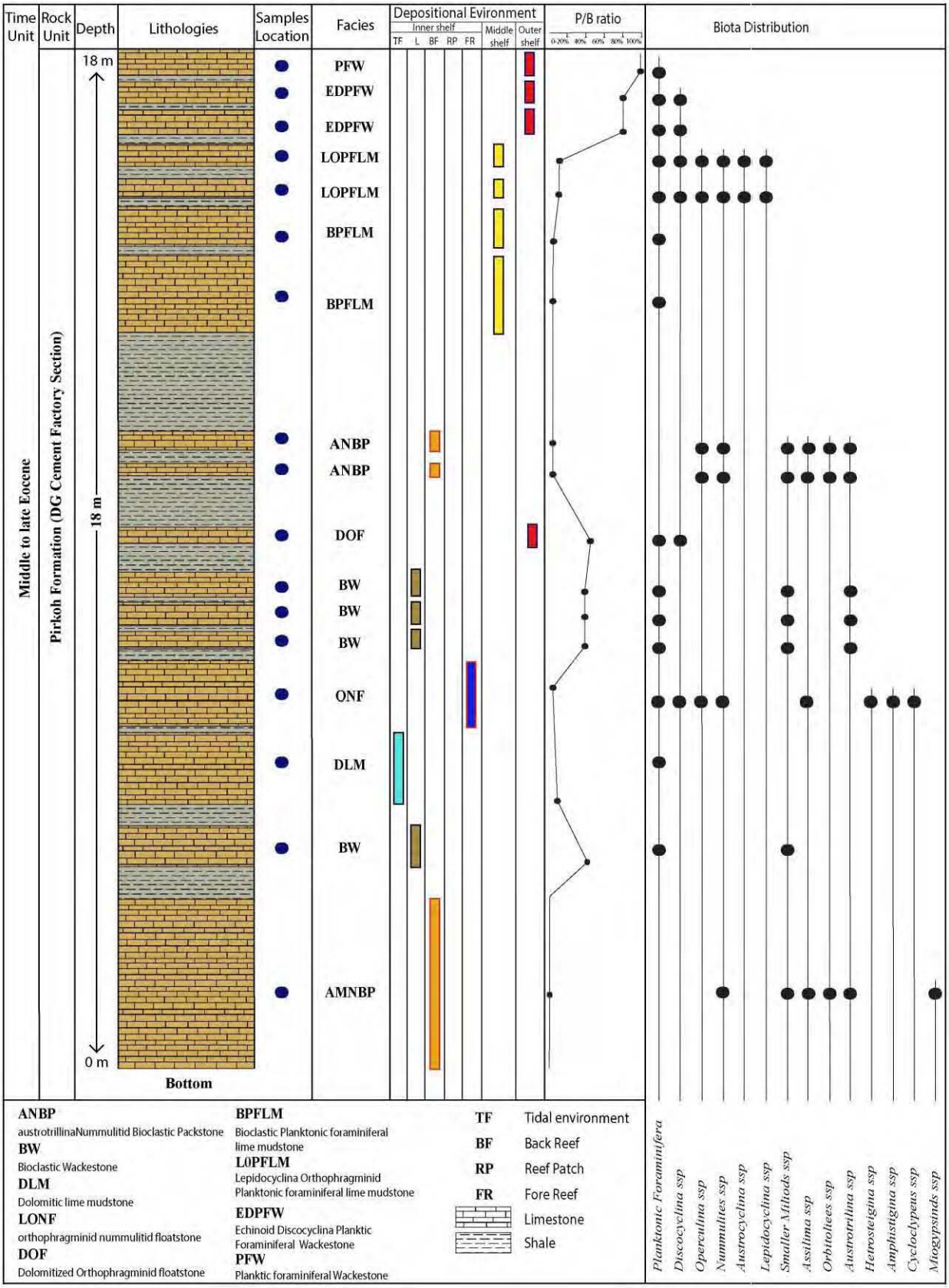


Fig 5.5: showing litho-log and biota distribution of Pirkoh Formation in DG cement factory section.

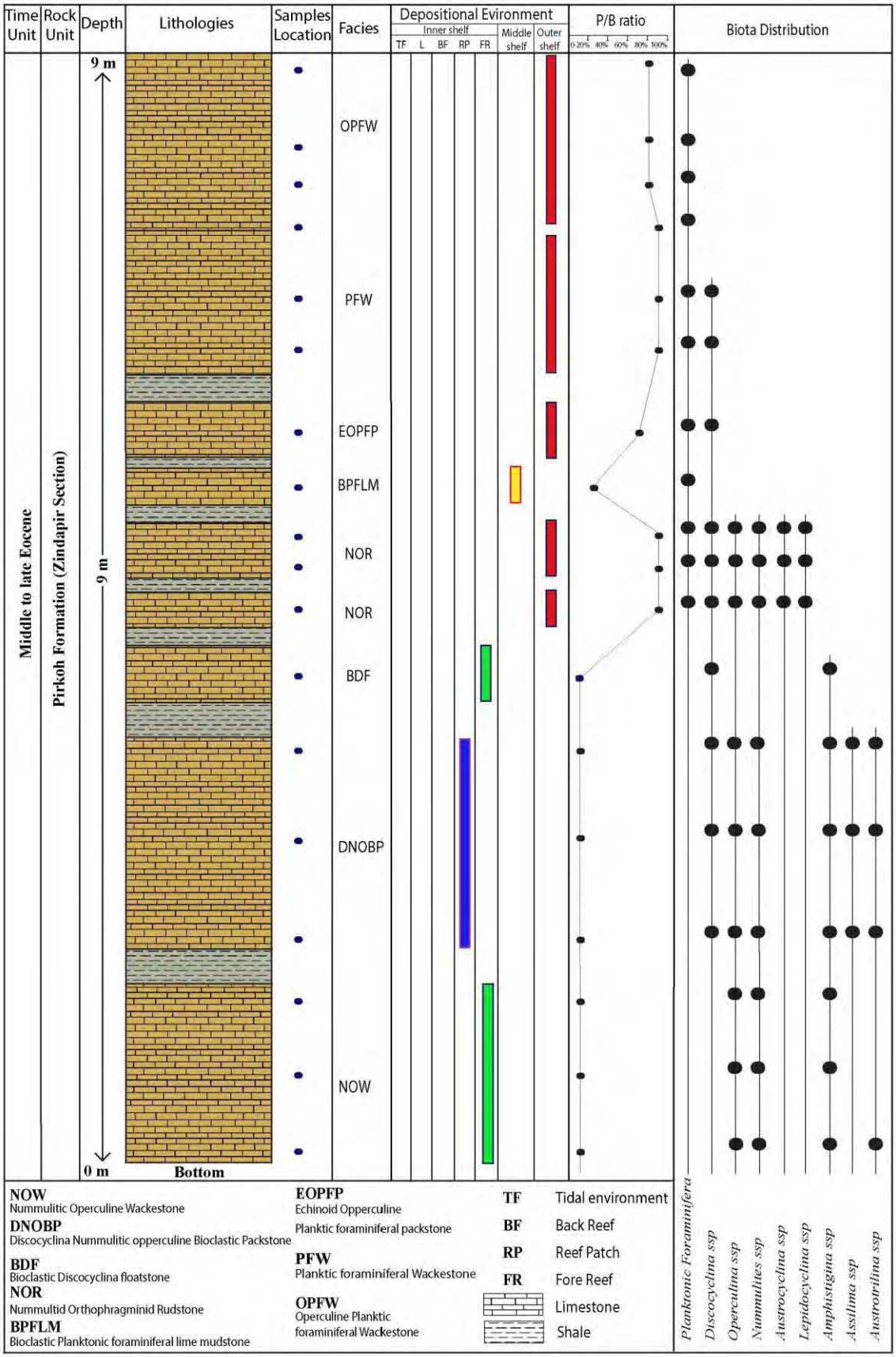


Fig 5.6: showing the litho-log and biota distribution of Pirkoh Formation in Zindapir section.

### 5.3 Depositional Model of Pirkoh Formation

The microfacies analyses of Pirkoh Formation is representing total fifteen microfacies (MF1-MF15) categorized in three major facies assemblages i.e., inner, middle, and outer shelf based on their depositional setting on carbonate platform. The facies assemblages are typical representative of Tethyan carbonate shelf. The inner shelf facies are deposited on tidal setting (MF1), open lagoons (MF2), backreef shelf (MF3). reef patch (MF4), forereef shelf (MF5-MF7). The middle shelf facies are represented by (MF8-9) while the outer shelf facies are (MF10-15) as shown in model.

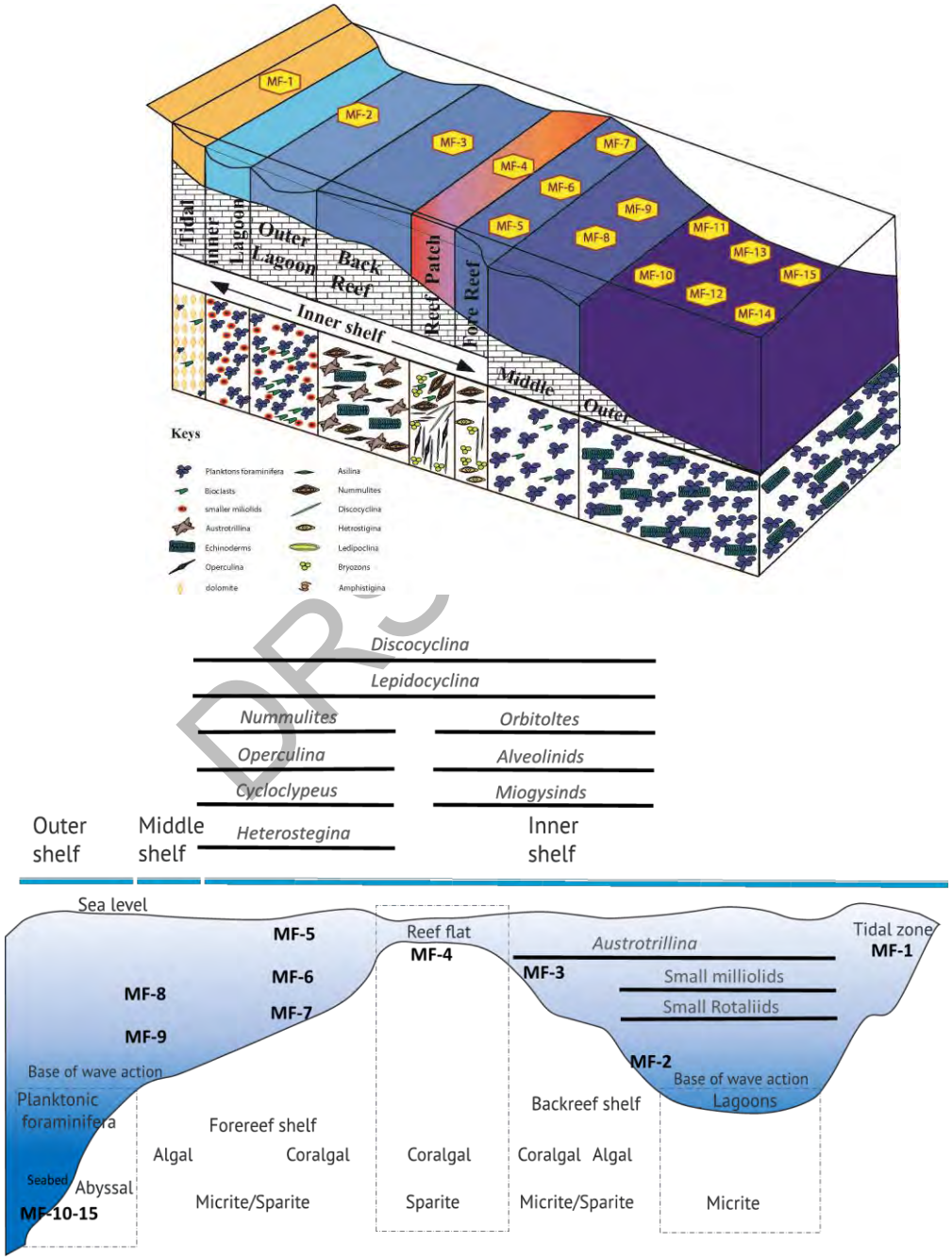


Fig 5.7: showing the detail depositional model of Pirkoh Formation as 3D and 2D display.

**CHAPTER 6**

# DIAGENESIS

## 6.1 Introduction

The term diagenesis refers to the sum of all biological, physical, and chemical process which influence the original depositional facies. The process of diagenesis take place soon after deposition and terminate until the zone of metamorphism. The process of diagenesis are categorized into eogenesis, mesogenesis and telogenesis. The eogenesis is further categorized into shallow and deep marine setting, while in mesogenesis the diagenesis take place in meteoric vadose and phreatic environment. The burial diagenesis is a generally associated late-stage diagenesis, while the telogenesis (uplift) is associated with late-stage uplift (Choquette and James, 1990).

## 6.2 Realm of Diagenesis

The regime of diagenesis is categorized by (Machel 1999) follow as:

### 6.2.1 Sear surface diagenesis

It is associated with lithification and take place at very shallow depth during the initial burial of carbonate sediments. The diagenetic fluids associated with near surface diagenesis are mostly originated from marine and brackish water. The meteoric diagenetic fluids is least significant in near surface diagenesis.

### 6.2.2 Shallow realm diagenesis

The diagenesis at shallow regime associated with physical and chemical compaction with possibility of suture zone development at depth of 600-1000m.

### 6.2.3 Intermediate realm of diagenesis

The shallow depth diagenesis is associated with multiple episodes of calcite cementation as well as dissolution (fabric and non-fabric selected) at depth equivalent to boundary of oil window.

### 6.2.4 Deep realm of diagenesis

It is the lower most boundary of diagenesis below which diagenesis terminate and low-grade metamorphism occur.

### 6.3 Diagenesis of Pirkoh Formation

The detail diagenesis of Pirkoh Formation is studied in Zindapir and DG cement factory section, Zindapir Anticline in the eastern Sulaiman province. The petrographic studies were conducted at scale of (100- 200 microns) under plan polarized light. The Pirkoh Formation has undergone various diagenetic events follow as:

#### 6.3.1 Eogenetic stage (Marine realm)

##### 6.3.1.1 Carbonate sedimentation and lithification

The carbonate sedimentation take place and deposited the limestone as well as the shale deposition on the shelf environment during middle to late Eocene which is followed by the lithification during earliest stage of diagenesis.

##### 6.3.1.2 Micritization

The fluid rock interaction in carbonate rocks take place in during eogenetic stage of diagenesis particularly at shallow depth in the marine phreatic zone, where the biogenic activities influence the carbonate sediments (Reid & MacIntyre, 2000; Vincent et al., 2007; Flugel, 2010; Beigi et al., 2017). Micritization take place in shallow marine setting during early diagenesis indicating slow sedimentation rate. The micritization in Pirkoh Formation has occurred along the edges of bioclasts (Fig.1 A, B). The micritization is common and widespread in Samana Suk Formation and indicates slow sedimentation rate.

##### 6.3.1.3 Dolomitization (Shallow marine)

The fine-crystalline dolomite (very fine anhedral with a few well-developed euhedral rhombs) shown in (Fig.6.1 C, D) embedded in micritic matrix (dolomicrite) indicates early diagenetic stage dolomitization in a peritidal environment (Tucker and Wright, 1990; Wanas, 2008).

##### 6.3.1.4 Isopachous rim cement

The shallow marine zone displays the high-Mg aragonite and calcite composition isopachous rim cements as first-generation cement take place during eogenesis, but it unusual in marine phreatic setting (Flugel, 2010). The growth isopachous rim cements found on the outer boundaries of planktonic foraminifera (Fig. 6.1 E, F). It is postdating postdates micritization (Adabi and Rao, 1991).

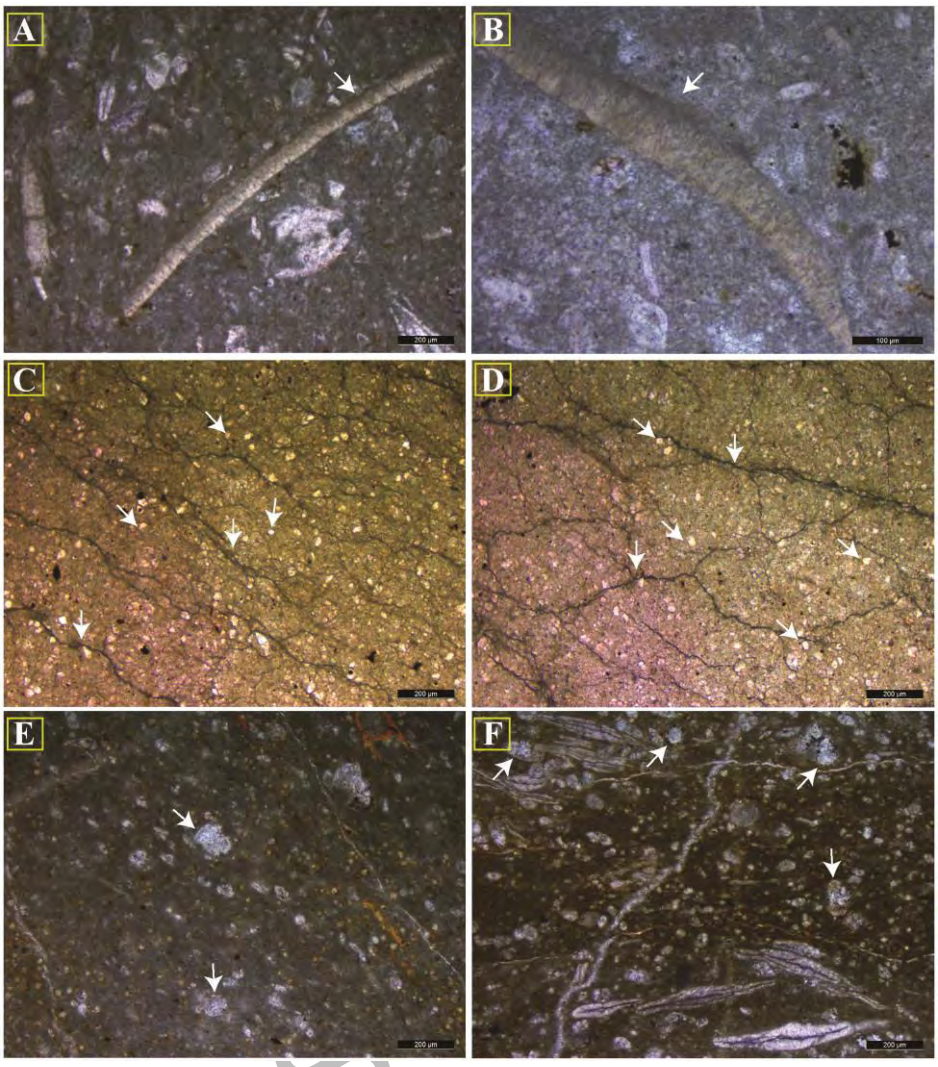


Fig 6.1: (A, B) shows micritization, (C, D) shows fracturing and dolomitization in micritic lime, (E, F) shows isopachous rim cements.

### 6.3.2 Mesogenetic stage (Meteoric realm)

#### 6.3.2.1 Fabric Selected Dissolution

The Pirkoh Formation shows dissolution widely distributed at outcrop and petrographic scale. The dissolution has occurred in eogenetic, mesogenetic, and telogenetic stage. It is playing an important role in enhancing the potential of the reservoir. During the eogenetic and mesogenetic stage fabric selective dissolution is reported in Pirkoh formation shown in (Fig. 6.2 A, B). The non-fabric selected dissolution also observed in place, but it is least significant due the precipitation of blocky calcite.

#### 6.3.2.2 Blocky calcite

The blocky calcite is associated with meteoric zone (Phreatic) during of mesogenetic stage and shallow burial late stage. The blocky calcite display characteristics of Phreatic cements such as its uniformly distribution, which is reflecting the complete saturation of pores with water in the given setting (James and Choquette, 1984). In the chronological sequence, the early stages of meteoric vadose cementations are followed by initial dissolution in meteoric vadose zone, which is later on further followed by dissolution in phreatic zone. The extended meteoric diagenesis it results to fabric inversion resulting to secondary pores, where the blocky calcite precipitate until the complete filling of secondary pore and its precipitation further proceed to burial late diagenesis (Fig. 6.2 C, & D).

#### 6.3.2.3 Physical Compaction

The physical compaction take place at shallow to deep burial compaction due to overlying deposition. In the Pirkoh Formation the physical compaction resulted to deformation of skeletal grains and minor fracturing during late mesogenetic and early burial stage (Fig. 6.2 E). This mechanical compaction has resulted to high reduction of porosity in grainstone and Packstone texture as compare to mudstones and wackestone.

### 6.3.3 Burial stage

#### 6.3.3.1 Chemical Compaction

In the Pirkoh Formation no suture zones are reported at outcrop scale and very minor suture seems are observed in the petrographic results. Although it is a common phenomenon

of diagenesis which takes place due to pressure solution (Lloyd, 1977; Choquette & James, 1990). The minor chemical compaction is observed (Fig. 6.2 F).

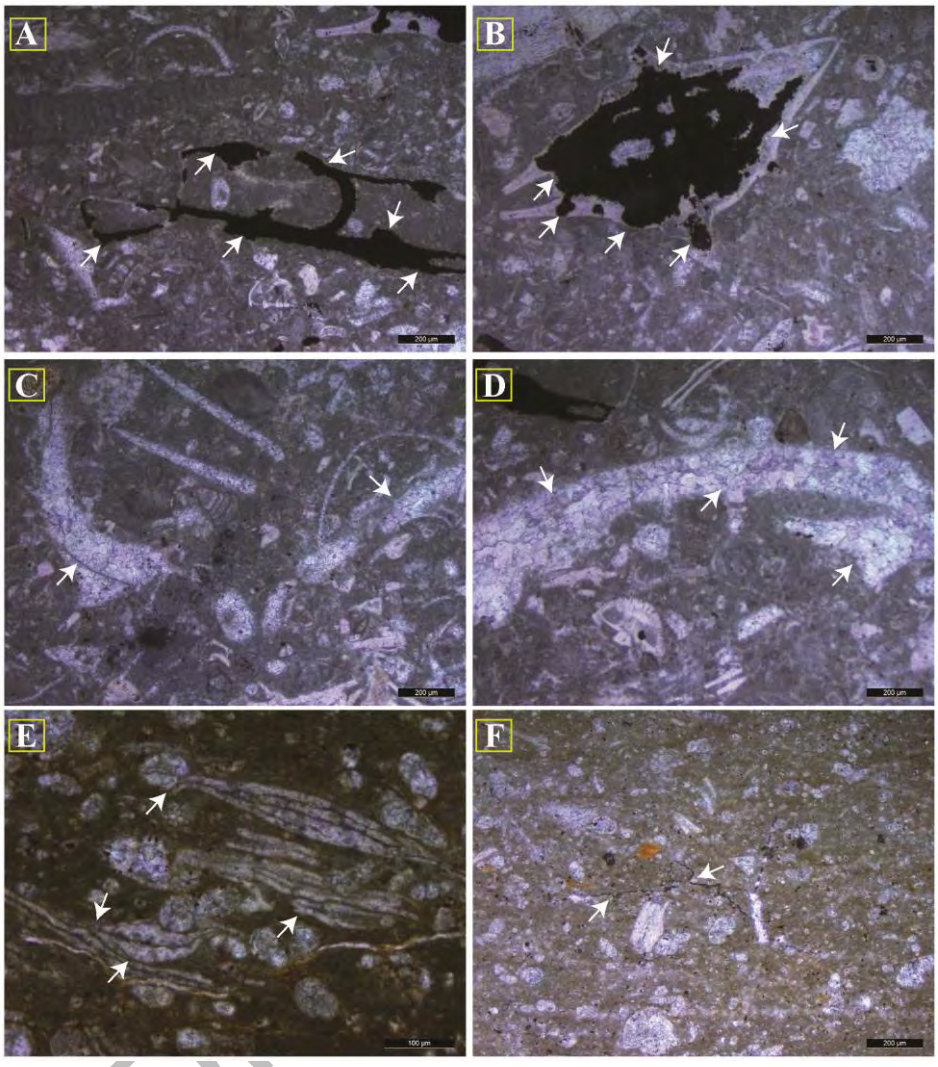


Fig 6.2: (A, B) shows fabric selective dissolution, (C, D) shows blocky calcite cement, (E) shows operculina deformation due physical compaction, (F) stylolitation due to chemical compaction.

### 6.3.3.2 Selective Dolomitization

The selective dolomitization take place along the fracturing where fluids squeezed out due to burial chemical and mechanical compaction. The dolomite rhombs are showing well developed euhedral rhombs and a few subhedral texture. The presence of high iron leaching indicates burial depth selective dolomitization (Fig. 6.3 A, B).

### 6.3.4 Telogenesis

### 6.3.4.1 Fracturing and veins Filling

The field study and petrographic scale display high density fractures in Pirkoh Formation. The fractures are filled with various phases of calcite cements and display telogenetic transparent calcite which is associated with uplift after collision during late Eocene (Fig. 6.3 C, D).

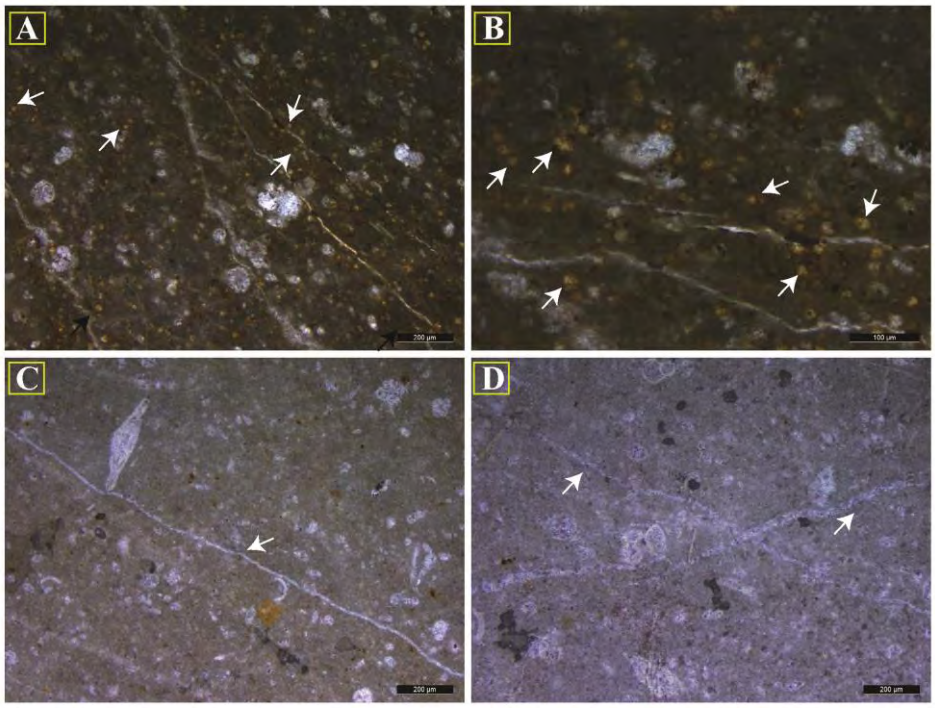


Fig 6.3: (A, B) shows selective dolomitization, (C, D) shows late stage telogenetic calcite.

### 6.4 Paragenetic sequence

1. The eogenesis show micritization mostly in the shallow marine settings with shallow marine dolomitization.

2. The first generation isopachous rim cements are observed in shallow marine to deep marine setting of eogenetic stage, such cements are mostly found on the edges of planktonic foraminifera of open lagoonal and open marine outer shelf facies.

3.During the eogenetic and early mesogenetic stage in marine and meteoric (vadose) regime the fabric selected dissolution is evident.

4. The later stage of mesogenesis display blocky calcite cements precipitate in meteoric (phreatic) and which continue till the late stage of burial diagenesis.

5. The physical compaction tend to start at later stage of mesogenesis and terminate at shallow burial depth resulting to very minor fracturing.

6. At burial depth, the mechanical compaction transformed to chemical compaction resulting to stylolites and selective `dolomitization along the fluids patterns.

7. The telogenesis (tectonic uplift) resulted to fracturing of Pirkoh Formation.

8. In the latest stage of diagenesis the former factures are filled with transparent telogenetic calcite (vein filling calcitization) last episode of diagenesis as a result of late Eocene collision.

The episodes of diagenesis in various diagenetic realms are shown in (fig. 6.4)

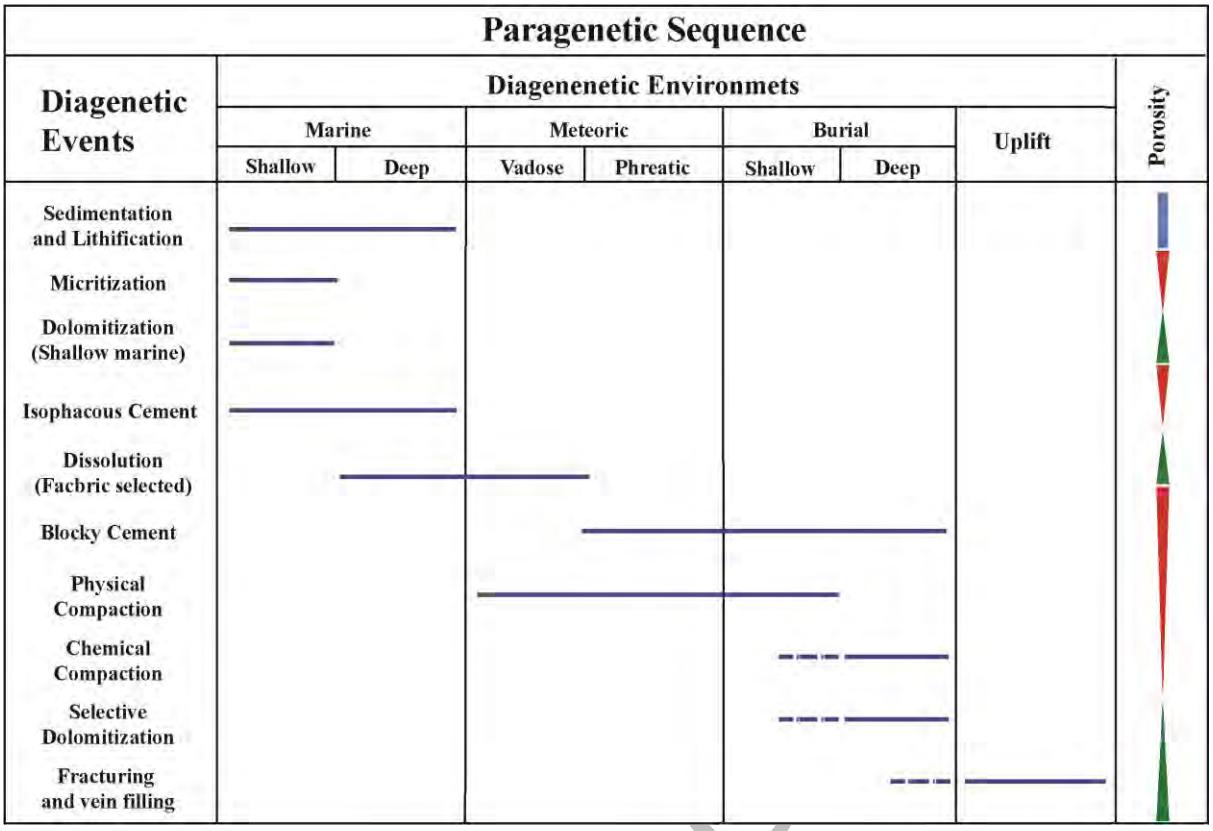


Fig 6.4: showing the paragenetic sequence of Pirkoh Formation.

# CHAPTER 7

# RESERVOIR CHARACTERIZATION

## 7. 1 Reservoir quality Classification

The reservoir quality is classified into the following 4 groups and further categorized into classes based on their variation in permeability and porosity. In general, the group 1 is classified into class High I and High II reservoir quality, the group 2 is into class III good and class IV moderate reservoir quality, the group 3 having class V Cautionary-1 and class VI Cautionary-2 reservoir quality and the final group 4 into class VII and class VIII of low and very low reservoir quality respectively (Khanin, 1965, 1969) modified by (Shogenov et al., 2015). The detail of each group and their respective classes are followed as:

### 7.1.1 Group 1

The group 1 of the reservoir quality classification is the highest quality having both the permeability and porosity high values, the class I (very high) of the group is having very high permeability ranging from 300 and more while their porosity % range greater the 18%. While their class II (high) has the same permeability and but its porosity % varies from 9-18 % in the reservoir quality classification

### 7.1.2 Group 2

The group 2 of the classification has class III (good) reservoir quality having the permeability and the porosity % of 100-300 mD and greater than 18 % respectively, while the class IV (moderate) reservoir quality having the same permeability but different porosity ranging from 9-18 % in the reservoir quality classification.

### 7.1.3 Group 3

The group 3 of the classification are cautionary rocks having the permeability of 10-100 mD and is further classified into the class V and class IV called the cautionary 1 and 2 having the porosity of 18-23 and 7-9 % respectively.

### 7.1.4 Group 4

The last group of the reservoir quality classification having the low reservoir quality has class VII and class VIII of low and very low reservoir quality having permeability of 1-10 and 0.001-1 mD and having the porosity of 7-9 and 0-7 % respectively.

| Group | Class | Reservoir quality | Permeability (mD) | Porosity (%) |
|---|---|---|---|---|
| **1** | I | High-1 | >300 | >23 |
| | II | High-2 | >300 | 9-18 |
| **2** | III | Good | 100-300 | >23 |
| | IV | Moderate | 100-300 | 9-18 |
| **3** | V | Cautionary-1 | 10-100 | 20-23 |
| | VI | Cautionary-2 | 10-100 | 7-9 |
| **4** | VII | Low | 1-10 | 7-9 |
| | VIII | Very low | 0.001-1 | 0-7 |

Table 7.1: shows hydrocarbon reservoir quality of (Khanin, 1965, 1969) modified by (Shogenov et al., 2015).

### 7.2 Reservoir Rank Classification

The reservoir rank classification is introduced for the reservoir to rank it, whether the rock sample is a having the reservoir parameters which is porosity within the rock sample, the permeability within the sample, rock quality ranking and their flow zone index upon which the rock is classified into 6 different ranks that is rank1 excellent, rank 2 very good, rank 3 good, rank4 fair, rank 5 poor and rank 6 which is tight (Nabawy et al., 2018)

The quality parameters i.e., quality index and flow index are introduced by (Amaefule et al., 1993), which are based in air porosity (%) and air permeability (mD).

1. Quality index: 0.0314 (√ (k / Ø))
2. Normalized Porosity: ØHe in decimal / (1 - ØHe in decimal)
3. Flow index: Quality index / Normalized Porosity in decimal

#### 7.2.1 Rank 1

Rank 1 has greater than 25 % porosity, and greater than 1000 (mD) permeability. It has RQI greater than 5.00 (µm), and FZI greater than 15 (µm). It is excellent rank.

#### 7.2.2 Rank 2

Rank 2 has less than or equal to 25 % and greater than 20 % porosity, less than 1000 (mD) and greater than 100 (mD) permeability. The RQI is less than or equal to 5.00 (µm) and greater than 2 (µm), while the FZI is less than or equal to 15 (µm) and greater than 10 (µm). It is very good rank.

#### 7.2.3 Rank 3

Rank 3 has less than or equal to 20 % greater than 15 % porosity. It has less than 100 (mD) and greater than 10 (mD) permeability. The RQI less than or equal to 2.00 (µm) and

greater the 1(µm), while the FZI is less than or equal to 10 (µm) and greater than 5.0 (µm). It is good rank.

### 7.2.4 Rank 4

Rank 4 has less than or equal to 15 % greater than 10 % porosity, greater than 1 (mD) and less than 10 (mD) permeability, RQI greater than 0.5 (µm) and lesser than or equal to 1 (µm), FZI of less or equal than 5 (µm) and greater than 2.5 (µm). It is fair rank.

### 7.2.5 Rank 5

Rank 5 has less than or equal to 10 % and greater than 5 % porosity, greater than 0.1 (mD) and lesser or equal to 1 (mD) permeability. It has RQI of less than or equal to 0.5 (µm) and greater than 0.25(µm). The FZI is less than or equal 2.5 (µm) and greater than 1 (µm). It is poor rank.

### 7.2.6 Rank 6

Rank 6 has less than or equal to 5 % and greater than 0 % porosity. It has less or equal to 0.1 (mD) and greater than 0 (mD) permeability. It has RQI less than or equal to 0.5 (µm) and greater than 0.00 (µm). The FZI of less than or equal to 1.0 (µm) and greater than 0.00 (µm). Overall such reservoir is ranked as tight.

| Porosity (%) | Rank | Permeability (md) | Rank | RQI (µm) | Rank | FZI (µm) | Rank | RPI | Rank |
|---|---|---|---|---|---|---|---|---|---|
| 25 < Ø | 1 | 1000 < k | 1 | 5.00 < RQI | 1 | 15.0 < FZI | 1 | Excellent | 1 |
| 20 < Ø ≤ 25 | 2 | 100 < k ≤ 1000 | 2 | 2.00 < RQI ≤ 5.00 | 2 | 10.0 < FZI ≤ 15.0 | 2 | Very good | 2 |
| 15 < Ø ≤ 20 | 3 | 10 < k ≤ 100 | 3 | 1.00 < RQI ≤ 2.00 | 3 | 5.0 < FZI ≤ 10.0 | 3 | Good | 3 |
| 10 < Ø ≤ 15 | 4 | 1.0 < K ≤ 10 | 4 | 0.50 < RQI ≤ 1.00 | 4 | 2.50 < FZI ≤ 5.0 | 4 | Fair | 4 |
| 5 < Ø ≤ 10 | 5 | 0.1 < k ≤ 1.0 | 5 | 0.25 < RQI ≤ 0.50 | 5 | 1.00 < FZI ≤ 2.50 | 5 | Poor | 5 |
| 0 < Ø ≤ 5 | 6 | 0 < k ≤ 0.1 | 6 | 0.00 < RQI ≤ 0.25 | 6 | 0.00 < FZI ≤ 1.00 | 6 | Tight | 6 |

Table 7.2: shows reservoir rank classification of (Nabawy et al., 2018), and integrated reservoir parameters of (Amaefule et al., 1993).

## 7.3 Reservoir Ranking and quality classification of Pirkoh Formation

The field samples of the Pirkoh Formation were analyzed for the air permeability and air porosity to study their reservoir behavior and the result of selected samples compared with the standard classification which was discussed later.

### 7.3.1 Mudstone texture

1. The bioclastic planktonic foraminiferal lime mudstone of the middle shelf environment has the air permeability of 0.07 mD and air porosity is 2.89 %, which is classified based on the reservoir quality classification and reservoir rank classification falling in the group 4 class 8 and ranked 6 respectively.

2. The planktonic foraminiferal lime mudstone of middle shelf environment having the air permeability of 0.06 mD and the air porosity of 2.78% classified based on the reservoir quality and reservoir rank classification falling in the class 8 of group 4 and ranked 6 respectively.

3. The dolomitic lime mudstone of tidal setting display air permeability of 0.08 mD and their porosity is 2.93% has also classified in class 8 of group 4 of reservoir quality classification and ranked 6 in reservoir rank classification.

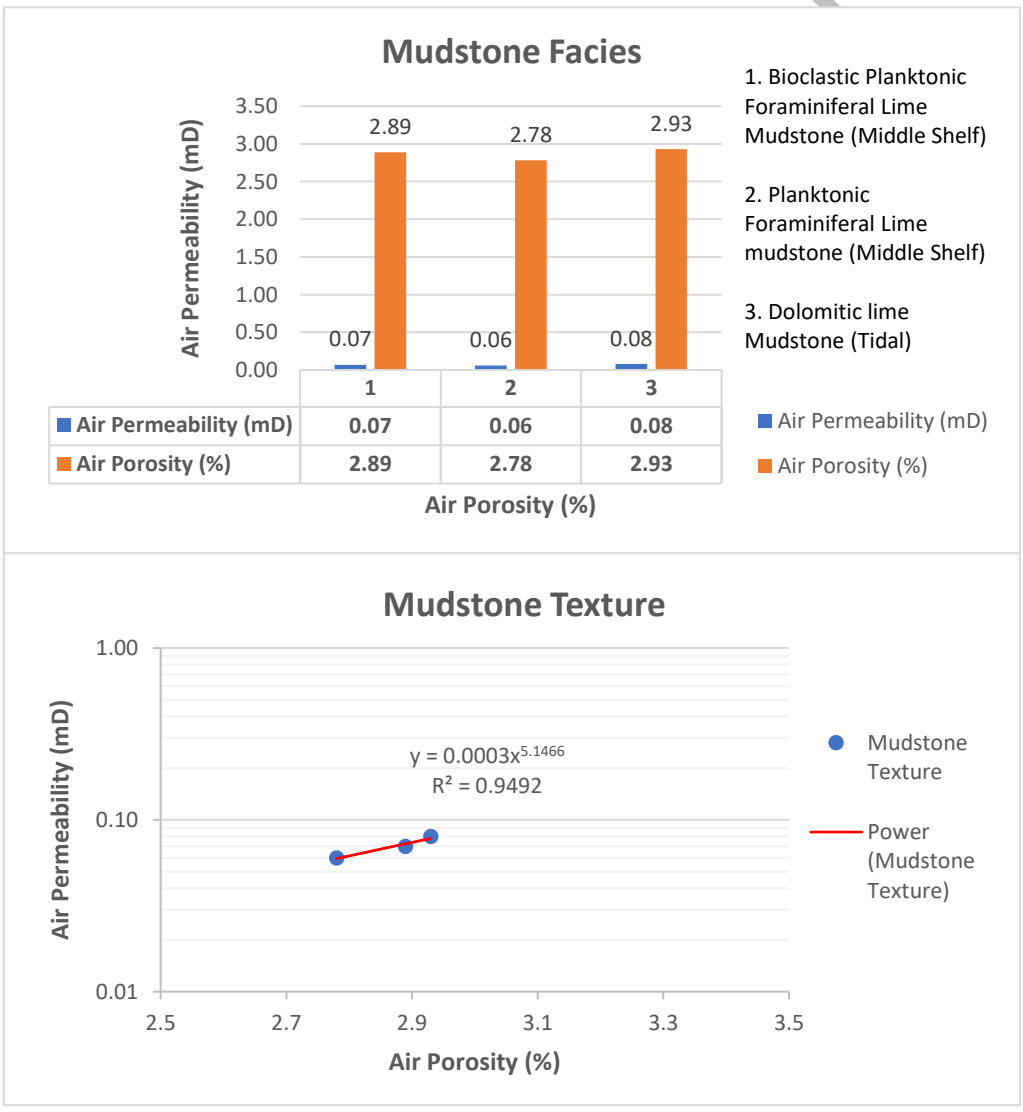


Fig 7.1: shows air porosity and air permeability of mudstone texture facies and $R^2 = 0.9436$.

### 7.3.2 Rudstone Texture

The Pirkoh formation is investigated for three sample of same facie rudstone texture for air porosity and permeability.

1. Nummulitid orthophragminid Rudstone of outer shelf environment having the air Permeability of 0.09, 0.07, and 0.06 (mD) and their air porosity of 3.1, 3.0, and 3.04 (%). The rudstone sample are classified in the same group rank based on reservoir quality and rank classification which are class 8 of group 4 and rank 6 respectively. It signifies to poor diagenesis in rudstone texture.

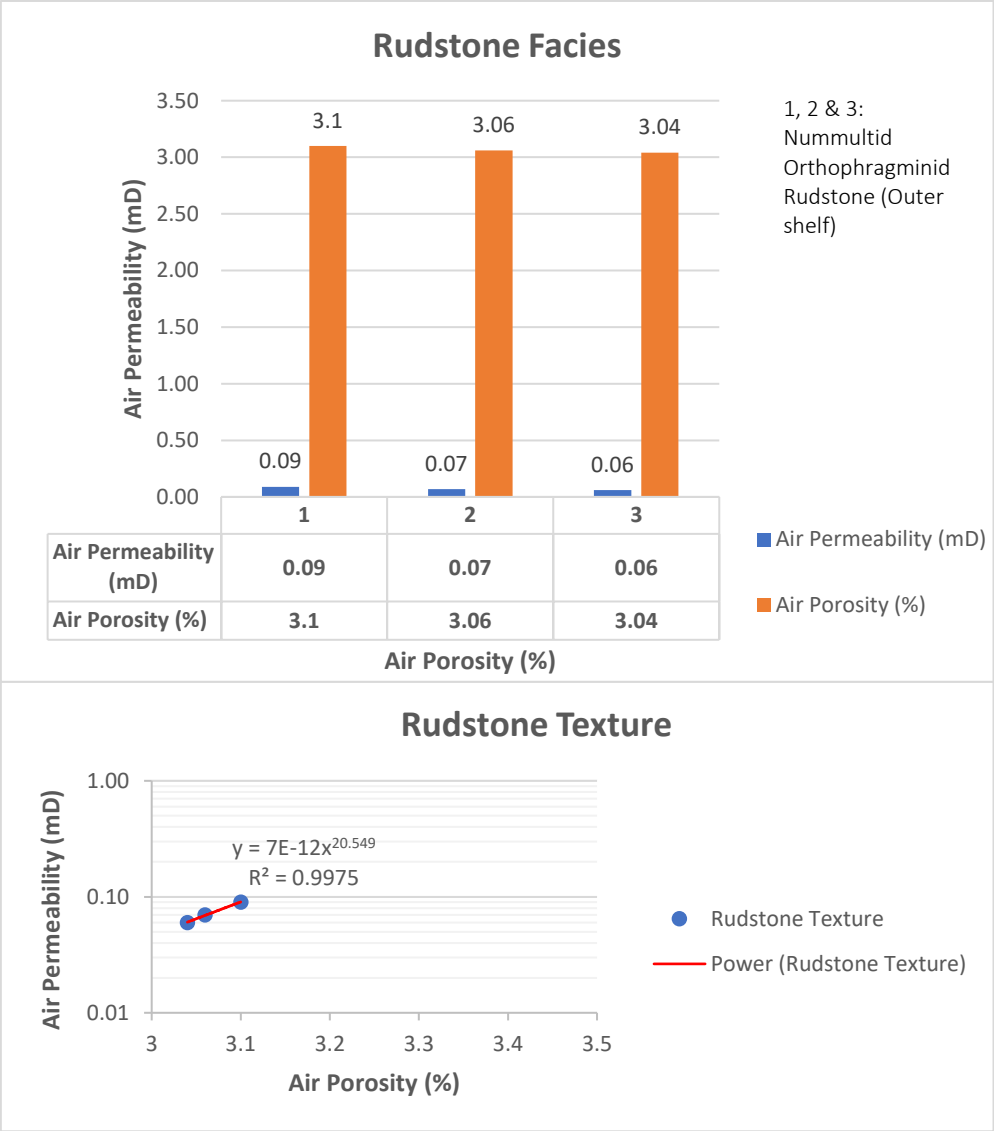


Fig 7.2: shows air porosity and air permeability of mudstone texture facies, and $R^2 = 0.9979$.

### 7.3.3 Wackestone Texture

1. Bioclastic wackestone of lagoonal environment showing the air permeability of 0.08 mD and their air porosity of 5%. It is classified on reservoir quality and rank classification in class 8 group 4 and rank 6 of the classification respectively.

2. Nummulitic operculine wackestone of forereef shelf setting display air permeability of 0.10 mD and their air porosity of 4.8 %. It is categorized in class 8 group 4 and rank 6 on reservoir quality classification and reservoir rank classification respectively.

3. Planktic foraminiferal wackestone of outer shelf environment display air permeability 0.06 mD and air porosity 3.1% and is classified on the reservoir quality and rank classification in group 4 class 8 and rank 6 respectively.

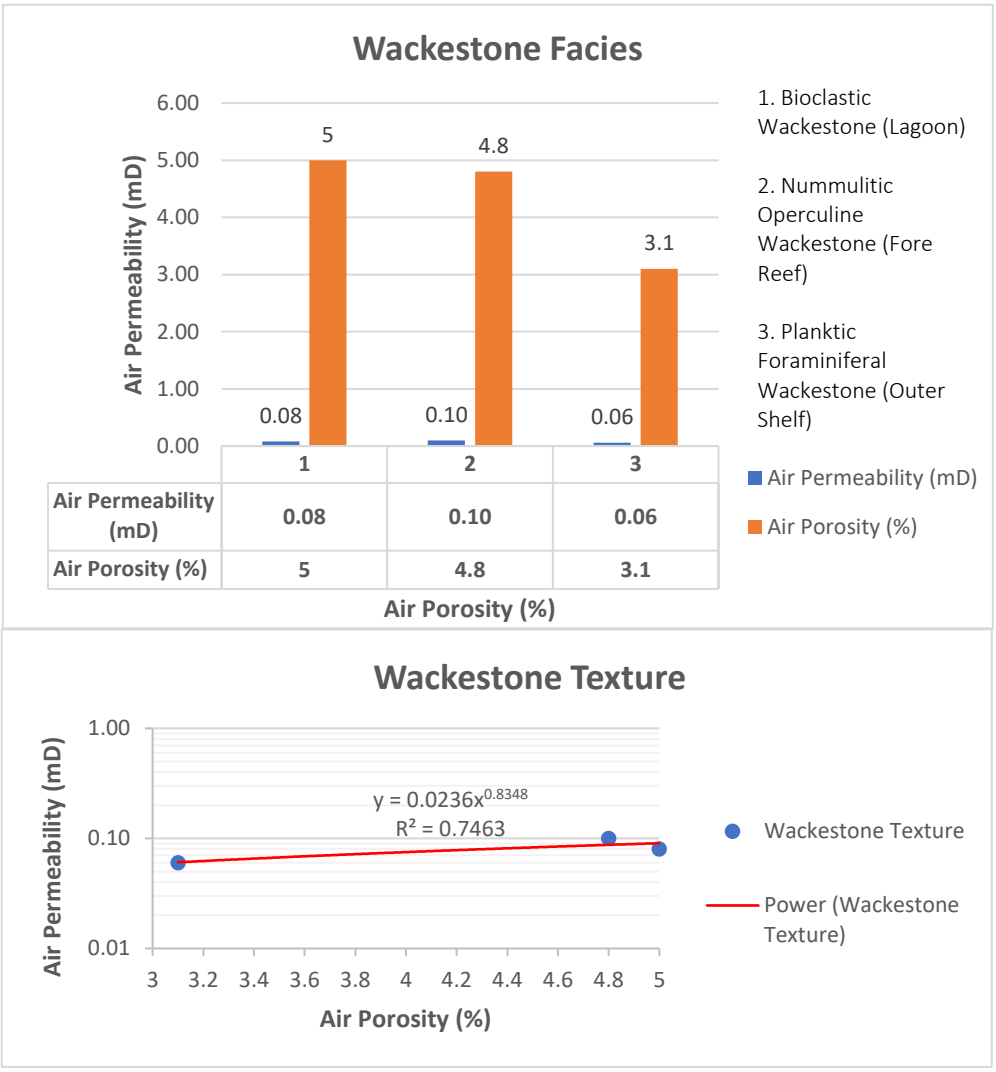


Fig 7.3: shows air porosity and air permeability of mudstone texture facies, and $R^2 = 0.6659$.

### 7.3.4 Packstone Texture

1. Austrotrillina nummulitid bioclastic packstone of back reef display air permeability of 0.29 mD and air porosity of 5.64%, which is classified based on reservoir quality and rank classification categorized in the class 8 group 4 of the quality classification and rank 5 of the reservoir rank classification.

2. Discocyclina nummulitic operculine bioclastic packstone of reef patch setting display air permeability 0.19 mD and air porosity 3.28%, which is classified in the group 4 class 8 of reservoir quality classification and rank in between 5 to 6 on reservoir rank classification.

3. Echinoid operuline planktic foraminiferal packstone of outer shelf setting has air permeability of 0.24 mD and air porosity 3.93% is classified as group 4 class 8 of reservoir quality classification and rank in between 5 to 6 in the reservoir rank classification.

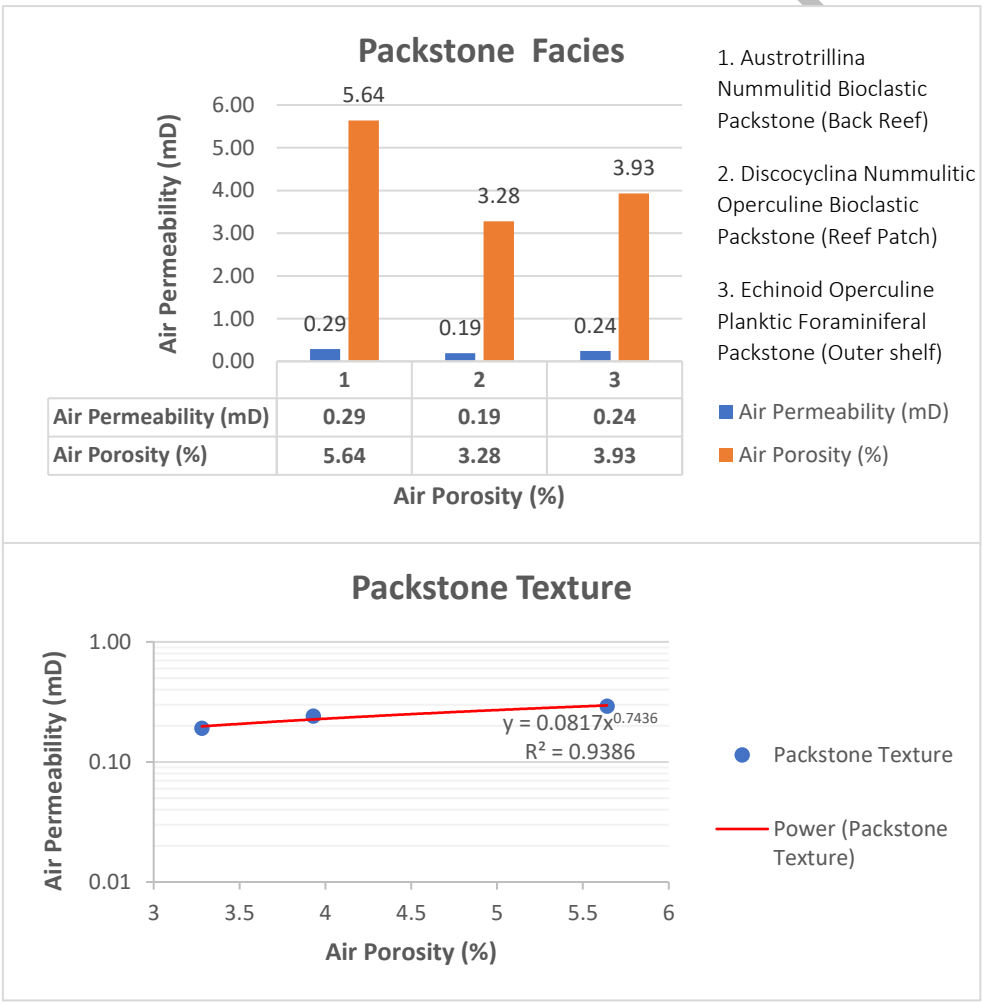


Fig 7.4: shows air porosity and air permeability of packstone texture, and $R^2 = 0.9444$.

### 7.3.5 Floatstone Texture

1. Orthophragminid nummulitid floatstone of fore reef having the air permeability 0.06 mD and air porosity 2.67 % is classified as group 4 class 8 of the reservoir quality classification and rank 6 of the reservoir rank classification.

2. Dolomitized orthophragminid bioclastic floatstone of outer shelf setting display air permeability 0.14 mD and air porosity 3.04%, which is classified in group 4 class 8 of reservoir quality classification and is rank 6 in the reservoir rank classification.

3. Bioclastic discocyclina floatstone of fore reef environment display air permeability 0.09 mD and air porosity 2.8%, which is classified in group 4 class 8 according to the reservoir quality classification and is rank 6 according to the reservoir rank classification.

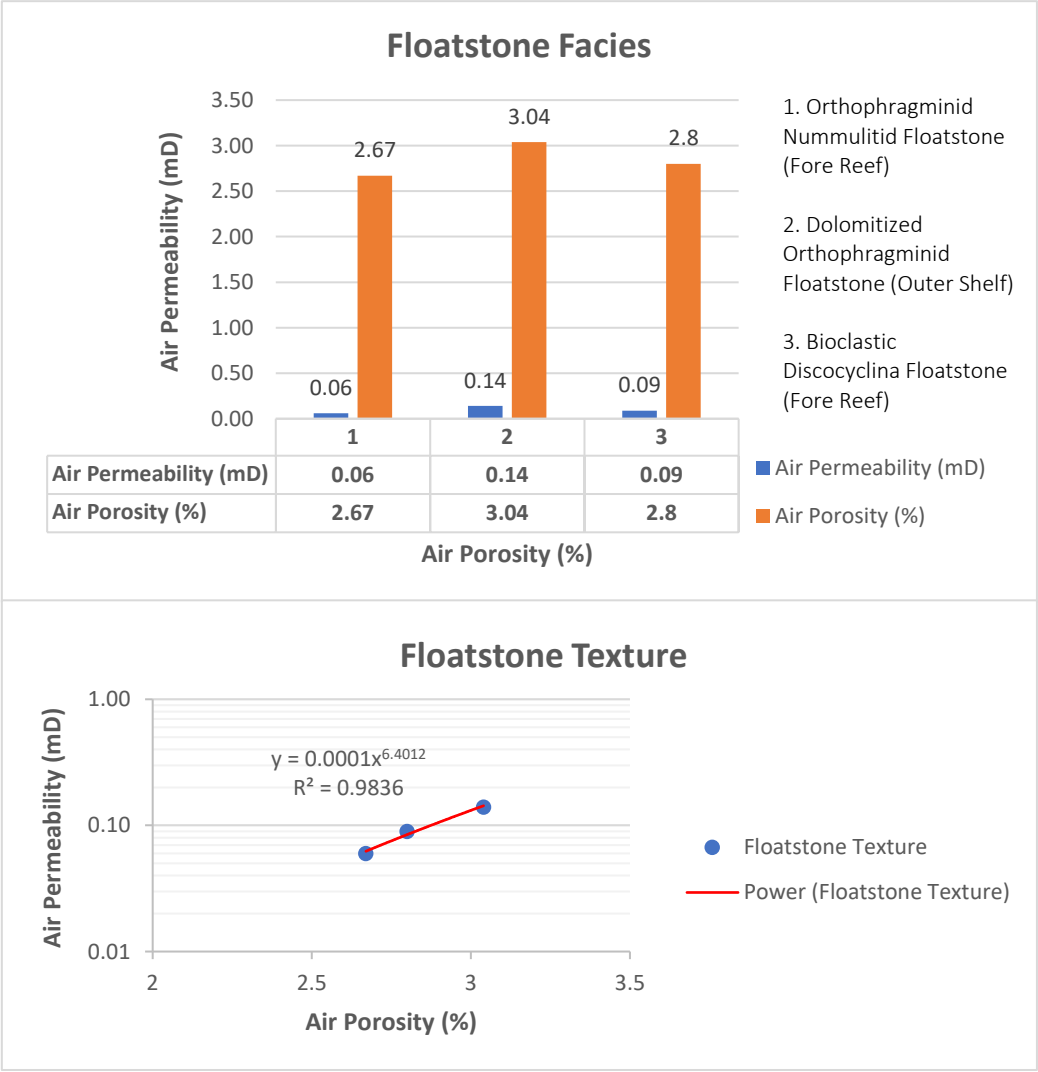


Fig 7.5: shows air porosity and air permeability of floatstone texture, and $R^2 = 0.9877$.

### 7.4 Reservoir rank classification of Pirkoh Formation

The overall results of the selected samples are studied and according to the reservoir rank classification of (Nabawy et al., 2018), and integrated reservoir parameters of (Amaefule et al., 1993), the Pirkoh Formation is poor ranked, categorized as tight in the reservoir behavior as shown in (Fig. 7.4).

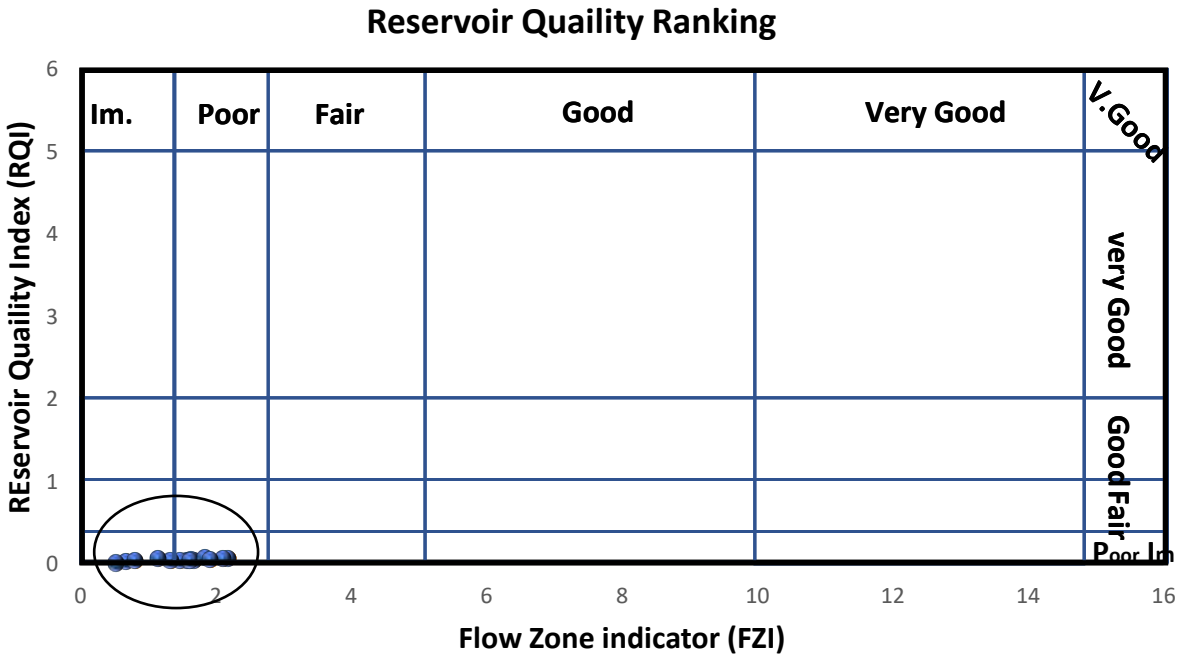


Fig 7.6: showing reservoir rank classification of Pirkoh Formation (Nabawy et al., 2018), and integrated reservoir parameters of (Amaefule et al., 1993).

### 7.5 Reservoir Quality classification of Pirkoh Formation

The overall results of the selected samples are studied and according to the Reservoir Quality classification of (Khanin, 1965, 1969) modified by (Shogenov et al., 2015). The Pirkoh Formation is of poor quality as shown in (Fig. 7.7).

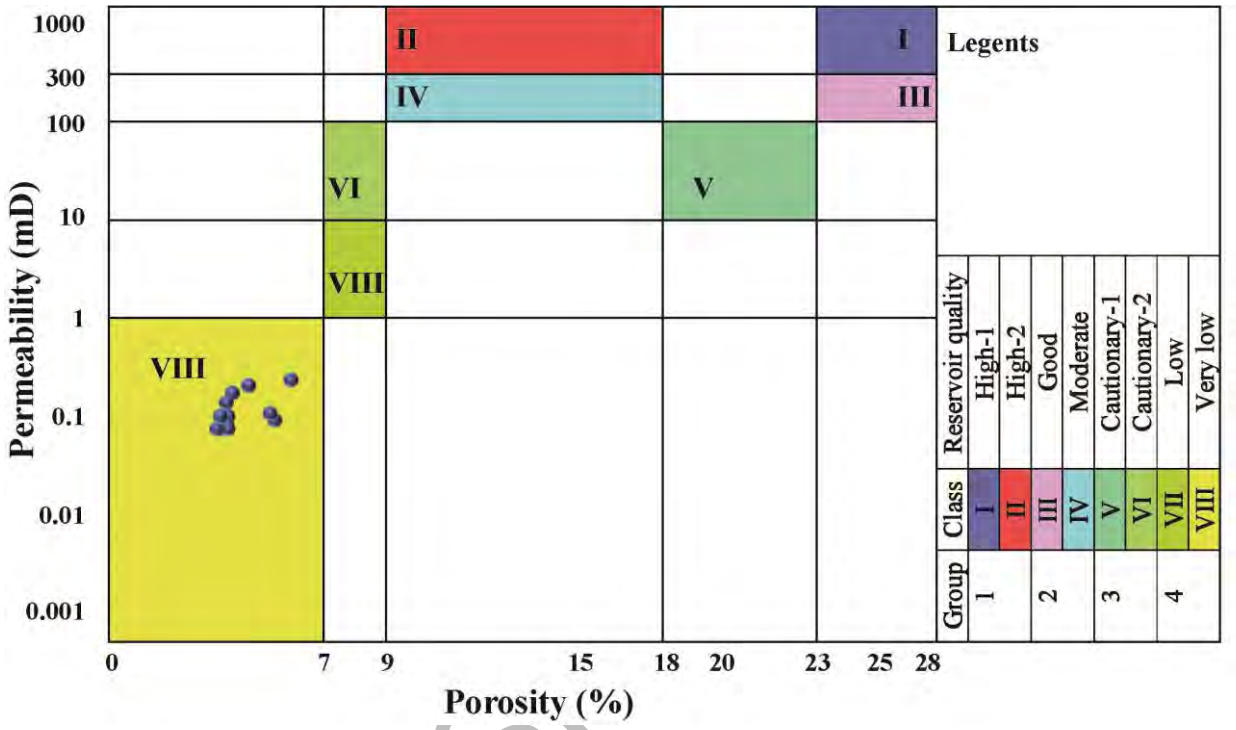


Fig 7.7: showing reservoir quality of classification of Pirkoh Formation (Khanin, 1965, 1969) modified by (Shogenov et al., 2015).

### 7.6 Textural summary of Pirkoh Formation

The Pirkoh Formation is showing good power regression for same texture (Fig. 7.8 A) and poor relationship of both variable in different texture (Fig. 7.8 B). Moreover, the depositional porosity is well preserved and least influenced by diagenesis is noticed from petrographic studies. The results show that wackestone and packstone display relatively high porosity as compared to mudstone, floatstone and rudstone facies. Moreover, the inner shelf facies found to be more porous as compared to open marine facies.

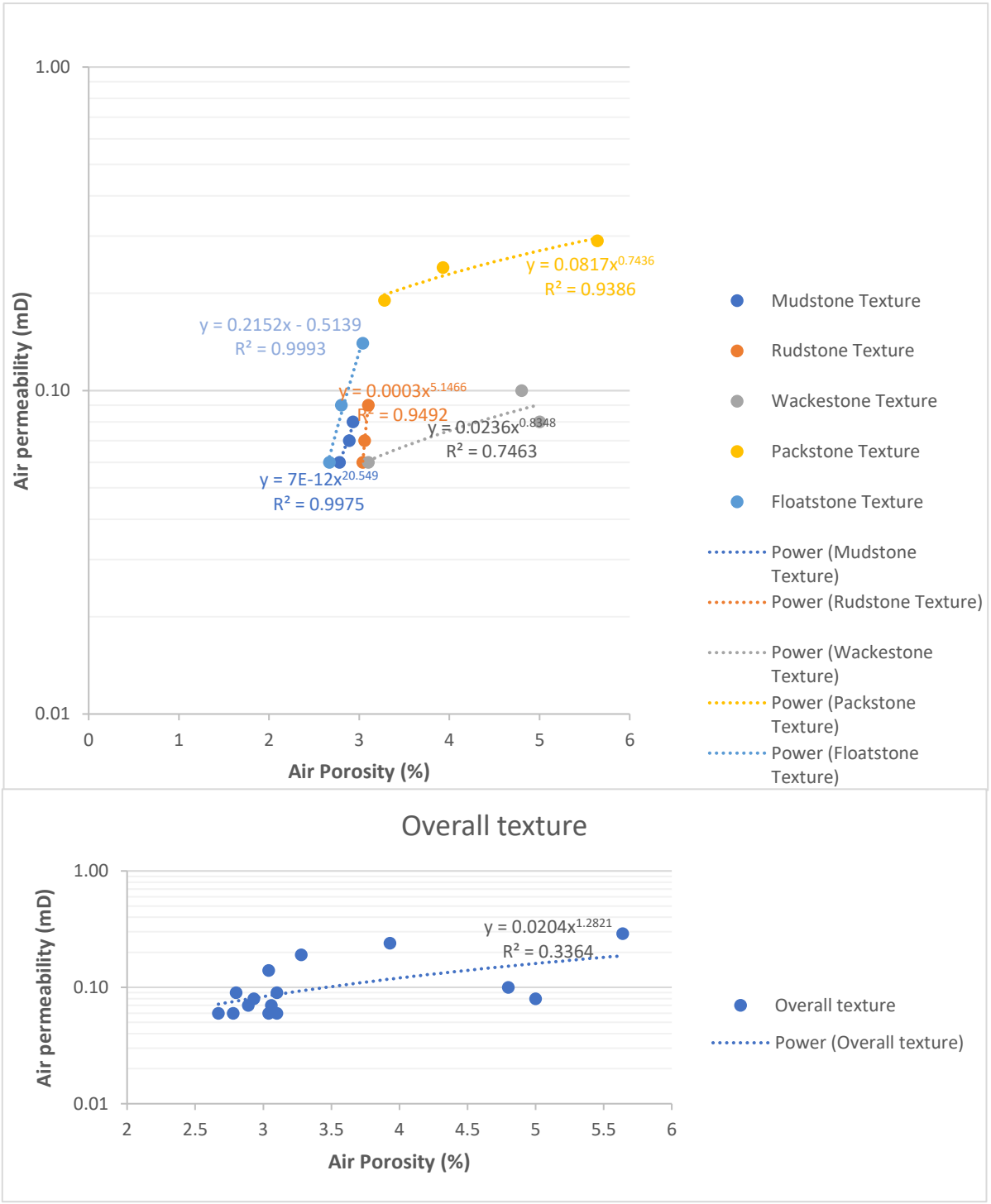


Fig 7.8: showing summary of porosity and permeability relation of depositional texture.

# CHAPTER 8

## SOURCE ROCK

### 8.1 TOC and Rock eval pyrolysis

The total organic carbon (TOC wt.%) and rock eval pyrolysis of selected field samples were conducted to determine the source rock quality of Pirkoh Formation.

The term TOC refer to total organic carbon, which is measured in weight percentage, while the abbreviations S1, S2 and S3 refer to free hydrocarbons, thermal breakage of kerogen, carbon dioxide during the temperature dropping respectively.

**S1:** The flame ionization detector is used to detect and measure S1 peak upon the evaporation of loose hydrocarbon at isothermally condition for 7 mints at the initial temperature of 335°C.

**S2:** At the temperature of 314-610°C (rise of 32°C/min) result to evaporation of organic matter starts and unstable content begins to break up, these hydrocarbons were registered as S2 peak. **T.max**: It is the value measured when the S2 values reached to his peak depending on thermal maturity and the organic matter. It is the maximum temperature at which maximum pyrolysis take place.

**S3:** The trapped CO2 at temperature 310-380°C is released during cooling stage. The temperature increased, the CO2 is released, and during the temperature drop it is detected by the detector called the thermal conductivity detector, which is S3 values (Horsfield, 1985).

The following are the derivates from the later mentioned parameters.

1. Oxygen index (O.I): It is the 100 into the ratio of S3 and TOC in weight percent.
2. Hydrogen index (H.I) It is the 100 into the ratio of S2 and TOC in weight percentage. The cross plot of (H.I) and (O.I) is the function of organic richness in sediments.
3. Production Index (P.I): It is the ration of S1 and sum of S1 and S2.
4. Genetic potential (G.P) is the sum S1 and S2.

## 8.2 Kerogen type and environments

To evaluate the potential of the source rock the type of organic matter is an important factor to be determined. The organic matter present in the rock has influence on the hydrocarbon product, as each types of kerogen has a specific chemical structure and hydrocarbon product. There are four different types of kerogen in a sedimentary rock i.e. type-I (Oil prone) found in the lacustrine and some of the marine facies are oil prone. The type-II (Oil and gas prone) are derived from the sediments of marine comprises of hydrogen organic matter of oil-prone, the oil is the main product of production but also produces more gas. The types III (Gas prone), has low hydrocarbon and generating more gas are the woody plant material derived terrestrial organic matter, while the type-IV kerogen has no capacity of generation, these kerogens are dead or inert carbon (Peters, 1986; Merrill, 1991).

The kerogen type of Pirkoh Formation is determined by the following Van Krevelen diagram indicating type-II kerogen (Fig. 8.1 A). The kerogen environment can be determined by plotting hydrogen index vs oxygen index. The results suggest that more anoxic environment (Fig. 8.1 B).

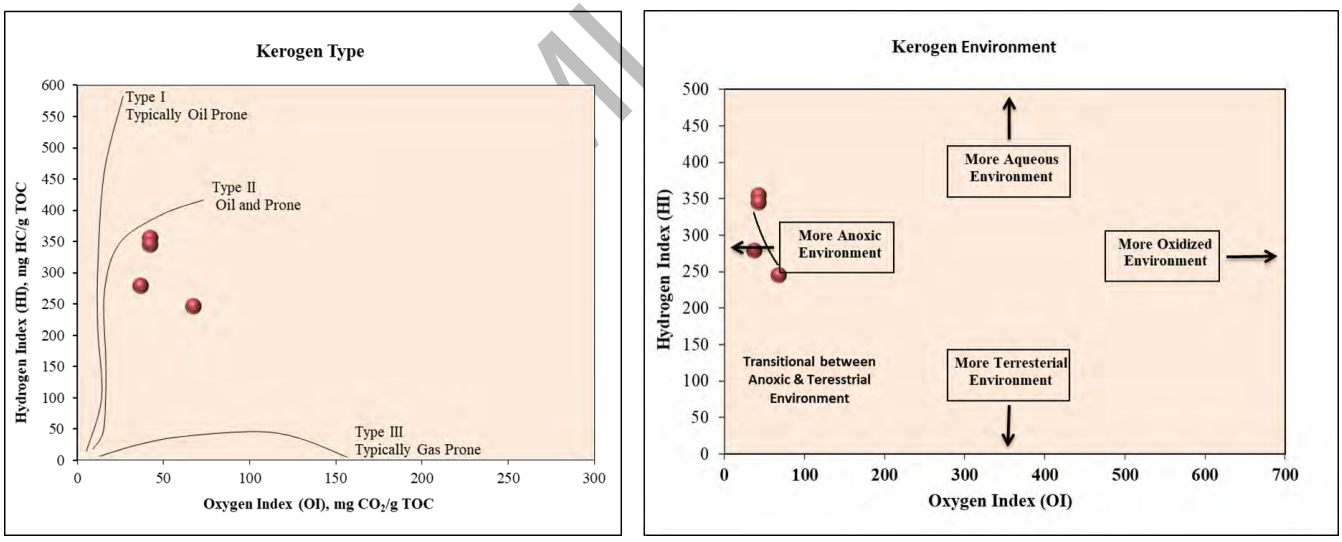


Fig 8.1: (A) showing Kerogen type-II of Pirkoh Formation on modified Van Krevelen diagram,1984 (B) showing plot of H.I vs O.I indicate more anoxic environment of Pirkoh Formation (after Last and Ginn, 2005).

### 8.3 Origin of organic matter generative and potential of source rock

The Indigenous vs non-indigenous hydrocarbons (Hint, 1995) is indicating the autochthonous origin of hydrocarbons of the Pirkoh Formation (Fig. 8.2 A). The limestone preserved in situ well preserved biota, which has good generative potential even with low TOC as compared to that of shale. The total organic content is used to determine the richness of the organic matter of the source rock, which is by weight percent of the organic matter/kerogen. (TOC wt.%).

The higher the total organic content the higher will be the generation potential of source rock. According to (Peters, 1986), the total organic content of the source rock will be of poor generative potential when its values range from 0 to 0.5%. The total organic content between the range of 0.5 to 1% shows the generative potential of the source rock is fair. The total organic content from 1 to 2%, 2 to 4% and greater than 4% signify to good, very good and excellent generative potential of source rock respectively (Fig. 8.2 B table). The Pirkoh Formation shows generative and potential of source rock (Fig. 8.2 B).

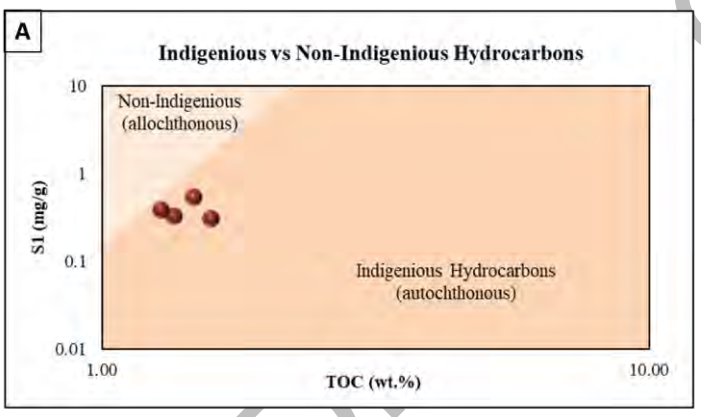


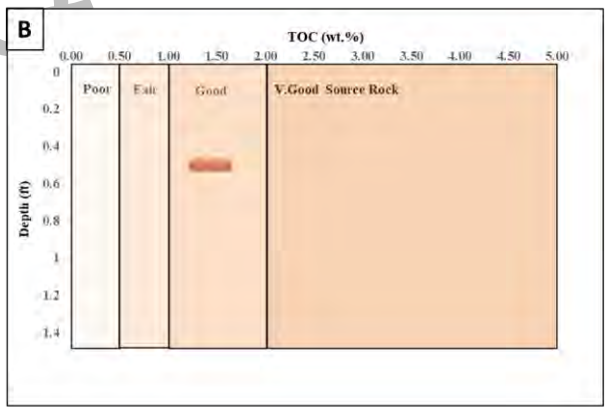


| TOC (wt.%) | Generative potential source rock |
|---|---|
| 0- 0.5 | Poor |
| 0.5-1.0 | Fair |
| 1-2 | Good |
| 2-4 | Very Good |
| >4 | Excellent |

Fig 8.2: (A) showing indigenous vs non-indigenous hydrocarbons (Hint, 1995), and (B) showing the generative potential of source rock (Peters, 1986) of Pirkoh Formation.

## 8.4 Source rock quality

The source rock quality can be determined by plotting genetic potential of source rock versus the total organic content, while the origin of organic matter that produce hydrocarbons can be determined by plotting S1 versus total organic carbon. The Pirkoh Formation shows fair to good source rock quality (Fig. 8.3).

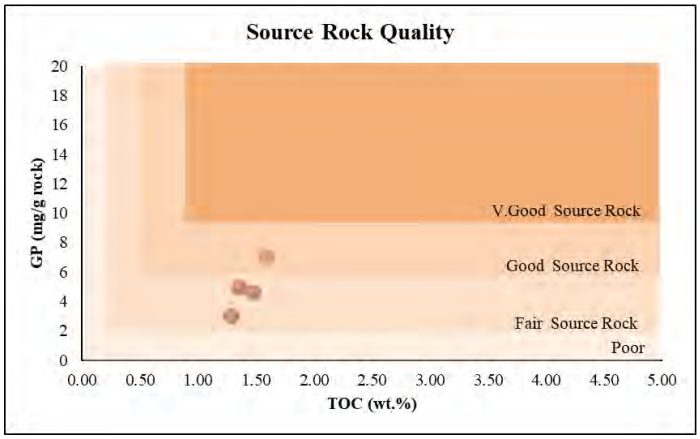


| GP (mg/g) | Genetic potential |
|---|---|
| < 2 | Poor |
| 2-6 | Fair |
| > 6 | Good |

| TOC (wt.%) | Generative potential/quality of source rock |
|---|---|
| 0- 0.5 | Poor |
| 0.5-1.0 | Fair |
| 1-2 | Good |
| 2-4 | Very Good |
| >4 | Excellent |

Fig 8.3: showing source rock quality (Welte and Tissot, 1984; Peters, 1986) of the Pirkoh Formation as fair to good source rock quality.

## 8.5 Maturity and thermal alteration of organic matter

The Maturity of source rock is alteration degree by heating of an organic matter. The influencing factors like the type of organic matter in a source rock, the free hydrocarbon access with combination of other contents i.e., mineral matter and the age and depth of burial influenced the thermal maturity (Welte and Tissot, 1984). The Tmax, Vitrinite Reflectance, and production index is used to assume the evolution of thermal alteration of the organic matter in sedimentary rock. The increase in Tmax, increases the organic matter maturity level. This is related to the nature of chemical reaction with thermal breaking, the stronger the bonds the more temperature is required to break the hydrocarbon chains, while the weaker bond breaks quickly upon low temperature (Whelan and Thompson, 1993)

Tmax and PI is used to calculated the thermal maturity of the organic matter in rocks. The maturity of the rock sample can be calculated by the combination of Tmax and PI. The material is immature if the Tmax is less than 430 ºC and PI is less than 0.2. The organic matter having the Tmax greater than 435 ºC to 465 and PI between 0 to 0.4 is mature. The organic content is considered as post mature, when the Tmax is greater than 465 to 500 and their PI is greater than 0.4 (Peters and Cassa, 1994; Bacon et al., 2000). The Pirkoh Formation shows low degree of thermal alteration of Pirkoh Formation as immature source rock. (Fig. 8.4).

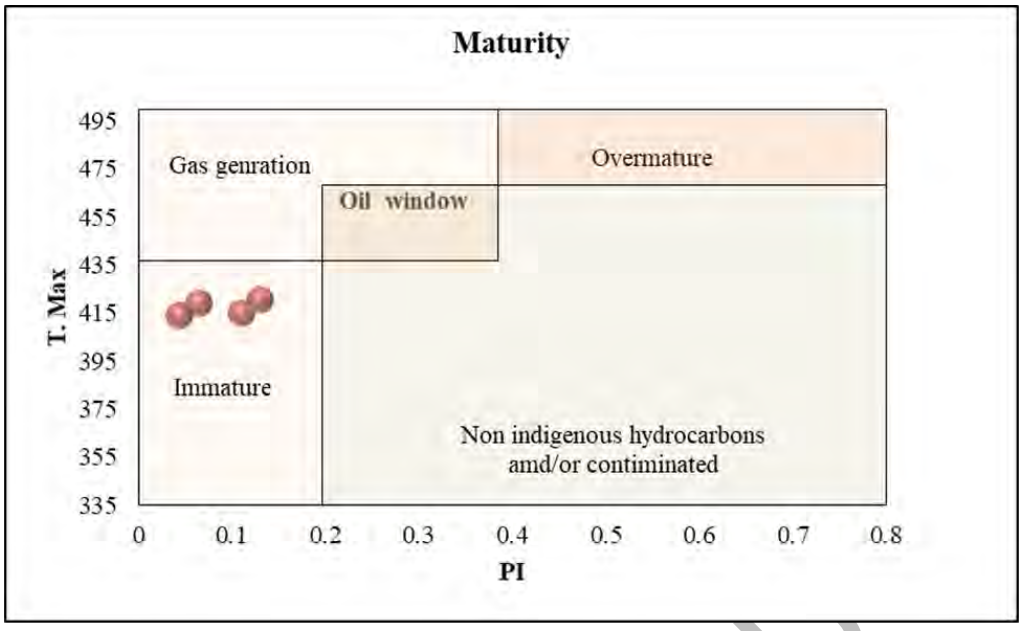


| PI | Tmax (°C) | Maturity | Hydrocarbon zone |
|---|---|---|---|
| < 0.2 | <435 | Immature | None |
| 0.20 - 0.40 | 435-465 | Mature | Oil window |
| >0.4 | >465 | Over mature | Gas generation |

Fig 8.4 showing plot of T. Max vs P.I illustrates maturity and thermal alteration of organic matter (Espitalie et al., 1985; Peters, 1986), indicating low degree of thermal alteration of Pirkoh Formation as immature source rock.

### 8.6 Kerogen type and maturation level

The kerogen type and maturation level of source can be also collectively determined by hydrogen index vs T. Max. The Pirkoh Formation shows mix type II and III kerogen of Pirkoh Formation as immature source rock categorized in pre-oil window (Fig. 8.5).

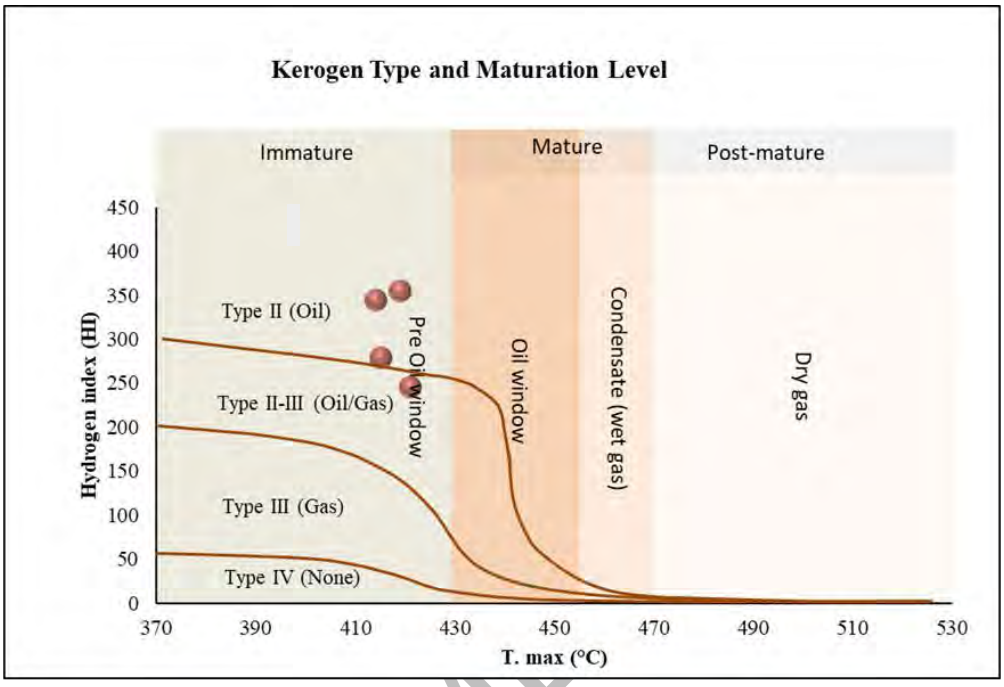


| Kerogen type | HI | Maturity | | Tmax (°C) |
|---|---|---|---|---|
| I | > 600 | Immature | | <430 |
| II | > 300-600 | Mature | Early Mature | 430-445 |
| II/III | 200 - 300 | | Peak Mature | 445-450 |
| III | 50-200 | | Late Mature | 450-470 |
| IV | <50 | Post Mature | | >470 |



Fig 8.5: showing kerogen type and maturation level (Peters and Cassa, 1994) indicating mix type II and III kerogen of Pirkoh Formation as immature source rock fall in pre-oil window.

### 8.7 Genetic potential

The genetic potential (GP) is the sum of S1+S2, which can be defined as the total amount of oil and gas that unit quantity of the source rock could produce if the rock were buried deep enough and long time. According to (Welte and Tissot, 1984), the GP (mgHC/g) ranging less than 2, range between 2 to 6 and greater than 6 signify to considered as poor, moderate, and good source rocks respectively. The Pirkoh Formation shows moderate to good potential (Fig. 8.6).

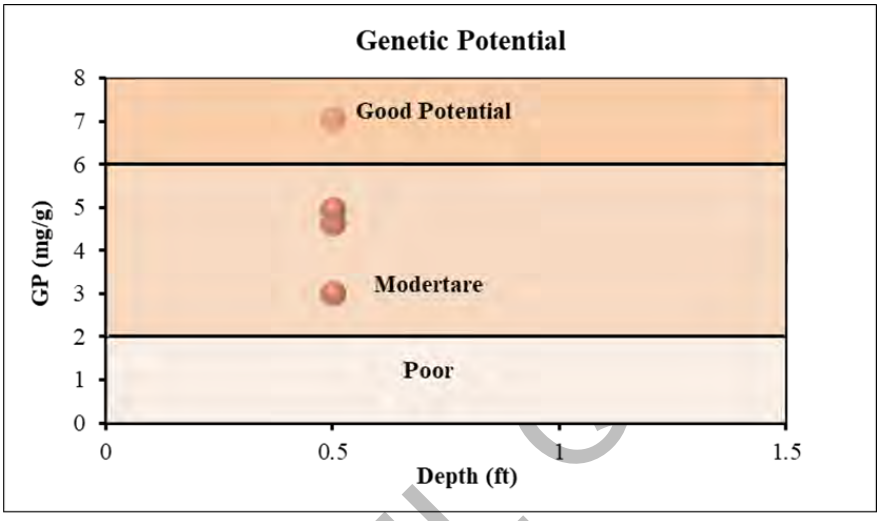


| GP (mg/g) | Genetic potential |
|---|---|
| < 2 | Poor |
| 2-6 | Fair |
| > 6 | Good |

Fig 8. 6 showing genetic potential (Welte and Tissot, 1984) illustrating Pirkoh Formation has moderate to good potential.

### 8.8 Production index (P.I)

The production index (PI) is the ratio of S1 to sum of S1 and S2. The production index is used to measure maturity of source rock as over mature, mature, and immature. The over mature source rock has PI >0.4. The PI indicates to mature source rock if its values range between 0.10 to 0.40, while the immature source rock has PI greater than 0.20. The production index of Pirkoh Formation is indicating immature source rock (Fig. 8.7).

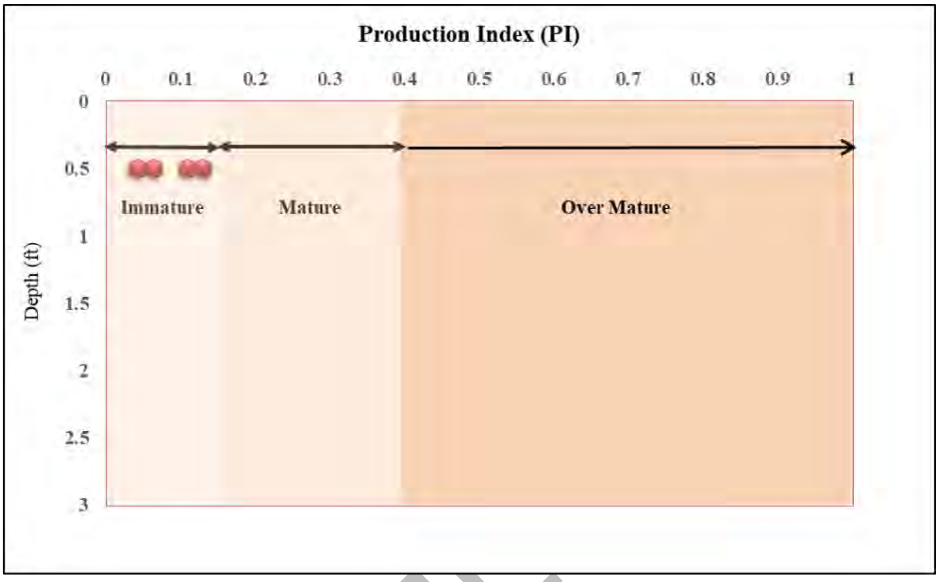


| PI | Maturity |
|---|---|
| < 0.2 | Immature |
| 0.10-0.40 | Mature |
| >0.4 | Over mature |

Fig 8.7: showing Production index (Espitalie et al., 1985), indicating Pirkoh Formation as immature source rock.

## CHAPTER 9

# DISCUSSIONS

The Pirkoh Formation in Zindapir area display white to pale yellow limestone consist of thick bedding in the lower and upper part and thin to medium bedding in the middle part. Although the shale intercalations are present through the outcrop. In Zindapir area Pirkoh Formation has upper transitional contact with Drazinda Formation, and lower conformable contact Domanda Formation. In the exposed outcrop section, the Pirkoh Formation display well preserved shallow benthic foraminifera in the lower part and open marine planktonic foraminifera in the upper part.

The microfacies analyses of Pirkoh Formation unravel the depositional facies, which display the deposition from inner shelf to open outer shelf setting. The inner shelf facies consist of deposition on tidal, open lagoons, inner forereef shelf, reef patch and backreef shelf (MF-MF7). The tidal setting of inner shelf display lime mud texture with early diagenetic dolomitization. The lagoonal facies comprise of abundant planktonic foraminifera with smaller miliolids below the FWWB, in the present study the bioclastic wackestone facie of lagoonal setting display abundant planktonic foraminifera but less small miliolids with scattered bioclast signify to open lagoon with significant water circulation and well oxygenated regime. The backreef shelf facie are display abundant orbitolites and austrotrillina along with nummulites and operculina species. The reef patch facie of inner shelf is evident from the co-occurrence of nummulites, operculina and assilina and from the reworked biota assemblage of back and forereef shelf together. The forereef of inner shelf shallow benthic foraminifera majorly includes nummulites *sp.*, operculina *sp.*, assilina *sp.*, hetrostegina *sp,* and amphistigina *sp*.

The middle shelf facies (MF8 -MF9) are characterized by lime mudstone texture with less than 5% of planktonic foraminifera. The large flat and well preserved orthophragminids, lepidocyclinids, extensive echinoids fragments and abundant of planktonic foraminifera is signifying to open marine outer shelf facies (MF10-MF15) of Pirkoh Formation. The depositional facies of Pirkoh Formation display various diagenetic events in chronological order. The P/B ratio is very low in the inner shelf and middle shelf (less than 5%) expect lagoon facie (40-55%), and it high in the outer shelf setting (greater 90 %).

The eogenesis show micritization mostly in the shallow marine settings with shallow marine dolomitization. The isopachous rim cements are observed in shallow marine to deep marine setting of eogenetic stage, such cements are mostly found on the edges of planktonic

foraminifera of open lagoonal and open marine outer shelf facies. The deep marine and vadose meteoric regime display the fabric selected dissolution in Pirkoh Formation. During mesogenesis, blocky calcite cements precipitate in meteoric (phreatic) and the precipitation continue till the late burial stage of diagenesis. Similarly, the physical compaction continued from mesogenesis and terminate at shallow burial depth resulting to very minor fracturing. At burial depth, the mechanical compaction transformed to chemical compaction resulting to stylolites and selective `dolomitization along the fluids patterns. The last stage of diagenesis during uplifting/telogenesis is resulting fracturing and transparent telogenetic calcite vein filling.

The depositional porosity and permeability of Pirkoh Formation overall results of the selected samples are studied and according to the reservoir rank classification is ranked poor and categorized tight reservoir, and the quality of depositional facies display overall impervious reservoir. However, in field observation the outcrop shows significant fractures, and dissolution thus it is classified as secondary reservoir in the petroleum play. The source rock results display fear to good reservoir potential but consist of immature source rock. However, at greater depth the Pirkoh Formation can be a good source rock.

## CONCLUSION

The present study is revealing the depositional facies of middle to late Eocene Pirkoh Formation in Zindapir anticline of eastern Sulaiman province, Dera Ghazi Khan, Pakistan. The carbonate rocks in the study area are of great importance because it is typical representative of tethyan carbonate shelf deposits with well-preserved marine biota. Moreover, the study is virgin to literature with very minor to no past research. The microfacies analyses of Pirkoh Formation is representing total fifteen micro-facies (MF1-MF15) categorized in three major facies assemblages i.e., inner, middle, and outer shelf based on their depositional setting on carbonate platform. The facies assemblages are typical representative of Tethyan carbonate shelf. The inner shelf facies are deposited on tidal setting facie is characterized by lime mudstone, open lagoon facie showing reworked bioclasts with planktonic foraminifera and smaller miliolids. The backreef shelf facies of inner shelf display orbitolites, austrotrillina, flat nummulites, and operculina species. The reef flat setting shows the diversity of larger benthic foraminifera of both forereef shelf and backreef shelf. The forereef shelf facies are exhibiting well preserved amphistigina in association with other LBF. The middle shelf facies are represented by characterized by lime mud-stone texture and low P/B ratio less than 5%, while the outer shelf facies are consisting of wackestone and packstone texture display high P/B ratio greater than 90%, with co-occurrence of extensive occurrence of echinoid fragments and large flat and well-preserved nummulites and orthophragminids in pelagic matrix. The outcrop after detail investigation showing shallow to deep marine facies trending west to east from the lower part to upper part of the formation. The depositional facies show reservoir rank as tight and impervious, but secondary reservoir based on high density fractures at outcrop scale. Moreover, it displays immature source rock of fear to good quality. The Pirkoh Formation is a candidate for representing the reconstruction of tethyan carbonate shelf on the edge of Indian plate exposed in Zindapir Anticline in DG Khan, Pakistan.

## REFERENCES


Abuamarah, B.A. and Nabawy, B.S., 2021. A proposed classification for the reservoir quality assessment of hydrocarbon-bearing sandstone and carbonate reservoirs: A correlative study based on different assessment petrophysical procedures. Journal of Natural Gas Science and Engineering, 88, p.103807.

Adabi, M.H., and Rao, C.P., 1996. Petrographic, elemental and isotopic criteria for the recognition of carbonate mineralogy and climates during the Jurassic (examples from Iran and England). In 13th Australian Geological Convention (Vol. 41, p. 6).

Adabi, M.H., Zohdi, A., Ghabeishavi, A. and Amiri-Bakhtiyar, H., 2008. Applications of nummulitids and other larger benthic foraminifera in depositional environment and sequence stratigraphy: an example from the Eocene deposits in Zagros Basin, SW Iran. Facies, 54(4), pp.499-512.

Adams, C.G., 1965. The foraminifera and stratigraphy of the Melinau Limestone, Sarawak, and its importance in Tertiary correlation. Quarterly Journal of the Geological Society, 121(1-4), pp.283-338.

Aigner, T., 1983. Facies and origin of nummulitic buildups: an example from the giza pyramids plateau (middle eocene, egypt). fossil-lagerstaetten nr. 57.

Alabere, A.O., Akangbe, O.K. and Akande, S.O., 2020. Petrography and paleo-depositional environment of the campanian-maastrichtian patti formation exposed at AHOKO North Central Nigeria. IOSR J Appl Geol Geophys, 8(5), pp.39-49.

Amaefule, J.O., Altunbay, M., Tiab, D., Kersey, D.G. and Keelan, D.K., 1993, October. Enhanced reservoir description: using core and log data to identify hydraulic (flow) units and predict permeability in uncored intervals/wells. In SPE annual technical conference and exhibition. OnePetro.

Arni, P. and Lanterno, E., 1972. Considérations paléoécologiques et interprétation des calcaires de l'Éocène du Véronais.

Arni, P., 1965. L'évolution des Nummulitinae en tant que facteur de modification des dépôts littoraux. Mémoires du BRGM (Paris), (32), pp.7-20.

Asis, J. and Jasin, B., 2015. Miocene larger benthic foraminifera from the Kalumpang Formation in Tawau, Sabah. Sains Malaysiana, 44(10), pp.1397-1405.

Bacon, C.A., Calver, C.R., Boreham, C.J., Leaman, D.E., Morrison, K.C., Revill, A.T. and Volkman, J.K., 2000. The petroleum potential of onshore Tasmania: a review.

Banks, C.J. and Warburton, J., 1986. 'Passive-roof'duplex geometry in the frontal structures of the Kirthar and Sulaiman Mountain belts, Pakistan. Journal of structural Geology, 8(3-4), pp.229-237.

Banner, F.T., Simmons, M.D. and WITTAKER, J., 1991. The Mesozoic chrysalidinidae (Foraminifera, Textulariacea) of the middle East: the Redmond (Aramco) taxa and their relatives. Bulletin of the British Museum, Natural History. Geology, 47(2), pp.101-152.

Beavington-Penney, S.J., Wright, V.P. and Racey, A., 2006. The middle Eocene Seeb Formation of Oman: an investigation of acyclicity, stratigraphic completeness, and accumulation rates in shallow marine carbonate settings. Journal of Sedimentary Research, 76(10), pp.1137-1161.

Beavington-Penny, S.J.W.V.P. and Racey, A., 2006. Carbonate sedimentation-The middle Eocene Seeb Formation of Oman: An investigation of acyclicity, stratigraphic completeness, and accumulation rates in shallow marine carbonate. Journal of Sedimentary Research, 76(9-10), pp.1137-1161.

Bernard, M., Shen-Tu, B., Holt, W.E. and Davis, D.M., 2000. Kinematics of active deformation in the Sulaiman Lobe and Range, Pakistan. Journal of Geophysical Research: Solid Earth, 105(B6), pp.13253-13279.

Blondeau, A., 1972, Les Nummulites. Vuibert, Paris, 245p.

Boudaugher-Fadel, M.K., 2018. Evolution and geological significance of larger benthic foraminifera. UCL press.

Brown, J.S., 1943. Suggested use of the word microfacies.Economic Geology, 38, p. 325

Burchette, T.P. and Wright, V.P., 1992. Carbonate ramp depositional systems. Sedimentary geology, 79(1-4), pp.3-57.

Buxton, M.W.N. and Pedley, H.M., 1989. Short paper: a standardized model for Tethyan Tertiary carbonate ramps. Journal of the Geological Society, 146(5), pp.746-748.

Chaproniere, G.C., 1975. Palaeoecology of Oligo-Miocene larger Foraminiferida, Australia. Alcheringa, 1(1), pp.37-58.

Choquette, P.W., James, N.P., McIlreath, I.A. and Morrow, D., 1990. Diagenesis. Geoscience Canada, 10(4).

Cole, W.S., 1957. Variation in American Oligocene species of Lepidocyclina. Paleontological Research Institution.

Coniglio, M., Sherlock, R., Williams-Jones, A.E., Middleton, K. and Frape, S.K., 1994. Burial and hydrothermal diagenesis of Ordovician carbonates from the Michigan Basin, Ontario, Canada. Dolomites: A Volume in Honour of Dolomieu, pp.231-254.

Ćosović, V., Drobne, K. and Moro, A., 2004. Paleoenvironmental model for Eocene foraminiferal limestones of the Adriatic carbonate platform (Istrian Peninsula). Facies, 50, pp.61-75002E

Cuvillier, J., 1952. Le notion de 'microfacies' et ses applications. – VIII Congreso Nazionale di Metano e Petroleo, sect. I, 1-7

Davies L.M. 1941.Correlation of Laki beds. Geol. Mag. Vol. 78, 151-152.

Davies, G.R. and Smith, L.B., 2006. Structurally controlled hydrothermal dolomite reservoir facies: An overview. AAPG bulletin, 90(11), pp.1641-1690.

Davis, D.M. and Lillie, R.J., 1994. Changing mechanical response during continental collision: active examples from the foreland thrust belts of Pakistan. Journal of Structural Geology, 16(1), pp.21-34.

Deschamps, R., Kohler, E., Gasparrini, M., Durand, O., Euzen, T. and Nader, F., 2012. Impact of mineralogy and diagenesis on reservoir quality of the Lower Cretaceous Upper Mannville Formation (Alberta, Canada). Oil & Gas Science and Technology–Revue d'IFP Energies nouvelles, 67(1), pp.31-58.

Ding, H., Zhang, Z., Dong, X., Tian, Z., Xiang, H., Mu, H., Gou, Z., Shui, X., Li, W. and Mao, L., 2016. Early Eocene (c. 50 Ma) collision of the Indian and Asian continents: Constraints from the North Himalayan metamorphic rocks, southeastern Tibet. Earth and Planetary Science Letters, 435, pp.64-73.

Dunham, R.J., 1962. Classification of carbonate rocks according to depositional textures.

Eames F.E. 1952. A contribution to the study of the Eocene in West Pakistan and western India; Part A, The geology of standard sections in the western Punjab and in the Kohat district. Part B, Description of the fauna of certain standard sections and their bearing on the classification and correlation of the Eocene in Western Pakistan and Western India. Quart. J. Geol. Soc. London, 107, pt. 2, 159-200.

Eichenseer, H. and Luterbacher, H., 1992. The marine Paleogene of the Tremp Region (NE Spain)-depositional sequences, facies history, biostratigraphy and controlling factors. Facies, 27, pp.119-151.

Espitalié, J., Madec, M., Tissot, B., Mennig, J.J. and Leplat, P., 1977, May. Source rock characterization method for petroleum exploration. In Offshore Technology Conference. OnePetro.

Fermont, W.J.J., 1982. Discocyclinidae from Ein Avedat (Israel) (Doctoral dissertation, Utrecht University).

Fermont, W.J.J., 1982. Discocyclinidae from Ein Avedat (Israel) (Doctoral dissertation, Utrecht University).

Flugel, E., 1982. Microfacies analysis of limestones. Berlin: Springer-Verlag. pp: 633.

Flügel, E., 2013. Microfacies of carbonate rocks: analysis, interpretation and application. Springer Science and Business Media, Berlin

Geel, T., 2000. Recognition of stratigraphic sequences in carbonate platform and slope deposits: empirical models based on microfacies analysis of Palaeogene deposits in southeastern Spain. Palaeogeography, palaeoclimatology, palaeoecology, 155(3-4), pp.211-238.

Goldsmith, J.W., MacLachlan, J.C. and Madge, M.R., 1959. Paleotectonic maps of the Triassic System: US Geol. Survey, Misc. Geol. Inv. Map, pp.1-300.

Harris, M.K., Thayer, P.A. and Amidon, M.B., 1997. Sedimentology and depositional environments of middle Eocene terrigenous-carbonate strata, southeastern Atlantic Coastal Plain, USA. Sedimentary Geology, 108(1-4), pp.141-161.

Hemphill W.R., Kidwai A.H. 1973. Stratigraphy of the Bannu and Dera Ismail Khan areas, Pakistan.U.S. Geol. Surv. Prof. Paper 716B, 36Pp.

Horsfield, B., 1997. The bulk composition of first-formed petroleum in source rocks. Petroleum and basin evolution: Insights from petroleum geochemistry, geology and basin modeling, pp.335-402.

Hottinger, L., 1993. Recent foraminifera from the Gulf of Aqaba, Red Sea. Opera/Academia Scientiarum et Artium Slovenica, Class IV: Historia noturalis, 33 and Znanstvenoraziskovalni Tsenter SAZU. Paleontoloski Institut lvana Rakovca, 3, pp.1-179.

Humayon, M., Lillie, R.J. and Lawrence, R.D., 1991. Structural interpretation of the eastern Sulaiman foldbelt and foredeep, Pakistan. Tectonics, 10(2), pp.299-324.

Hurley, N. F., and Ron Budros. "Albion-scipio and stoney point fields-USA, Michigan Basin." (1990): 1-37.

Iqbal M.W.A. 1969. The Tertiary pelecypod and gastropod fauna from Drug, Zinda Pir, Vidor (Distt. D.G. Khan), Jhalar and Charrat (Distt. Campbellpur), West Pak. GSP. Mem. Paleont. Pakistanica 6: 77p.

Iqbal M.W.A., Shah S.M.I. 1980. A guide to the stratigraphy of Pakistan. GSP Rec. 53.

Iqbal, M. and Helmcke, D., 2004. Geological interpretation of earthquakes data of Zindapir Anticlinorium, Sulaiman foldbelt, Pakistan. Pakistan journal of Hydrocarbon Research, 14, pp.41-47.

Iqbal, M. and Khan, M.R., 2012. Impact of Indo-Pakistan and Eurasian Plates Collision in the Sulaiman Fold Belt, Pakistan. Search and Discovery Article, 50575.

Jadoon, I.A., Lawrence, R.D. and Hassan, K.S., 1994. Mari-Bugti pop-up zone in the central Sulaiman fold belt, Pakistan. Journal of Structural Geology, 16(2), pp.147-158.

Jadoon, I.A.K. and Zaib, M.O., 2018. Tectonic map of Sulaiman fold belt: 1: 500,000 scale. COMSATS University Islamabad (Abbottabad Campus), Pakistan.

Jadoon, I.A.K., Lawrence, R.D. and Lillie, R.J., 1992. Balanced and retrodeformed geological cross-section from the frontal Sulaiman Lobe, Pakistan: Duplex development in thick strata along the western margin of the Indian Plate. Thrust tectonics, pp.343-356.

Jadoon, I.A.K., Lawrence, R.D. and Lillie, R.J., 1992. Balanced and retrodeformed geological cross-section from the frontal Sulaiman Lobe, Pakistan: Duplex development in thick strata along the western margin of the Indian Plate. Thrust tectonics, pp.343-356.

Jadoon, I.A.K., Lawrence, R.D. and Lillie, R.J., 1993. Evolution of foreland structures: An example from the Sulaiman thrust lobe of Pakistan, southwest of the Himalayas. Geological Society, London, Special Publications, 74(1), pp.589-602.

James, N.P. and Choquette, P.W., 1984. Diagenesis 9. Limestones-the meteoric diagenetic environment. Geoscience Canada, 11(4), pp.161-194.

Kadri, I.B., 1995. Petroleum geology of Pakistan. Pakistan Petroleum Limited.

Kamali, M.R. and REZAEE, R., 2012. Identification and evaluation of unconventional hydrocarbon reserves: examples from Zagros and Central Iran Basins.

Kazmi, A.H. and Jan, M.Q., 1997. Geology and tectonics of Pakistan. Graphic publishers.

Kazmi, A.H. and Rana, R.A., 1982. Tectonic map of Pakistan 1: 2 000 000: Map showing structural features and tectonic stages in Pakistan. Geological survey of Pakistan.

Khalifa, M.A. and Zaghloul, E.A., 1990. Carbonate lithofacies and depositional environments of the Lower Eocene Farafra Limestone, Farafra Oasis, Western Desert, Egypt. Journal of African Earth Sciences (and the Middle East), 11(3-4), pp.281-289.

Khan, Z.A. and Tewari, R.C., 2016. The facts and fictions of the Oceanic Tethys concept. Jour. Geosciences, 1, pp.12-41.

Khanin, A.A., 1965. Osnovnye ucheniya o porodakhkollektorakh nefti i gaza [Main Studies of Oil and Gas Reservoir Rocks]. Publishing House Nedra, Moscow.

Khanin, A.A., 1969. Porody-kollektory nefti i gaza i ikh izuchenie [Oil and Gas Reservoir Rocks and Their Study]. Publishing House Nedra, Moscow.

Kiessling, W., 2002. Secular variations in the Phanerozoic reef ecosystem.

Kiessling, W., Flügel, E. and Golonka, J., 1999. Paleoreef maps: evaluation of a comprehensive database on Phanerozoic reefs. AAPG bulletin, 83(10), pp.1552-1587.

Lan, C., Yang, M. and Zhang, Y., 2016. Impact of sequence stratigraphy, depositional facies and diagenesis on reservoir quality: A case study on the Pennsylvanian Taiyuan sandstones, northeastern Ordos Basin, China. Marine and Petroleum Geology, 69, pp.216-230.

Lapponi, F., Bechstaedt, T., Boni, M., Banks, D.A. and Schneider, J., 2014. Hydrothermal dolomitization in a complex geodynamic setting (Lower Palaeozoic, northern Spain). Sedimentology, 61(2), pp.411-443.

Lawrence, R.D., Yeats, R.S., Khan, S.H., Farah, A. and DeJong, K.A., 1981. Thrust and strike slip fault interaction along the Chaman transform zone, Pakistan. Geological Society, London, Special Publications, 9(1), pp.363-370.

Less, G., 1987. Paleontology and stratigraphy of the European Orthophragminae. Geologica Hungarica series Palaeontologica, 51, pp.1-373.

Lloyd, R.M., 1977. Porosity Reduction By Chemical Compaction-Stable-Isotope Model.

Lucia, F. J., 2007. Carbonate Reservoir Characterization: An Integrated Approach. 2nd edn. Berlin Heidelberg: Springer-Verlag. • Machel, H.G. and Anderson, J.H., 1989. Pervasive subsurface dolomitization of the Nisku Formation in central Alberta. Journal of Sedimentary Research, 59(6), pp.891-911.

Machel, H.G. and Anderson, J.H., 1989. Pervasive subsurface dolomitization of the Nisku Formation in central Alberta. Journal of Sedimentary Research, 59(6), pp.891-911.

Machel, H.G. and Buschkuehle, B.E., 2008. Diagenesis of the Devonian Southesk-Cairn Carbonate Complex, Alberta, Canada: marine cementation, burial dolomitization,

thermochemical sulfate reduction, anhydritization, and squeegee fluid flow. Journal of Sedimentary Research, 78(5), pp.366-389.

Machel, H.G. and Mountjoy, E.W., 1986. Chemistry and environments of dolomitization—a reappraisal. Earth-Science Reviews, 23(3), pp.175-222.

Machel, H.G., 1988. Fluid flow direction during dolomite formation as deduced from trace element trends.

Machel, H.G., 1999. Effects of groundwater flow on mineral diagenesis, with emphasis on carbonate aquifers. Hydrogeology Journal, 7(1), pp.94-107.

Machel, H.G., 2004. Concepts and models of dolomitization: a critical reappraisal. Geological Society, London, Special Publications, 235(1), pp.7-63. • Machel, H.G., 2005. Investigations of burial diagenesis in carbonate hydrocarbon reservoir rocks. Geoscience Canada.

Mansurbeg, H., Caja, M.A., Marfil, R., Morad, S., Remacha, E., Garcia, D., Martin-Crespo, T., El-Ghali, M.A.K. and Nystuen, J.P., 2009. Diagenetic evolution and porosity destruction of turbiditic hybrid arenites and siliciclastic sandstones of foreland basins: evidence from the Eocene Hecho Group, Pyrenees, Spain. Journal of Sedimentary Research, 79(9), pp.711-735.

Martín-Martín, J.D., Gomez-Rivas, E., Bover-Arnal, T., Travé, A., Salas, R., Moreno-Bedmar, J.A., Tomás, S., Corbella, M., Teixell, A., Vergés, J. and Stafford, S.L., 2013. The Upper Aptian to Lower Albian syn-rift carbonate succession of the southern Maestrat Basin (Spain): Facies architecture and fault-controlled stratabound dolostones. Cretaceous Research, 41, pp.217-236.

Maxwell, W.G.H., 1968. Atlas of the great barrier reef.

Maxwell, W.G.H., Day, R.W. and Fleming, P.J.G., 1961. Carbonate sedimentation on the Heron Island reef, Great Barrier reef. Journal of Sedimentary Research, 31(2), pp.215-230.

Merrill, R.K., 1991. Source and migration processes and evaluation techniques.

Middleton, K., Coniglio, M., Sherlock, R. and Frape, S.K., 1993. Dolomitization of Middle Ordovician carbonate reservoirs, southwestern Ontario. Bulletin of Canadian Petroleum Geology, 41(2), pp.150-163.

Nebelsick, J.H., Rasser, M.W. and Bassi, D., 2005. Facies dynamics in Eocene to Oligocene circumalpine carbonates. Facies, 51, pp.197-217.

Peresson, H. and Daud, F., 2009. Integrating Structural Geology and GIS: Wrench tectonics and exploration potential in the eastern Sulaiman fold belt. In Proceedings, Pakistan Association of Petroleum Geoscientists (PAPG)/Society of Petroleum Engineers (SPE) Annual Technical Conference, Islamabad, Pakistan, November 17th to 18th.

Peters, K.E. and Cassa, M.R., 1994. Applied source rock geochemistry: Chapter 5: Part II. Essential elements.

Peters, K.E., 1986. Guidelines for evaluating petroleum source rock using programmed pyrolysis. AAPG bulletin, 70(3), pp.318-329.

Petterson, M.G. and Windley, B.F., 1985. RbSr dating of the Kohistan arc-batholith in the Trans-Himalaya of north Pakistan, and tectonic implications. Earth and Planetary Science Letters, 74(1), pp.45-57.

Prouty, C.E., 1988. Trenton Exploration and Wrenching Tectonics--Michigan Basin and Environs: Chapter 14.

Quittmeyer, R.C. and Kafka, A.L., 1984. Constraints on plate motions in southern Pakistan and the northern Arabian Sea from the focal mechanisms of small earthquakes. Journal of Geophysical Research: Solid Earth, 89(B4), pp.2444-2458.

Racey, A., 2001. A review of Eocene nummulite accumulations: structure, formation and reservoir potential. Journal of petroleum geology, 24(1), pp.79-100.

Raza S.M., Khan S.H., Karim T., Ali M. 2001. Stratigraphic Chart of Pakistan, published by Geological Survey of Pakistan.

Shah S.M.I. 1980. Stratigraphy and economic geology of central salt range. GSP, Rec. 52, 104p.

Redfearn, D.P., Trim, G.M., Skanes, A.C., Petrellis, B., Krahn, A.D., Yee, R. and Klein, G.J., 2005. Esophageal temperature monitoring during radiofrequency ablation of atrial fibrillation. Journal of cardiovascular electrophysiology, 16(6), pp.589-593.

Reid, R.P. and Macintyre, I.G., 2000. Microboring versus recrystallization: further insight into the micritization process. Journal of Sedimentary Research, 70(1), pp.24-28.

Reiss, Z., Hottinger, L., 1984. The Gulf of Aqaba: Ecological Micropaleontology. Ecological Studies, Springer- Verlag, Berlin, 50, pp. 1– 354.

Reynolds, K., Copley, A. and Hussain, E., 2015. Evolution and dynamics of a fold-thrust belt: the Sulaiman Range of Pakistan. Geophysical Journal International, 201(2), pp.683-710.

Rikhtegarzadeh, M., Vaziri, S.H., Aleali, M., Bakhtiar, H.A. and Jahani, D., 2016. Microbiostratigraphy, microfacies and depositional environment of the Sarvak Formation in Bi Bi Hakimeh oil field (well no. 29), southwest Iran. International Journal of Geography and Geology, 5(10), pp.194-208.

Saif-Ur-Rehman, K.J., Ding, L., Jadoon, I.A., Baral, U., Qasim, M. and Idrees, M., 2019. Interpretation of the Eastern Sulaiman fold-and-thrust belt, Pakistan: A passive roof duplex. Journal of Structural Geology, 126, pp.231-244.

Searle, M.P., Khan, M.A., Fraser, J.E., Gough, S.J. and Jan, M.Q., 1999. The tectonic evolution of the Kohistan-Karakoram collision belt along the Karakoram Highway transect, north Pakistan. Tectonics, 18(6), pp.929-949.

Sengor, A.M.C., Altiner, D., Cin, A., Ustaomer, T. and Hsu, K.J., 1988. Origin and assembly of the Tethyside orogenic collage at the expense of Gondwana Land.

Shah, S.M.I., 1977, Precambrian and Paleozoic of Pakistan. In Shah, S.M.I, (ed.) Stratigraphy of Pakistan. Geol. Surv. Pakistan, Mem., Vol. 12, pp. 1-5.

Shogenov, K., Shogenova, A., Vizika-Kavvadias, O. and Nauroy, J.F., 2015. Reservoir quality and petrophysical properties of Cambrian sandstones and their changes during the experimental modelling of CO^ sub 2^ storage in the Baltic Basin. Estonian Journal of Earth Sciences, 64(3), p.199.

Siddiqui, N.K. and Jadoon, I.A.K., 2013. Indo-Eurasian plate collision and the evolution of Pak-Iran Makran Microplate, Pishin-Katawaz fault block and the Porali trough. Search and Discovery Article, 30265, pp.3-5.

Sinclair, H.D., Sayer, Z.R. and Tucker, M.E., 1998. Carbonate sedimentation during early foreland basin subsidence: the Eocene succession of the French Alps. Geological Society, London, Special Publications, 149(1), pp.205-227.

Sirotti, A., 1982. Phylogenetic classification of Lepidocyclinidae: a proposal. Bollettino della Societa Paleontologica Italiana, 21, pp.99-112.

Tahirkheli, R.K., 1979. The India-Eurasia suture zone in northern Pakistan: Synthesis and interpretation of recent data at plate scale. Geodynamics of Pakistan, pp.125-130.

Taylor, T.R., Giles, M.R., Hathon, L.A., Diggs, T.N., Braunsdorf, N.R., Birbiglia, G.V., Kittridge, M.G., Macaulay, C.I. and Espejo, I.S., 2010. Sandstone diagenesis and reservoir quality prediction: Models, myths, and reality. AAPG bulletin, 94(8), pp.1093-1132.

Treloar, P.J. and Izatt, C.N., 1993. Tectonics of the Himalayan collision between the Indian plate and the Afghan block: A synthesis. Geological Society, London, Special Publications, 74(1), pp.69-87.

Vincent, B., Emmanuel, L., Houel, P. and Loreau, J.P., 2007. Geodynamic control on carbonate diagenesis: petrographic and isotopic investigation of the Upper Jurassic formations of the Paris Basin (France). Sedimentary Geology, 197(3-4), pp.267-289.

Waheed, A. and Wells, N.A., 1990. Changes in paleocurrents during the development of an obliquely convergent plate boundary (Sulaiman fold-belt, southwestern Himalayas, west-central Pakistan). Sedimentary Geology, 67(3-4), pp.237-261.

Wanas, H.A., 2008. Cenomanian rocks in the Sinai Peninsula, Northeast Egypt: Facies analysis and sequence stratigraphy. Journal of African Earth Sciences, 52(4-5), pp.125-138.

Wanas, H.A., Shama, A.A. and El-Nahrawy, S.A., 2020. Depositional model and sequence stratigraphy of the Paleocene-Lower Eocene succession in the Farafra Oasis, Western Desert, Egypt. Journal of African Earth Sciences, 162, p.103706.

Welte, D.H. and Tissot, P., 1984. Petroleum formation and occurrence. Springer-verlag.

Whelan, J.K. and Thompson-Rizer, C.L., 1993. Chemical methods for assessing kerogen and protokerogen types and maturity. Organic Geochemistry: Principles and Applications, pp.289-353.

Wilson, J.L., 1975. Carbonate facies in geologic history Springer-Verlag. New York, 471.

Yazdi-Moghadam, M., Sarfi, M., Ghasemi-Nejad, E., Sadeghi, A. and Sharifi, M., 2021. Early Miocene larger benthic foraminifera from the northwestern Tethyan Seaway (NW Iran): new findings on Shallow Benthic Zone 25. International Journal of Earth Sciences, 110, pp.719-740.

Yoo, C.M., Gregg, J.M. and Shelton, K.L., 2000. Dolomitization and dolomite neomorphism: Trenton and Black River limestones (middle Ordovician) northern Indiana, USA. Journal of Sedimentary Research, 70(1), pp.265-274.

Zahid, M.A., Chunmei, D., Lin, C., Gluyas, J., Jones, S., Zhang, X., Munawar, M.J. and Ma, C., 2016. Sequence stratigraphy, sedimentary facies and reservoir quality of Es4s, southern slope of Dongying Depression, Bohai Bay Basin, East China. Marine and Petroleum Geology, 77, pp.448-470.

Zenger, D.H., Dunham, J.B. and Ethington, R.L., 1980. Concepts and models of dolomitization.

Zhao, Z.J., Zhang, Y.B., Pan, M., Wu, X.N. and Pan, W.Q., 2010. Cambrian sequence stratigraphic framework in Tarim Basin. Geological Review, 56(5), pp.609-620.

Ahmed Jr, S., Rigby, S., Kroon, D., Khan, S., Hanif, M. and Ahmed Sr, S., 2011. Integrated Paleogene sequence stratigraphy of the Kohat Basin, Northwest Pakistan. Pakistan Journal of Hydrocarbon Research, 21, pp.41-47.

## Appendix-I

(Plug Analysis)

| Sample No. | Texture | Air Permeability K (mD) | Air Porosity ØHe (%) | Normalized Porosity ØZ (dec) | RQI | FZI |
|---|---|---|---|---|---|---|
| CS3 | Mudstone | 0.07 | 2.89 | 0.02976 | 0.0481 | 1.616263 |
| CS13 | Mudstone | 0.06 | 2.78 | 0.02859 | 0.0454 | 1.587968 |
| CS11 | Mudstone | 0.08 | 2.93 | 0.03018 | 0.0511 | 1.693174 |
| ZS8 | Rudstone | 0.09 | 3.1 | 0.03199 | 0.05266 | 1.646139 |
| ZS9 | Rudstone | 0.07 | 3.06 | 0.0315 | 0.0468 | 1.485714 |
| ZS10 | Rudstone | 0.06 | 3.04 | 0.03135 | 0.0511 | 1.629984 |
| CS2 | Wackestone | 0.08 | 5 | 0.056 | 0.0387 | 0.691071 |
| ZS1 | Wackestone | 0.10 | 4.8 | 0.054 | 0.0442 | 0.818519 |
| ZS13 | Wackestone | 0.06 | 3.1 | 0.03199 | 0.043 | 1.34417 |
| CS1 | Packstone | 0.29 | 5.64 | 0.05977 | 0.0691 | 1.156098 |
| ZS5 | Packstone | 0.19 | 3.28 | 0.03391 | 0.0743 | 2.191094 |
| ZS12 | Packstone | 0.24 | 3.93 | 0.0409 | 0.076 | 1.858191 |
| CS4 | Floatstone | 0.06 | 2.67 | 0.0274 | 0.01469 | 0.536131 |
| CS8 | Floatstone | 0.14 | 3.04 | 0.03135 | 0.0663 | 2.114833 |
| ZS7 | Floatstone | 0.09 | 2.8 | 0.0288 | 0.0555 | 1.927083 |

**Appendix-II**

(Source Rock Analysis)

| Sample no. | TOC (wt %) | S1 (HC mg/g) | S2 (HC mg/g ) | S3 (CO2 mg/g) | T max | GP | PI | OI | HI |
|---|---|---|---|---|---|---|---|---|---|
| ZS8 | 1.47 | 0.54 | 4.1 | 0.54 | 415 | 4.64 | 0.11 | 36.73 | 278.91 |
| ZS12 | 1.35 | 0.33 | 4.8 | 0.57 | 419 | 4.96 | 0.064 | 42.22 | 355.55 |
| ZS5 | 1.58 | 0.31 | 6.88 | 0.68 | 414 | 7.06 | 0.043 | 42.03 | 345.44 |
| CS1 | 1.28 | 0.39 | 2.61 | 0.71 | 421 | 3 | 0.13 | 66.98 | 246.22 |